**MDOT**





**Research**

# CONDITION ASSESSMENT AND METHODS OF ABATEMENT OF PRESTRESSED CONCRETE BOX-BEAM DETERIORATION

## PHASE I

### FINAL REPORT – NOVEMBER 2005

**MichiganTech**

**CENTER FOR STRUCTURAL DURABILITY
MICHIGAN TECH TRANSPORTATION INSTITUTE**

Technical Report Documentation Page

| 1. Report No.<br>**Research Report RC-1470** | 2. Government Accession No. | 3. MDOT Project Manager<br>**Steve Kahl, P.E.** | |
|---|---|---|---|
| 4. Title and Subtitle<br>**Condition Assessment and Methods of Abatement of Prestressed Concrete Box-Beam Deterioration** | | 5. Report Date<br>**November 30, 2005** | |
| 7. Author(s)<br>**Dr. Theresa M. Ahlborn, Mr. Christopher G. Gilbertson (MTU)**<br>**Dr. Haluk Aktan, Mr. Upul Attanayake (WSU)** | | 6. Performing Organization Code<br>**MTU and WSU** | |
| 9. Performing Organization Name and Address<br>**Center for Structural Durability – A joint effort between:**<br><br>**Michigan Technological University**<br>**1400 Townsend Drive**<br>**Houghton MI 49931-1295** / **Wayne State University**<br>**5050 Anthony Wayne Drive**<br>**Detroit MI 48202** | | 8. Performing Org Report No.<br>**CSD-2005-09** | |
| 12. Sponsoring Agency Name and Address<br>**Michigan Department of Transportation**<br>**Construction and Technology Division**<br>**PO Box 30049**<br>**Lansing MI 48909** | | Work Unit No. | |
| | | 11. Contract Number | |
| | | 11(a). Authorization Number | |
| 15. Supplementary Notes | | 13. Type of Report and Period Covered<br>**Final Report, 2004-2005** | |
| | | 14. Sponsoring Agency Code | |

16. Abstract

**Phase I of the box-beam deterioration project provides a solid base for understanding the issues involved in the maintenance of Michigan's side-by-side box-beam bridges. The literature review explains the structural behavior of these bridges and provides a history of box-beam bridge design. Background information on durability and deterioration issues, tools for identifying distress, and the effects of premature deterioration and how to make proper repairs are identified. The Pontis database was used to identify 15 side-by-side box-beam bridges in Michigan to be field inspected. These bridges were inspected and forms of distress identified during the literature review were found and documented. An inspection handbook was created to aid a bridge inspector during a scoping or damage assessment bridge inspection. This handbook provides guidance on what to look for and what sort of impact it may have on the structural integrity of the beam. Flowcharts are included to aid a design engineer in determining proper repair techniques. Additionally, sample load rating calculations are provided to show the engineer how to assess a load rating for a distressed bridge. Lastly, a finite element analysis was conducted for a single box-beam section. The finite element model gave a detailed look at the effects of deterioration on the stresses and strains within a box-beam and provided an advanced method for determining the structural capacity of the beams.**

| 17. Key Words:<br>**Box-Beam, Deterioration, Prestressed Concrete** | | 18. Distribution Statement<br>**No restrictions. This document is available to the public through the Michigan Department of Transportation.** | |
|---|---|---|---|
| 19. Security Classification (report)<br>**Unclassified** | 20. Security Classification (Page)<br>**Unclassified** | 21. No of Pages<br>**169** | 22. Price |

**Report RC-1470**

# CONDITION ASSESSMENT AND METHODS OF ABATEMENT OF PRESTRESSED CONCRETE BOX-BEAM DETERIORATION

## PHASE I

Submitted by the
### CENTER FOR STRUCTURAL DURABILITY
A Michigan DOT Center of Excellence

Submitted to:

**MDOT**

## Final Report – November 2005

Wayne State University
Civil & Environmental Eng. Dept.
5050 Anthony Wayne Dr.
Detroit, Michigan 48202
Fax: 313/577-9850

Dr. Haluk Aktan, P.E.
Professor
313/577-3825
Haluk.Aktan@wayne.edu

Mr. Upul Attanayake
Graduate Research Assistant
313/577-9293
upul@wayne.edu

Michigan Technological University
Civil & Environmental Eng. Dept.
1400 Townsend Dr.
Houghton, Michigan 49931
Fax: 906/487-1620

Dr. Theresa M. Ahlborn, P.E.
Associate Professor
906/487-2625
tess@mtu.edu

Mr. Christopher Gilbertson, P.E.
Graduate Research Assistant
906/487-2021
cggilber@mtu.edu

**ACKNOWLEDGEMENTS**

**DISCLAIMER**

# TABLE OF CONTENTS

# LIST OF FIGURES

CENTER FOR STRUCTURAL DURABILITY – Condition Assessment and Methods
of Abatement of Prestressed Concrete Box-Beam Deterioration

v

# LIST OF TABLES

CENTER FOR STRUCTURAL DURABILITY – Condition Assessment and Methods
of Abatement of Prestressed Concrete Box-Beam Deterioration

vii

# Executive Summary

## *INTRODUCTION*

A previous study (Needham and Juntunen 1997) revealed that highway bridges in Michigan deteriorate due to freeze-thaw action, corrosive effects of deicing salts, and collision with high loads (vehicles that exceed maximum overhead clearance). This previous study recommended that the deterioration trends in prestressed concrete box-beams be identified. Side-by-side box-beam bridges became popular beginning in the 1970's because of economy and construction advantages. This type of bridge is typically constructed by placing precast/prestressed box-beams adjacent to each other, grouting full depth shear keys, applying transverse post-tensioning, and casting a six-inch thick reinforced concrete deck. The resulting superstructure is expected to behave as a plate simply supported at two ends. The integrity of the plate becomes compromised when longitudinal cracks form along the shear keys, allowing surface water to penetrate and become trapped between the box-beams. Water saturated with deicing salts penetrates along the full length of the beams and initiates corrosion of prestressing tendons. Though there are significant advantages to this type of superstructure, premature deterioration is a major concern for this particular type of bridge superstructure. This project (Phase I) was initiated to look into causes and cures of premature deterioration.

Five objectives were identified for this project:

- Detailed identification of common types and levels of box-beam distress or deterioration.

- Develop guidelines to assist inspectors in assessing the effect of section loss on structural capacity.

- Provide guidelines for the load capacity assessment of bridges with distressed beams by finite element modeling and analysis.

- Identify effective maintenance or protection techniques for deteriorated regions of box-beam that are in good or fair condition.

- Develop recommendations for changes or modifications to the design of side-by-side box-beam bridges based on the results of the analytical modeling.

CENTER FOR STRUCTURAL DURABILITY – Condition Assessment and Methods
of Abatement of Prestressed Concrete Box-Beam Deterioration

ix

## FIELD INSPECTION

Criteria were established for the selection of fifteen side-by-side prestressed concrete box-beam bridges for inspection. The pool of bridges selected for inspection were separated into two groups; those built before 1974 and after 1985. Significant changes were made to the design of side-by-side box-beam bridge superstructures in 1974 and 1985. Bridges built between 1974 and 1985 were not studied due to short lived design changes and a lack of sufficient number of such bridges in current use.

It was essential that bridges over a range of ages be incorporated into the inspection to extract the progression of distress and the mechanisms which cause it. Eight bridges were chosen from the list of 27 built before 1974 and seven bridges were chosen from the list of 50 that were built after 1985.

Deterioration of individual box-beams comes in many forms. The visual symptoms usually consist of cracks and/or spalls. These areas are of concern because they may allow salt-laden water to penetrate into the structural member and cause further deterioration of both concrete and steel. Corrosion of the shear reinforcement and the prestressing tendons greatly impacts the capacity of the structure; not only does it cause loss of a key component in a prestressed system, but corroding steel may expand three to six times the original volume and cause further loss of concrete section due to cracking and spalling (Teng 2000).

A predominant distress observed in all new and old side-by-side box-beam bridges that were inspected is the reflective cracking of the deck along the shear keys between box-beams. This is a serious problem as it allows penetration of surface water with the deicing chemicals through the deck and between the beams. Older bridges may have been constructed with an asphalt wearing surface instead of a concrete deck over the box-beams. This practice was stopped in the 1980's and a six-inch reinforced concrete deck was introduced due to water leakage between the shear keys. Yet, the deck reflective cracking distress persisted. Reflective cracking of the deck may be a sign of functional problems with the shear keys between adjacent box-beams and/or loss of force in the transverse post-tensioning strands. The purpose of the shear keys and the transverse post-

tensioning is to tie the beams in the system for providing moment and shear stiffness in the transverse direction. This causes the beams to behave conjointly with full load transfer between any two adjacent box-beams. Reflective cracking of the bridge deck infers differential movement between beams. Should this happen, the bridge system may no longer behave as designed and overloading of individual elements may occur.

## *INSPECTION HANDBOOK*

Thirteen conditions of deterioration documented during field inspection are listed and identified in the inspection handbook. The types of distress are ranked according to their level of structural significance by an alphabetical condition rating specific to this project. The condition nomenclature determined by the Federal Highway Administration (FHWA) for the National Bridge Inventory (NBI) is provided to help correlate between the two systems. The grades of deterioration provided in this handbook are specific to prestressed box-beams and therefore contain more box-beam-specific detail than the NBI condition ratings. The condition ratings assigned to Michigan prestressed concrete box-beam bridges are summarized below.

**Table 1: Summary of condition states for Michigan prestressed concrete box-beams**

| Box-Beam Rating | Description of Possible Conditions Present | FHWA Rating | FHWA Description |
|---|---|---|---|
| A | 1. No cracks or staining | 9-8 | Excellent to very good condition |
| B | 2. Map cracks<br>3. Hairline cracks | 7-6 | Good to satisfactory condition |
| C | 4. Minor spalling or delamination<br>5. Narrow cracks w/ water or corrosion<br>6. Water stains at joints<br>7. Longitudinal cracks on deck | 5 | Fair condition |
| D | 8. Medium cracks w/o water<br>9. Evidence of displacement between beams | 4 | Poor condition |
| E | 10. Medium cracks w/ water or corrosion | 4 | Poor condition |
| F | 11. Wide cracks w/ water or corrosion | 4 | Poor condition |
| G | 12. Spalling w/ exposed or corroded reinforcement<br>13. Shear or flexure cracking | 3-2 | Serious to critical condition |

The purpose of the inspection handbook is to aid the inspector by illustrating typical forms of distress in box-beam bridges and help reduce the likelihood of overlooking items which may be needed for additional analysis of the structure. Use of the inspection handbook may be beneficial to all levels of bridge inspection. However, due to the level of detail, it will prove most useful to inspectors conducting in-depth/scoping inspections, or damage assessment inspections.

## INSPECTION REPORT FORMS

Specialized inspection worksheets and forms have been developed for use during in-depth / scoping or damage assessment inspections of Michigan box-beam bridges. The level of detail attained in these forms may be greater in scope than inventory and routine levels of inspection. However, the forms provide clear and concise documentation of the inspection for the design engineer in determining the appropriate repair. Use of these forms help ensure that enough information is gathered during a bridge inspection to properly assess the structural capacity.

## REPAIR OPTION FLOWCHARTS

Flowcharts were created which may be used by the design engineer to assess the proper repairs for distress identified by the field inspector. These flowcharts provide means to first identify the type of distress (structural or material). Failure to differentiate between material and structural deteriorations may result in inappropriate repair choices.

The intent of these flowcharts is to determine the proper repair for the identified distress. Many of the repairs may be made following the Michigan DOT *Standard Specifications for Construction* (MDOT 2003c). A design engineer may be required to design repairs for material related or severe forms of distress. There may also be unique site or project specific conditions for which an engineer with experience in distress related repair should be consulted.

## *LOAD RATING CALCULATIONS*

The *Manual for Condition Evaluation of Bridges* (AASHTO 2003b) in conjunction with the *Bridge Analysis Guide* (MDOT 2003a) were used to conduct the sample load ratings. The *Manual for Condition Evaluation of Bridges* provides a series of equations specific to prestressed concrete superstructures which must be checked. The equations are presented in two groups; inventory and operating levels. The inventory level uses factors which represent loads of frequent application. The factors contained in the operating level equations correspond to larger loads of less common application. Both sets of equations require knowledge of material and cross-sectional beam properties. Those properties which have been affected by distress must be changed and a new load rating must be calculated.

Sample load ratings were performed for two bridges, both 27x36-inch side-by-side box-beam superstructures. The loading, span length, and material properties were different between the two. The first example, Bridge A, is from example problem 6 in the *Bridge Analysis Guide* (MDOT 2003a). The second example, Bridge B, was derived from information collected during the bridge inspection selection stage of the project. Bridge B represents a configuration representative of existing Michigan bridges. Table 2 indicates the simulated distress applied to each beam. Simulation of the spalled scenarios in both example A and B were conducted by recalculating the cross-sectional properties of the beam to account for the loss of concrete and/or strand. Deterioration of the shear keys was simulated by modifying the distribution factors for live and dead load to reflect a 10% reduction in load distribution. This represents extreme degradation because even severe cracks in shear keys have been found to only cause a 10% reduction in load distribution between adjacent box-beams (Miller et al. 1998). The condition states listed in Table 2 corresponds to the box-beam rating in Table 1.

**Table 2:  Scenarios studied in load rating**

| Case | Scenario | Box-Beam Rating (Table 1) |
|---|---|---|
| **Bridge A** | **Bridge Analysis Guide, Example 6** | |
| A-1 | Control condition | A |
| A-2 | Spalling of concrete, 30 inches$^2$ (5.9%) of section loss. | C |
| A-3 | Spalling of concrete and loss of strand, 30 inches$^2$ (5.9%) of section loss and 30% corrosion of strands. | E, F, G |
| | | |
| **Bridge B** | **Typical Bridge from Phase I Inspection** | |
| B-1* | Control condition | A |
| B-2* | Spalling of concrete, 103 inches$^2$ (20%) of section loss. | G |
| B-3* | Spalling of concrete and loss of strand, 103 inches$^2$ (20%) of section loss and 2 severed strands (6.7%). | G |
| B-4* | Spalling of concrete and loss of strand, 133 inches$^2$ (26%) of section loss and 4 severed strands (13.2%). | G |
| B-5 | Spalling of concrete and loss of strand, 133 inches$^2$ (26%) of section loss and 25% corrosion of strands. | G |
| B-6 | Ineffective shear keys and/or post-tensioning, 10% increase in load distribution factors | D |
| * Normalized live load capacity is available from finite element analysis | | |

Results of the inventory level load rating are shown in Table 3.  The values presented are the lowest values from the six equations for inventory level ratings as printed in the *Manual for Condition Evaluation of Bridges* (AASHTO 2003b).  The controlling failure mechanism is also indicated for each of the simulated forms of distress.

**Table 3:  Inventory level load rating results for prestressed concrete box-beams**

| Case | Inventory Load Rating Factor (HS-20 Truck) | Percent of Control Case Rating | Controlling Equation |
|---|---|---|---|
| A-1 | 1.26 | 100% | Prestress Steel Tension |
| A-2 | 0.97 | 77.0% | Prestress Steel Tension |
| A-3 | 0.83 | 69.9% | Concrete Tension |
| | | | |
| B-1 | 1.80 | 100% | Shear Strength |
| B-2 | 1.73 | 96.1% | Concrete Tension |
| B-3 | 1.50 | 83.3% | Concrete Tension |
| B-4 | 1.28 | 71.1% | Concrete Tension |
| B-5 | 0.85 | 47.2% | Concrete Tension |
| B-6 | 1.63 | 88.8% | Shear Strength |

Deterioration had a significant impact on the inventory rating of the bridge structures. The inventory rating was greatly reduced (listed as a percentage of the control case rating in Table 3) due to the presence of deterioration.  The shear strength of the beam and the

tensile stress in the prestressing strand and concrete were the factors which controlled the inventory rating.

## *ANALYTICAL MODELING*

Finite element analysis was utilized for the evaluation of shear and flexural capacities of individual box-beams with the common types and levels of distress. Side-by-side box-beam bridge designs specify a cast-in-place concrete deck, full-depth grouted shear keys, and transverse post-tensioning for the orthotropic action of the bridge superstructure. However, longitudinal reflective deck cracking may limit the monolithic action. Spalling of shear key grout, significant water leakage through shear keys, concrete delamination and spalls, and corroded and broken prestressing strands are among the documented beam distresses. With the uncertainty of transverse load transfer among the adjacent beams, superstructure capacity may be limited by the capacity of a single beam. It can be assumed that in the extreme case a single beam carries as much as a single wheel line load, although, more likely some load transfer would still occur (10% reduction mentioned in the 'Load Rating Calculations' section). A single beam model was developed for the FE analysis to be conservative and simplify computations.

The objective of the FE modeling and analysis was to determine the impact of this distress on shear and flexural capacities of the box-beams. The physical condition of the bridge and the beams were documented through the field inspection of fifteen in-service side-by-side box-beam bridges. The inspection data revealed the most common distress types and levels of structural significance. The common distress types were incorporated in the two FE models developed for flexure critical and shear critical beam lengths.

In the case of the flexure critical model, distresses were incorporated at the mid span and at quarter-point locations of the model. The length of distress along the beam was assumed as 54 inches or 12 elements. In beams with broken tendons, the effective distress length is increased by the length of transfer of stresses back to concrete. The design transfer lengths calculated from *AASHTO Standard Specifications 9.20.2.4* (AASHTO 2002) (50 x tendon diameter) and *AASHTO LRFD 5.11.4* (AASHTO 2004)

CENTER FOR STRUCTURAL DURABILITY – Condition Assessment and Methods
of Abatement of Prestressed Concrete Box-Beam Deterioration

xv

(60 x tendon diameter) are 18.75 inches and 22.50 inches, respectively. In the FE model a transfer length of 20 inches is incorporated that also needs to match the element length.

Beam capacities are defined independently for the flexure critical and shear critical beams. In flexural critical beams, beam live load capacity is defined as the percentage of truck load (11 axle truck with 145.4 kips – *Bridge Analysis Guide* (MDOT 2003a) Truck # 17) generating a maximum tensile stress equal to the tensile stress limit specified in the *AASHTO Standard Specifications 9.15.2.2* (AASHTO 2002) and *AASHTO LRFD 5.9.4.2* (AASHTO 2004) for severe corrosive exposure conditions at or near the bottom fibers ($3\sqrt{f'_c}$). In shear critical beams, the fracture critical zone is defined between 18 and 27 inches from the support. Within this zone, principal stresses are obtained. The beam live load capacity is defined as the percentage of truck load (Truck # 17) generating a maximum tensile stress equal to the tensile stress limit of $3\sqrt{f'_c}$ on the web and within the fracture critical zone. The normalized live load capacities of flexure and shear critical beams are calculated and shown in Table 4 and Table 5, respectively.

The flexural capacity of the beam was calculated directly from the cross sectional stresses obtained under the level of wheel line load generating the critical tensile stress. In calculating the capacities, the section is assumed fully cracked and the tensile stress is neglected. In analytical methods (procedures given in design manuals), it is assumed that the flexural stress distribution across the beam width, at a particular distance from the neutral axis, is uniform. However, in a 3D box-beam, the stress distribution across the beam width resembles to a parabolic curve giving the maximum stress levels near the beam corners or sides. The stress distribution patterns used in calculations caused the differences of box-beam capacities calculated from analytical and FE methods. The beam capacities calculated from FE method is more accurate than that calculated from analytical methods because the FE method is capable of representing the stress distribution on a 3D box-beam model.

## CONCLUSIONS

Phase I of the box-beam deterioration project provides a solid base for understanding the issues involved in the maintenance of Michigan's side-by-side box-beam bridges.

Maintenance and inspection of Michigan's prestressed concrete box-beam bridges is imperative to the preservation of the state's infrastructure. Side-by-side box-beam bridges have many advantages over other bridge types in ease of construction, aesthetics, and cost. However, inspection of these bridges is different from other bridge types for two reasons. First, the designed interaction between beams makes inspection of the grouted keyways and transverse post-tensioning system important, and second, due to the placement of beams, many beams may only be inspected along the bottom flange and other indicators must be reviewed for signs of distress in the beams. The inspection handbook for early identification of common forms of distress, in conjunction with the inspection report forms and repair flowcharts, are beneficial tools for achieving increased service life of side-by-side box-beam bridges.

Field inspection data and the literature review indicate that cracking of shear keys is a major cause of deterioration via salt laden water intrusion. In addition, there is evidence of water collecting inside box-beams. Rust stains around drain holes and longitudinal cracks along the bottom flanges were noted. Longitudinal cracking may have occurred due to expansive forces exerted on the beam by corroding tendons or by the freezing of water collected inside box-beam cavity. Even though styrofoam is now used to form the box-beam cavity, moisture will likely continue to collect between the styrofoam and concrete on the inside of the bottom flange. Hence, tendons near the inner cavity may be subject to a more severe exposure than that of the outmost layer. From Phase I it is recommended that the concrete cover above the prestressing tendons near the top of the bottom flange be reviewed.

Phase I provided an in-depth review of existing literature on concrete box-beam deterioration, its history, theory and design, and provided tools available for identifying distress of both concrete and steel. Phase II of this project will expand upon the foundation laid out in Phase I by developing experimental methods of testing the

durability and effectiveness of repairs to side-by-side prestressed box-beam bridges. In addition, finite element models of box-beam assemblage including transverse posttensioning and barriers will be developed for verifying the design assumptions, load rating the bridge deck with box-beams at various levels of deterioration, and for damage assessment after a high load hit to the fascia beam. Finite element models require material properties of concrete and shear key grout. Material properties of prestressed concrete are well established and by knowing the 28-day compressive strength, which can be obtained from bridge plans, it is possible to estimate elasticity modulus using the formulation given in AASHTO Specifications. A series of laboratory testing will be performed to obtain the mechanical properties of commonly used grout material. Further, the finite element models of the assemblage will be used for load capacity assessment of the assemblage with repaired box-beams. This analysis will require mechanical properties of repair and/or patching materials that will be provided by MTU. Additional tasks are identified and detailed in the contract proposal for Phase II.

# Action Plan

The inspection handbook from the Phase I report along with custom designed inspection report forms and worksheets have been designed for use during in-depth/scoping or damage level bridge inspections. Aspects of these materials may be useful for other levels of bridge inspections, however the level of detail achieved through use of the forms and worksheets may be more than needed for a routine inspection. The handbook will still be useful in identifying forms of distress visible to the routine inspector which may then be noted for a future scoping level inspection. The inspection handbook has been written to serve as a separate document and may be published accordingly and distributed to those responsible for conducting bridge inspections. Updates and future additions of the inspection handbook could be provided on a contractual basis through the Center for Structural Durability at Michigan Technological University. Implementation of the inspection handbook may be achieved by distribution to those who conduct bridge inspections.

Repair flowcharts and load rating examples were produced in response to the bridge inspections and inspection handbook. The intended recipients of this information are the engineers responsible for determining the need and type of repair for distress found by inspectors in the field. This information is contained within the Phase I report and should be made available to design engineers for implementation. Work during Phase II will lead to more specific recommendations on material and repair methods. Phase II will validate the effectiveness of certain repairs.

The finite element analysis of the box-beam will be implemented through design modification suggestions. During Phase I of this project, an FE model was created to determine the stress distribution within a single box-beam with various forms and categories of distress under applied dead and live loads. Phase II of this project will develop this model to represent the interaction of other beams with the deck and transverse post-tensioning as found in a side-by-side box-beam bridge. Experimental work on a prototype bridge in conjunction with the FE model of the full bridge will allow

the understanding of the parameters controlling the orthotropic behavior of the side-by-side box-beam bridge. Design modifications may be presented upon review of the internal stresses with full consideration of load distribution within the bridge. Implementation of these findings will rely on the incorporation of the design modifications to the future box-beam standard designs.

Use of the Box-Beam Inspection Handbook, repair flowcharts, and distressed load rating calculation examples rely on distribution of the materials to those responsible for conducting inspections or repair assessment and design. The finite element modeling of a box-beam structure will produce suggestions for modifications to the standard Michigan design of box-beams, this will occur following additional research conducted during the second phase of the project.

## *Action Plan Summary:*

Fifty copies of the final report were delivered to MDOT by the Centers for Structural Durability at Michigan Technological and Wayne State Universities. Internal distribution of the documents shall be performed by MDOT. Training on the use of these guidelines and future updates and revised editions could be provided by the Center for Structural Durability at Michigan Technological University.

Based on the results of the field inspection it is recommended that a design change be considered for the bottom flange. Specifically, the concrete cover above the prestressing tendons should be increased to create more protection against strand corrosion.

The second phase of this project will focus on expanding upon the results of this phase. The finite element model will be expanded to represent the entire bridge system, and thus provide information on shear key performance and load distribution effects. Full scale monitoring of a prestressed box-beam from production through construction and into service is also planned.

# Chapter 1:    Introduction

## 1.1   Overview

Studies revealed that highway bridges in Michigan deteriorate at a rate greater than anticipated due to freeze-thaw action, corrosive effects of deicing salts, and collision with high loads (vehicles that exceed maximum overhead clearance).  Deterioration effects all bridge types, however, it is particularly difficult to assess in side-by-side box-beam bridges due to limited access and visibility.  The bridge is constructed by placing precast/prestressed box-beams adjacent to each other, grouting full depth shear keys, applying transverse post-tensioning, and casting a six-inch thick reinforced concrete deck.  However, longitudinal cracks form along the shear keys allowing surface water to penetrate and become trapped in between the box-beams.  Water saturated with deicing salts penetrates along the full length of the beams and initiates corrosion of prestressing tendons.  Though there are significant advantages to box-beam construction, this premature deterioration mechanism must be understood and addressed in future construction to justify these advantages.

## 1.2   Objectives

This project, Condition Assessment and Methods of Abatement of Prestressed Concrete Box-Beam Deterioration, is funded by the Michigan Department of Transportation (MDOT) through the joint Centers for Structural Durability at Wayne State University (WSU) and Michigan Technological University (MTU) as a collaborative effort.  The research dealt primarily with condition assessment through field inspection and analytical modeling of a single box-beam.

The objectives of this study are presented below:

- Identify common types and states of deterioration in side-by-side prestressed concrete box-beam bridges in Michigan.  Develop inspection techniques that result in early identification of cracking and strand corrosion at the ends of the prestressed box-beams.

CENTER FOR STRUCTURAL DURABILITY – Condition Assessment and Methods
of Abatement of Prestressed Concrete Box-Beam Deterioration

1

- Develop guidelines to assist/direct inspectors in determining when section loss may reduce structural capacity.

- Provide guidelines for load capacity assessment of bridges with distressed beams (due to deterioration and/or high load hits on the fascia beam) based on finite element modeling.

- Identify effective maintenance and/or repair techniques for the deteriorated regions of side-by-side prestressed concrete box-beams, especially for bridges in good or fair condition.

- Develop recommendations for changes or modifications to the design of side-by-side precast prestressed box-beam bridges based on analytical modeling.

To satisfy the objectives, this project was organized with the following tasks:

- Task 1:  State-of-the-Art Literature Review

  A literature review was conducted to identify, review, and synthesize information related to condition assessment and methods of abatement of side-by-side precast prestressed box-beam bridge deterioration.  This was an ongoing task throughout the project and the resulted in a comprehensive chapter describing many different aspects of side-by-side precast prestressed box-beam bridges ranging from history to types and causes of deterioration, inspection procedures, condition assessment techniques, design related issues, construction techniques and procedures, analytical studies, finite element modeling techniques, and repair techniques.

- Task 2:  Field Investigation/Observations of Prestressed Concrete Box-Beam Deterioration

  The major objective of this task was to identify the types of distress or deterioration of side-by-side precast prestressed box-beam bridges in Michigan. The distress types, mechanisms, and the distress states were established from the inspection data collected visually at arms length.  The inspection looked at the condition of each beam, deck, and the bearings.  It was essential to inspect bridges of all ages to be able to extract the distress progression and mechanisms which

occur over time.  Bridges for inspection were selected from the National Bridge Inventory (NBI) based on age, inspectability, location, and condition.  Fifteen bridges from across the state were inspected.  The selection process was determined through collaboration with the Research Advisory Panel (RAP).

Photos depicting varying condition states showing the progression of beam failure and severity levels of damage were taken and selected for inclusion in the inspector's guidebook developed in Task 4.  Common levels and locations of beam deterioration were identified for use with analytical modeling in Task 3.

- Task 3:  Analytical Modeling

This task developed an analytical model of a single precast prestressed concrete box–beam to be used for evaluating the load capacities at various states of concrete deterioration and various levels of tendon corrosion.  Finite element analysis programs were utilized in the modeling and analysis.  With this process, bridge load capacities were established using analytical models and results were used to develop guidelines in Task 4.

- Task 4:  Development of Guidelines

Guidelines were developed for scoping engineers, inspectors, and structural analysts.  Inspector's Guidebook to Prestressed Concrete Box-Beam Deterioration used photos from Task 2 and/or tables and/or flowcharts from Tasks 3 to assist the inspector in identifying the condition state of a box-beam.  A table was developed that links condition states with suggested maintenance and repair actions.  Guidance is given in Appendix D on how to prepare inspection reports in a form and content useful for further analysis by the bridge engineer.

Analysis guidelines for load ratings were developed from Tasks 3 such that information obtained from inspector's reports can be used to determine if a section exhibits a reduced load capacity.  Sample calculations are provided in Appendix G to estimate load capacity.

CENTER FOR STRUCTURAL DURABILITY – Condition Assessment and Methods of Abatement of Prestressed Concrete Box-Beam Deterioration

3

This report is organized into seven chapters. The first chapter contains an introduction to the project. The second chapter is a review of existing literature on the subject of concrete repair, box-beam bridges, finite element modeling and other topics specific to the subject matter of this report. A review of Michigan bridges was conducted and the process for this is presented in Chapter Three. Guidelines for the inspection process and load ratings are provided in the fourth chapter. Chapter Five contains results found from the inspection of fifteen bridges located throughout the lower peninsula of Michigan. Lastly, a finite element model was created for a single box-beam to determine the stress distribution within the beam. The procedure and results for this are contained in Chapter Six. The final chapter contains a summary of the project and suggestions for future work to be conducted in the second phase of this project. Appendices A through H are printed and located following the main body of the report. Appendices I through L have not been printed in their entirety. The complete appendices are located on the attached CD along with a single-sided electronic copy of the complete report in PDF format.

# Chapter 2:    State-of-the-Art Literature Review

## 2.1   Objective and Approach

The objective of the literature review is to identify, review, and synthesize information related to side-by-side precast prestressed concrete box-beam bridges with transverse post-tensioning.  The following aspects were addressed:

- Structural behavior of various superstructure components of a box-beam bridge

- History and background of side-by-side precast prestressed concrete box-beam bridges

- Design related issues of side-by-side precast prestressed concrete box-beam bridges with transverse post-tensioning (includes MDOT, national, and global practices)

- Types and causes of deterioration of different structural components of side-by-side box-beam bridges

- Overall inspection techniques including inspection of post-tensioned tendons (emphasis on concealed defects and identification of their indicators)

- Condition assessment techniques

- Finite element modeling techniques of bridge components

- Construction procedures

- Repair techniques

These topics were thoroughly reviewed and are presented within this chapter.  The information gathered in the literature review provided an adequate background for the remainder of the work presented in the other sections of this report.

## 2.2   Overview

Box-beams, which are referred to as thin-walled structures because of their cross-sectional dimensions, are preferred due to ease of construction, favorable span-to-depth ratios,  aesthetic appeal, high torsional stiffness of box-beams, and the ability to enclose utility lines within voids of box-beam sections (Fereig 1994).  In addition, these bridges can be constructed without cast-in-place concrete slabs, although this is not done in Michigan.  This reduces the time and money required for casting and curing of deck concrete.  If a cast-in-place concrete deck is required,

CENTER FOR STRUCTURAL DURABILITY – Condition Assessment and Methods
of Abatement of Prestressed Concrete Box-Beam Deterioration

5

formworks for the deck concrete are not required as they are in other design types.  These features facilitate rapid construction of the bridge (Miller et al. 1999).

## 2.3 Structural Behavior of Side-by-Side Precast Prestressed Concrete Box-Beam Bridge with Transverse Post-Tensioning

### 2.3.1 General

Before the development of the design procedure for side-by-side precast prestressed concrete box-beam bridges with transverse post-tensioning, the designer's conceptual model was a continuous bridge superstructure, similar to a plate.  Due to the difficulty of construction quality assurance with such a large, continuous structure, a model was developed that can be practically implemented in the field.  The idea was to place precast prestressed concrete box-beams adjacent to each other and provide fully interconnected joints between the beams.  These joints are identified as flexure and shear joints.  This type of interconnection is enhanced with shear keys and transverse post-tensioning, shear keys and a cast-in-place concrete overlay, or a combination of shear keys, transverse post-tensioning, and a cast-in-place concrete overlay.  Based on this practically implementable system, the design procedure was developed and a large number of side-by-side precast prestressed concrete box-beam bridges were constructed.

### 2.3.2 Plate Behavior

Designers envisioned that the behavior of concrete bridge deck resembles the behavior of an orthotropic plate, with two opposite edges that are simply supported and the other two edges are free.  Several papers discuss the behavior of an orthotropic plate under uniform loading.  Following a series of papers published by M.T. Huber on the application of the theory of anisotropic plates to reinforced concrete slabs, Timoshenko discusses the behavior of a reinforced concrete slab under uniform loading (Timoshenko 1987).

Flexural rigidities ($D_x$, $D_y$, and $D_{xy}$) of a slab with two-way reinforcement in the directions of x and y can be expressed as follows.

$$D_x = \frac{E_c}{1-v_c^2}\left[I_{cx}+(n-1)I_{sx}\right] \tag{1}$$

$$D_y = \frac{E_c}{1-v_c^2}\left[I_{cy}+(n-1)I_{sy}\right]$$
(2)

$$D_{xy} = \frac{1-v_c}{2}\sqrt{D_x D_y}$$
(3)

where, $n = E_c/E_s$, $E_c$ and $E_s$ are modulus of elasticity of concrete and steel respectively, $v_c$ Poisson's ratio of concrete, $I_{cx}$ and $I_{cy}$ are the moment of inertia of concrete, and $I_{sx}$ and $I_{sy}$ are the moment of inertia of reinforcement steel taken about the neutral axes in the section. The subscripts $x$ and $y$ denote the respective coordinate axes.

Equation (4) represents the differential equation of equilibrium for an orthotropic plate under uniform load ($q$) that causes downward deflection ($w$).

$$D_x\frac{\partial^4 w}{\partial x^4}+2\sqrt{D_x D_y}\frac{\partial^4 w}{\partial x^2 \partial y^2}+D_y\frac{\partial^4 w}{\partial y^4}=q$$
(4)

The bending stresses and the shear stress can be calculated from the following equations.

$$\sigma_x = -z\left(E_x\frac{\partial^2 w}{\partial x^2}+E\frac{\partial^2 w}{\partial y^2}\right)$$
(5)

$$\sigma_y = -z\left(E_y\frac{\partial^2 w}{\partial y^2}+E\frac{\partial^2 w}{\partial x^2}\right)$$
(6)

$$\tau_{xy} = -2Gz\frac{\partial^2 w}{\partial x \partial y}$$
(7)

By knowing the four constants $E_x$, $E_y$, $E$, and $G$ in the case of plane stress, the elastic properties of concrete can be characterized.

Designers implemented their understanding of orthotropic plate behavior for the superstructure design. The continuity between the adjacent beams is achieved with shear keys, transverse post-tensioning, and cast-in-place concrete overlay to make the entire system behave as a plate.

CENTER FOR STRUCTURAL DURABILITY – Condition Assessment and Methods
of Abatement of Prestressed Concrete Box-Beam Deterioration

7

### 2.3.3 Shear key Performance

Under the applied loads on side-by-side box-beam bridges, the beams are expected to deflect simultaneously due to transfer of vertical shear force through the shear keys at the beam joints. These shear keys are unable to transfer moments in the transverse direction. These joints exhibit hinging action; therefore, the transfer of vertical shear forces from one beam to the other in the transverse direction is due to torsional rigidity of the beams (Miller et al. 1999). *AASHTO LRFD* (AASHTO 2004) Section 5.14.4.3.2 requires that the depth of shear keys between the beams shall not be less than 7 inches. According to these specifications, longitudinal shear transfer joints are permitted to be modeled as hinges for purposes of the analysis. The non-shrinking grout material used for the shear keys requires a minimum strength of 5 ksi at 24 hours. Figure 2-1 shows the most common location of a shear key between side-by-side box-beams in the United States.
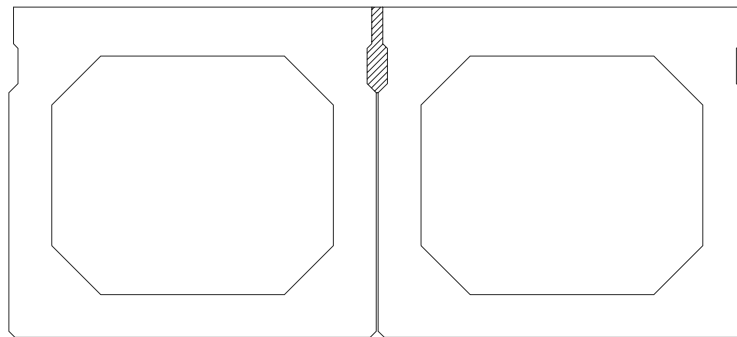


**Figure 2-1: Typical geometry for box-beam grouted shear key used in the U.S.**

Based on the means of connecting the beams, The AASHTO LRFD Specifications (AASHTO 2004) provides lateral load distribution factors to be used in beam designs. Therefore, the individual box-beams are designed only for a fraction of the expected live loads (Huckelbridge et al. 1995). The most common observed problem of the side-by-side box-beam bridges appears to be failure of shear keys and consequent longitudinal cracking. When analyzing the results of a full-scale testing of shear keys for side-by-side box-beam bridges, Miller et al. concluded that the location of the shear key and the non-shrink grout material has a significant potential for cracking due to thermal stresses (Miller et al. 1999). Temperature stresses initiate cracking and subsequent loading appears to cause crack propagation. These cracks allow water penetration that increases the rate of deterioration of the grout material and other bridge components.

Finally, the failure of the shear keys leads to individual beams being required to carry live loads greater than those for which they were designed. Overstressed beams show excessive relative displacements, which results in failure of the waterproofing system or the cast-in-place concrete deck. The magnitude of relative displacement of the beams depends on the actual length of the fractured shear key, the stiffness of the beams, and the magnitude and the proximity of the wheel load to the cracked joint (Huckelbridge et al. 1995).

The shear key used in most of the DOTs in the United States is relatively small (Figure 2-1). As shown in Figure 2-2 and Figure 2-3, Japanese practice is to place cast-in-place concrete in relatively wide and deep joints between the beams (Yamane et al. 1994; and El-Remaily et al. 1996). It is reported that longitudinal cracks are very rare on side-by-side box-beam bridges in Japan.
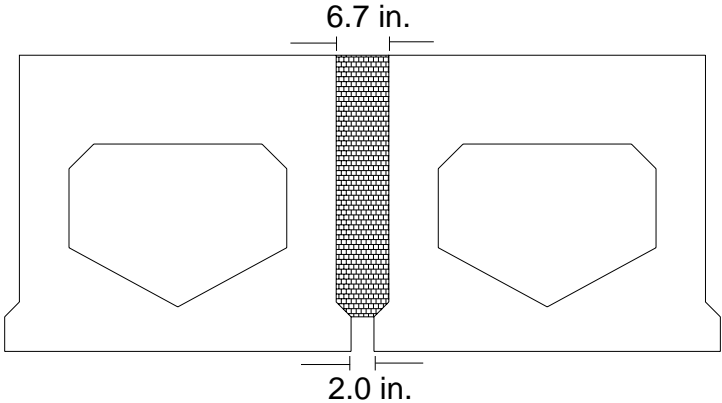


**Figure 2-2: Typical geometry for box-beam grouted shear key detail used in Japan**
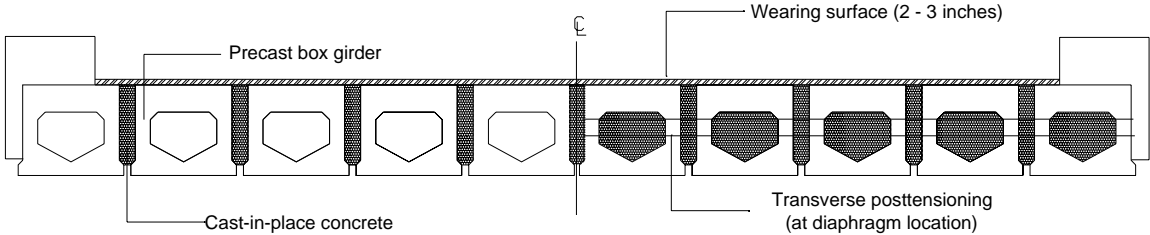


**Figure 2-3: Precast prestressed concrete box-beam bridge system in Japan**

Previous research on shear key performance (Yamane et al. 1994; Huckelbridge et al. 1995; El-Remaily et al. 1996; and Miller et al. 1999) is aimed at two areas, i.e., improving the mechanical behavior of the joint and improving the grouting material used for the shear key. Providing

CENTER FOR STRUCTURAL DURABILITY – Condition Assessment and Methods
of Abatement of Prestressed Concrete Box-Beam Deterioration

9

adequate transverse post-tensioning, thereby reducing or eliminating the initiation of cracks, can improve mechanical behavior of the shear keys.  This can further be enhanced by providing continuous or discrete full depth shear keys.  Discrete full depth shear keys are commonly positioned at the location of internal diaphragms through which the transverse post-tensioning is applied.  The shape of the shear key also has an impact on its performance.

Miller et al. studied the performance of the shear key at different locations along the beam depth (Miller et al. 1999).  Materials considered were non-shrink grout and epoxy.  Non-shrink grout shear keys located close to the top edge of the beam cracked before any load was applied.  It was concluded that these cracks were induced by temperature stresses.  The use of epoxy grout made it possible to prevent cracking under either temperature or load effects, but the coefficient of thermal expansion of epoxy is two to three times greater than that of concrete.  According to research findings at Case-Western Reserve University, substrate concrete cracks rather than the shear key if epoxy is used (Miller et al. 1999).  This failure mode is also undesirable.  By investigating the behavior of standard non-shrink grout and magnesium ammonium phosphate ($Mg$-$NH_4$-$PO_4$) mortars, Galuta and Cheung concluded that performance of the shear keys could be improved with better grout materials( Gulyas and Cheung 1995).

### 2.3.4  Transverse Post-Tensioning

Transverse post-tensioning  strands are used for side-by-side box-beam bridges constructed in Michigan.   Several other State DOTs use tie bars for the application of transverse post-tensioning.  Based on the results of six field tests, Huckelbridge et al. concluded that the tie bars have little or no impact on shear key performance (Huckelbridge et al. 1995).  *AASHTO LRFD Specifications* (AASHTO 2004) Section 5.14.4.3.3c requires that the stress of the transverse post-tensioning, after all losses, shall not be less than 0.25 ksi.  The area of contact between beams for transverse post-tensioning of box-beam bridges is not clearly defined by AASHTO.  This contact area could be regarded as the shear key area, the diaphragm-to-diaphragm contact area, or the entire side surface of the box-beam.   (El-Remaily et al. 1996) recommends considering the diaphragm-to-diaphragm contact area for the design.

### 2.3.5   Cast-in-Place Concrete Overlay

Side-by-side box-beam bridges are designed with asphalt wearing surfaces or conventional cast-in-place reinforced concrete decks (Huckelbridge et al. 1995). The purpose of the composite deck is to combine the box-beams with the transverse post-tensioning and the shear keys, such that the superstructure acts as a single unit while facilitating the distribution of loads over the deck. After studying several designs with 2 to 3-inch wearing surfaces and 5 to 6-inch cast in place toppings, (El-Remaily et al. 1996) described the cast-in-place concrete topping as a structurally inefficient solution due to its inability to control differential rotation of the box-beams. Further, it is indicated that its cost is about four times as much as a thin bituminous concrete overlay. Therefore, the composite concrete topping is not considered to be an economical solution but rather a necessity for durability to protect the box-beam below. As illustrated in Figure 2-3, box-beam bridge decks in Japan are covered with a 2 to 3-inch thick concrete or asphalt concrete layer (Yamane et al. 1994). *The Michigan Design Manual* (MDOT 2003b) requires a 6-inch thick reinforced concrete cast-in-place slab to be placed over the box-beams. According to *AASHTO LRFD Specifications* (AASHTO 2004) Section 5.14.4.3.3f, the thickness of the reinforced concrete overlay shall not be less than 4.5 inches.

### 2.3.6   Load Distribution

#### 2.3.6.1   *AASHTO LRFD Specifications Load Distribution*

Live load distribution over a bridge deck depends on the design type. Zokaie conducted National Cooperative Highway Research Program (NCHRP) funded research project in 1991, entitled *Distribution of Live Loads on Highway Bridges* (Zokaie 2000). For this project, a large database of information about more than 800 actual bridges was randomly compiled from various states to provide national representation. This database contained bridge type (i.e., prestressed concrete box-beam, I-beam, T-beam or steel box-beam, I-beam), span length, skew angle, number of beams, slab thickness, edge-to-edge width, beam eccentricity, beam moment of inertia, and other geometric properties. For the analysis, a hypothetical bridge deck model was created using the mean values of the parameters. Bridge models were created for each of the bridge types. To identify the influential parameters for live load distribution, a sensitivity analysis was performed using finite element models. Only one parameter was varied from its minimum to maximum

CENTER FOR STRUCTURAL DURABILITY – Condition Assessment and Methods
of Abatement of Prestressed Concrete Box-Beam Deterioration

11
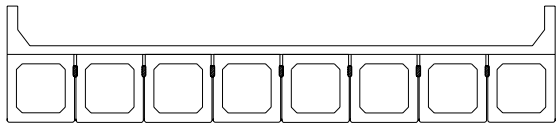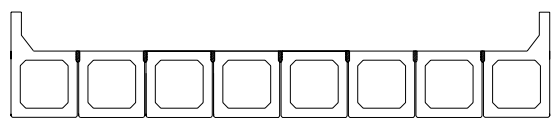
while holding all other parameters as mean values. From the sensitivity analysis results, Zokaie recognized influential parameters such as slab thickness ($t$), beam stiffness ($K_g$), beam spacing ($S$), and span length ($L$) (Zokaie 2000). The assumed model for the effects of each parameter was in the form of $ax^b$, where constants $a$ and $b$ were determined based on the variation of the distribution factor with the given parameter. Further, it was assumed that the effects of different parameters are independent of each other. Given these two assumptions, the live load distribution factor was modeled by an exponential formula as shown below:

$$g = (a)\ (S^{b1})\ (L^{b2})\ (t^{b3})\ (...) \qquad (8)$$

where, $g$ is the wheel load distribution factor; $S$, $L$, and $t$ are the beam spacing, span length, and slab thickness respectively; $a$ is a scale factor; $b_1$, $b_2$, and $b_3$ are determined from the variation of $g$ with $S$, $L$, and $t$ respectively. Based on this assumed relationship between the parameters, finite element models of the bridge deck for different design types, and the full axle load, distribution factors were derived. Later these formulations were included in *AASHTO LRFD Bridge Design Specifications* (Zokaie 2000).

In the *AASHTO LRFD Specifications* (AASHTO 2004), side-by-side box-beam bridges are categorized into two groups, (f) and (g), based on the type of deck, beam interconnection, and typical cross-section (Table 2-1).

**Table 2-1: Superstructure types with side-by-side box-beams**

| Supporting Components | Type of Deck | Typical Cross-Section |
|---|---|---|
| Precast solid, voided or cellular concrete boxes with shear keys | Cast-in-place concrete overlay | (f) |
| Precast solid, voided or cellular concrete boxes with shear keys and with or without transverse post-tensioning | Integral concrete | (g) |

Based on the connectivity between beams, the live load distribution factors published in *AASHTO LRFD Specifications* (AASHTO 2004) for moment and shear in interior beams are

given in Table 2-2 and Table 2-3, respectively. Load distribution over the exterior beam is different as compared to the interior beam. Live load distribution factors for moments and shear in exterior beams as specified by (AASHTO 2004) are given in Table 2-4 and Table 2-5, respectively. Load distribution of skew bridges is different from zero-skew bridges and the correction factors given in (AASHTO 2004) are shown in Table 2-6. Correction factors should be applied to each beam when calculating shear at the beam ends of a skew side-by-side box-beam bridge. These correction factors should be used in conjunction with the distribution factors given in Table 2-3 and Table 2-5.

The notations used in the distribution factor equations are given below:

| | | |
|---|---|---|
| $b$ | = | beam width, inch. |
| $D$ | = | width of distribution per lane, feet |
| $d$ | = | beam depth, inch. |
| $d_e$ | = | distance between the center of exterior beam and interior edge of curb or traffic  barrier, feet |
| $I$ | = | moment of inertia of beam, inches$^4$. |
| $J$ | = | St. Venant torsional constant, inches$^4$. |
| $L$ | = | span of beam, feet |
| $N_b$ | = | number of beams |
| $S$ | = | spacing of beams, feet |
| $W$ | = | edge-to-edge width of bridge, feet |
| $\theta$ | = | skew angle, deg. |
| $\mu$ | = | Poisson's ratio. |

CENTER FOR STRUCTURAL DURABILITY – Condition Assessment and Methods
of Abatement of Prestressed Concrete Box-Beam Deterioration

13

**Table 2-2: Distribution of live load per lane for moment in interior beams**

| Type of Beams | Applicable Cross-Section | Distribution Factors | Range of Applicability |
|---|---|---|---|
| Concrete beams used in multi-beam decks | **f** / **g** If sufficiently connected to act as a unit | One design lane loaded: $$k\left(\frac{b}{13.3L}\right)^{0.5}\left(\frac{I}{J}\right)^{0.25}$$ where: $k = 2.5\left(N_b\right)^{-0.2} \geq 1.5$ Two or more design lanes loaded: $$k\left(\frac{b}{305}\right)^{0.6}\left(\frac{b}{12.0L}\right)^{0.2}\left(\frac{I}{J}\right)^{0.06}$$ | $20 \leq L \leq 120$ $35 \leq b \leq 60$ $5 \leq N_b \leq 20$ |
| | **g** If connected only enough to prevent relative displacement at the interface | Regardless of number of loaded lanes: $S/D$ where: $C = K(W/L)$ $D = 11.5 - N_L + 1.4\,N_L\left(1-0.2C\right)^2$ when $C \leq 5$ $D = 11.5 - N_L \cdots$ when $\cdots C > 5$ $$K = \sqrt{\frac{(1+\mu)I}{J}}$$ | Skew $\leq 45^o$ $N_L \leq 6$ |

**Table 2-3: Distribution of live load per lane for shear in interior beams**

| Type of Superstructure | Cross-Section | One Design Lane Loaded | Two or More Design Lanes Loaded | Range of Applicability |
|---|---|---|---|---|
| Concrete box-beams used in multi-beam decks | **f, g** | $\left(\frac{b}{130L}\right)^{0.15}\left(\frac{I}{J}\right)^{0.05}$ | $\left(\frac{b}{156}\right)^{0.4}\left(\frac{b}{12.0L}\right)^{0.1}\left(\frac{I}{J}\right)^{0.05}\left(\frac{b}{48}\right)$ $\frac{b}{48} \geq 1.0$ | $35 \leq b \leq 60$ $20 \leq L \leq 120$ $25{,}000 \leq J \leq 610{,}000$ $40{,}000 \leq I \leq 610{,}000$ $5 \leq N_b \leq 20$ |

**Table 2-4: Distribution of live load per lane for moment in exterior beams**

| Type of Superstructure | Applicable Cross-Section | One Design Lane Loaded | Two or More Design Lanes Loaded | Range of Applicability |
|---|---|---|---|---|
| Concrete box-beams used in multi-beam decks | **f, g** | $g = e\ g_{interior}$ $e = 1.125 + \frac{d_e}{30} \geq 1.0$ | $g = e\ g_{interior}$ $e = 1.040 + \frac{d_e}{25} \geq 1.0$ | $d_e \leq 2.0$ |

**Table 2-5: Distribution of live load per lane for shear in exterior beams**

| Type of Superstructure | Applicable Cross-Section | One Design Lane Loaded | Two or More Design Lanes Loaded | Range of Applicability |
|---|---|---|---|---|
| Concrete box-beams used in multi-beam decks | **f, g** | $g = e \; g_{interior}$ <br><br> $e = 1.25 + \dfrac{d_e}{20} \geq 1.0$ | $g = e \; g_{interior} \left( \dfrac{48}{b} \right)$ <br> $\dfrac{48}{b} \leq 1.0$ <br><br> $e = 1 + \left( \dfrac{d_e + \frac{b}{12} - 2.0}{40} \right)^{0.5} \geq 1.0$ | $d_e \leq 2.0$ <br> $35 \leq b \leq 60$ |

**Table 2-6: Correction factors for load distribution factors of support shear**

| Type of Superstructure | Applicable Cross-Section | Correction Factor | Range of Applicability |
|---|---|---|---|
| Concrete box-beams used in multi-beam decks | **f, g** | $1.0 + \dfrac{12.0L}{90d} \sqrt{\tan \theta}$ | $0 < \theta \leq 60^0$ <br> $20 \leq L \leq 120$ <br> $17 \leq d \leq 60$ <br> $35 \leq b \leq 60$ <br> $5 \leq N_b \leq 20$ |

If two or more lanes of the bridge are loaded and the distribution factors for live load per lane for moment in an interior beam (Table 2-2) are going to be used for the design, interconnection of the beams is a concern. The fully connected joint should be able to transfer moment and shear between beams. Transverse post-tensioning (minimum 0.25 ksi) or reinforced concrete structural overlay or both can be used to enhance this type of interconnection. Use of other types of transverse connections like mild steel rods secured by nuts or similar unstressed dowels should not be considered sufficient to achieve full transverse flexural continuity unless proven by tests or experience (AASHTO 2004). To calculate the distribution factors for moment and shear in an exterior beam when one design lane is loaded, (AASHTO 2004) recommends using a lever rule. This rule requires summing up the moments about one support to find the reactions at another support. It is assumed that all the supported components are hinged at interior supports (Figure 2-4).

CENTER FOR STRUCTURAL DURABILITY – Condition Assessment and Methods
of Abatement of Prestressed Concrete Box-Beam Deterioration

15

Assumed Hinge
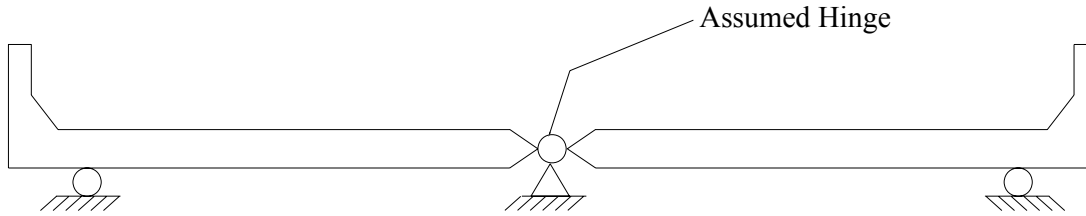
**Figure 2-4: Notional model for applying the lever rule**

Live load distribution between the box-beams depends on the connectivity between beams. Many researchers discuss the existing problems related to load transfer between beams (Ebeido and Kennedy 1996; El-Remaily et al. 1996; Huckelbridge et al. 1995; Juntunen 2000; Miller et al. 1999; and Sennah and Kennedy 1999).

### 2.3.6.2 AASHTO Standard Load Distribution (17th Edition)

In the *AASHTO Standard Specifications* (AASHTO 2002), to calculate bending moments in interior longitudinal beams, no longitudinal distribution of the wheel loads shall be assumed. The lateral distribution shall be determined as follows:

**Table 2-7: Distribution of live load for moment in interior longitudinal beams**

| Type of Floor | Bridge Designed for One Traffic Lane | Bridge Designed for Two or More Traffic Lanes |
|---|---|---|
| Concrete side-by-side box-beam | S/8.0 <br><br> If S exceeds 12-feet use foot note (1) | S/7.0 <br><br> If S exceeds 16-feet use foot note (1) |

(1) If S exceeds denominator, the load on the beam shall be the reaction of the wheels loads assuming the flooring between beams to act as a simple beam. Here S is the average stringer spacing in feet
(2) The sidewalk live load shall be omitted for interior and exterior box-beams designed in accordance with the wheel load distribution indicated herein.

The factor of the live load distribution for moment to the exterior beam shall be We/7.0, where We is the width of the exterior beam which shall be taken as the top slab width, measured from the midpoint between beams to the outside edge of the slab.

A multi-beam bridge is constructed with precast prestressed concrete beams that are placed side-by-side on the supports. The interaction between the beams is developed by continuous

longitudinal shear keys. In calculating bending moments for transverse beams, in multi-beam precast prestressed concrete bridges, no longitudinal distribution of wheel load shall be assumed.

The live load bending moment for each section of transverse beams shall be determined by applying to the beam the fraction of live load of a wheel load (both front and rear) determined by the following equation:

Load fraction $= S/D$ $\hspace{4cm}$ (1)

where,

$S$ = width of the precast member, when $S$ is less than 4-feet or more than 10-feet for precast stemmed members a special analytical investigation may be necessary and:

$$D = (5.75 - 0.5N_L + 0.7N_L(1 - 0.2C)^2 \hspace{3cm} (2)$$

where,

$N_L$ = number of traffic lanes

$$C = K\,(W/L)\ \text{for}\ W/L < 1 \hspace{3cm} (3)$$
$$\phantom{C} = K\ \text{for}\ W/L > 1$$

where,

$W$ = overall width of the bridge measured perpendicular to the longitudinal beams in feet

$L$ = span length measured parallel to longitudinal beams in feet, for beams with cast-in-place diaphragms use the length between diaphragms

$$K = \{(1 + \mu)I/J\}^{1/2} \hspace{3cm} (4)$$

where,

$I$ = moment of inertia

$J$ = Saint-Venant torsion constant

$\mu$ = Poisson's ratio for beams

For preliminary design, the value of K for multi-beam box section may be used as unity.

## 2.4　History and Background

### 2.4.1　General History

The modern development of prestressed concrete is attributed to Freyssinet of France, who started using high strength steel wires for pre- and post-tensioning concrete beams in 1928 (Troitsky 1994). The early development of the prestressed concrete industry in the United States and Canada, which started in the 1950s, was oriented toward factory production of precast prestressed elements for highway bridges. The first major prestressed concrete bridge built in the United States was Walnut Lane Bridge in Philadelphia in 1951. A record 787-feet long prestressed concrete twin box-beam for a highway bridge was built in 1976, 150 miles southwest of Tokyo, Japan. Prestressed concrete segmental bridges began in Western Europe in the 1950s. After World War II, the European transportation infrastructure needed to be rebuilt and extended. Box-beams were rapidly introduced in steel and concrete bridge construction as better understanding of the properties and the inherent advantages of closed hollow sections grew (Brown 1993). The use of high performance building materials and the development of powerful means for lifting and transportation together with an adequate combination of precast and cast-in-place, pre- and post-tensioning techniques, have impelled the development of precast concrete box-beam bridges (Mari 2000).

Prestressed concrete bridges quickly became popular because the beams could be built economically in plants and their span lengths could compete with that of steel beams (Needham and Juntunen 1997). According to the *Pontis 4.2* database, the first Michigan side-by-side box-beam bridge was built in 1955. The database shows that there are 1037 prestressed concrete bridges with the design types of side-by-side box-beams, spread box-beams, and I-beams under the jurisdiction of the Michigan Department of Transportation (MDOT). Of these prestressed concrete bridges, 236 are side-by-side box-beam bridges. Precast prestressed concrete box-beams are frequently used for short (20–60 feet) and short to medium span bridges (60–110 feet). The histogram shown in Figure 2-5 demonstrates the box-beam construction distribution over the last 49 years.
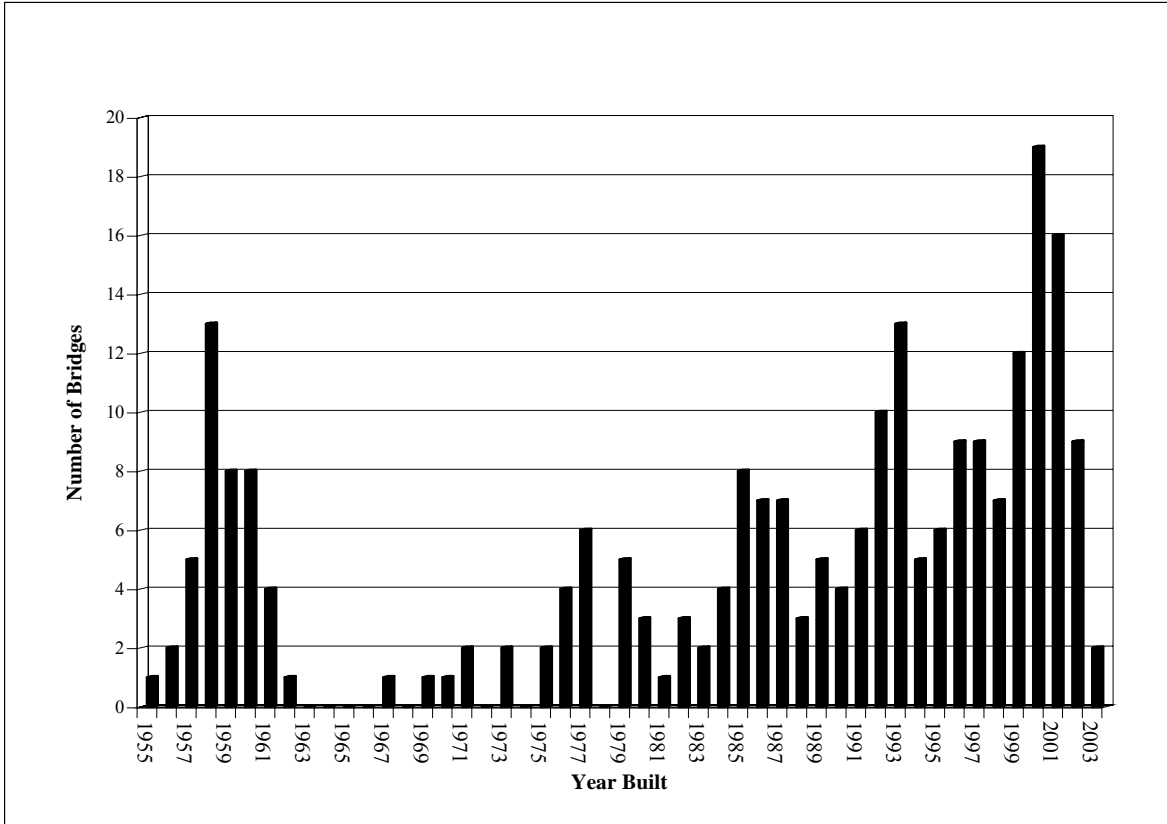
**Figure 2-5: Number of side-by-side prestressed concrete box-beam bridges under MDOT jurisdiction with respect to year built**

## 2.4.2   Michigan History of Prestressed Box-Beams

The prestressed side-by-side box-beam bridge was introduced to Michigan in 1955.  The earliest side-by-side precast prestressed concrete box-beam design configuration (1956), shows two box-beam configurations: single-cell of 36x27, 36x33, and 36x42 and double-cell of 36x17 and 36x21 (Figure 2-6).  The stirrups were open and did not extend to the bottom flange of the box-beam and the shear key configuration was narrower than the one used today.  The specified spacing between adjacent beams was ¼-inch.  For beams that span up to 40 feet, a tie-rod was used at the center of the span.  When the span was greater than 40 feet, tie-rods were used at each 1/3 location.  The specified wearing surface thickness was 3 inches.

CENTER FOR STRUCTURAL DURABILITY – Condition Assessment and Methods
of Abatement of Prestressed Concrete Box-Beam Deterioration

19
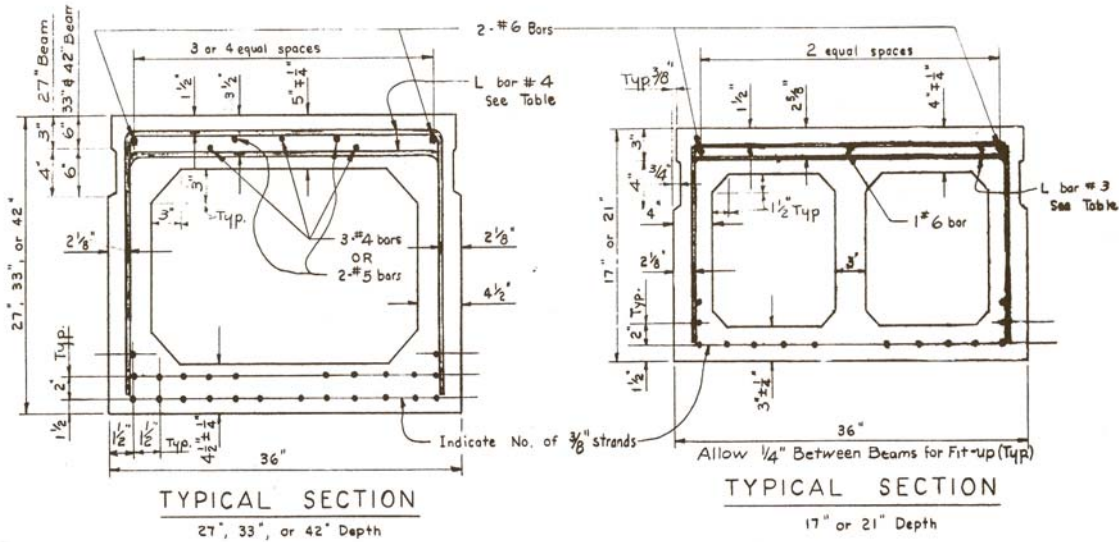
**Figure 2-6: Reinforcement details of (1956 box-beam sections)**

In 1958, deeper shear key configurations had been used at post-tensioning locations (Figure 2-7).
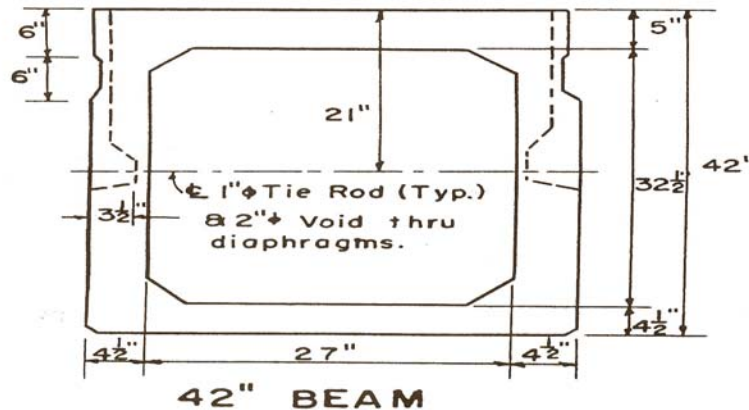


**Figure 2-7: Box-beam cross-section showing the 1958 tie rod location**

Another update in January 1959 revised the configuration of longitudinal bars.

Manufacturing difficulties discovered in 1961 saw an end to the design of concrete box-beams in Michigan. At this time, cardboard was used to form the void inside box-beams. It was discovered that during construction the cardboard could sometimes float upward, causing the top flange to be much smaller than designed. Between 1963 and 1966 no box-beam bridges were constructed and between 1967 and 1971 only four box-beam bridges were built. In 1974 box-beams were once again being used on a regular basis. However, there is no clear information

showing when cardboard was replaced with the currently used Styrofoam to form the box-beam void.

In 1974 significant changes were made to the box-beam design. Standard beams were single-cell 36x17-inch, 36x21-inch, 36x27-inch, 36x33-inch, 36x39-inch, and 36x42-inch except for a solid 36x12-inch box-beam section (Figure 2-8).
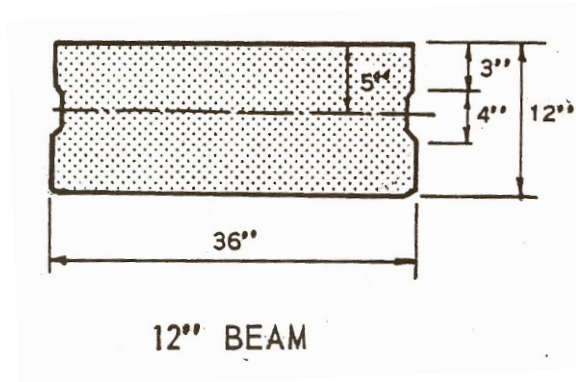


**Figure 2-8: 36x12 solid box-beam section from 1974**

The reinforcement details of the box-beams are shown in Figure 2-9. At this time all the sections contained closed stirrups. The spacing between adjacent beams was increased from ¼-inch to ½-inch.

CENTER FOR STRUCTURAL DURABILITY – Condition Assessment and Methods
of Abatement of Prestressed Concrete Box-Beam Deterioration

21
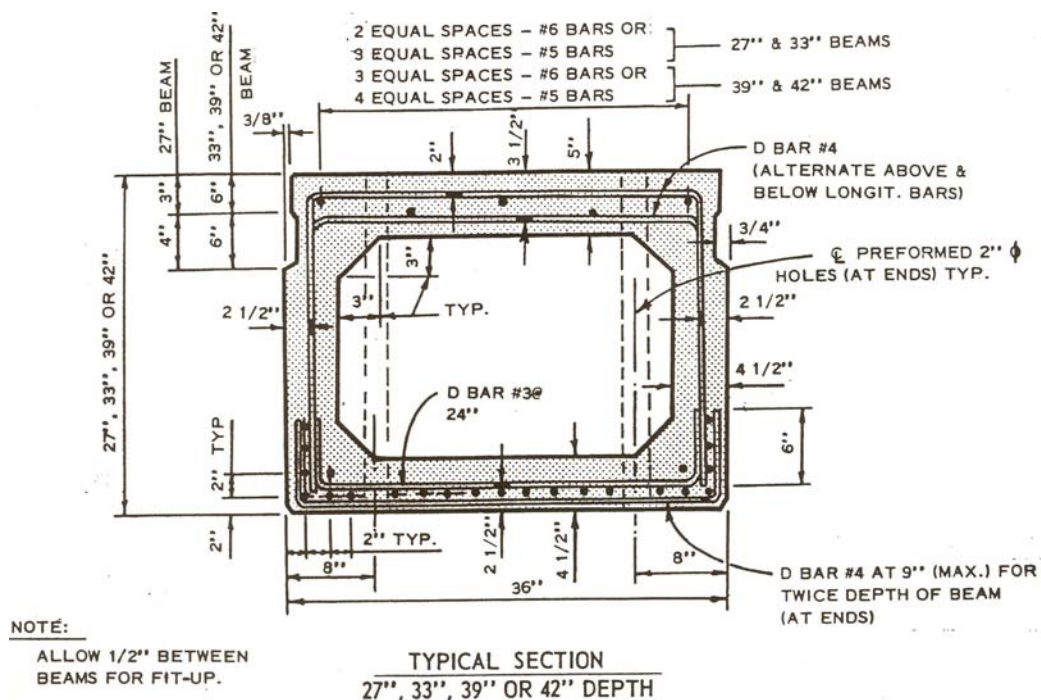
**Figure 2-9: Reinforcement details of box-beams in 1974**

In 1975 the design was updated to introduce bond breaker at the anchorage zone and in 1976 the bearing conditions of the beam were altered.  See Figure 2-10 (a) and (b) for details.
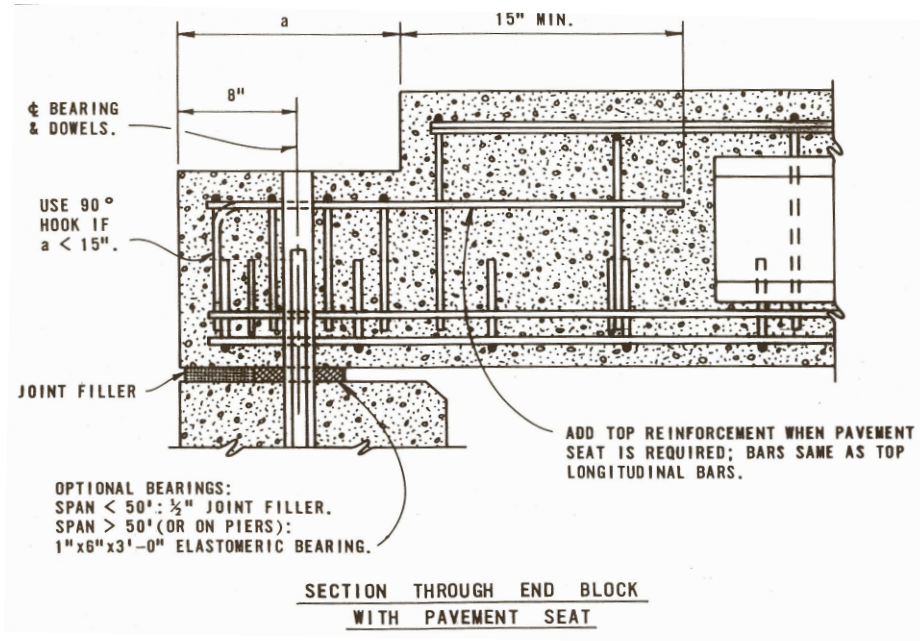


**(a) End block Details**
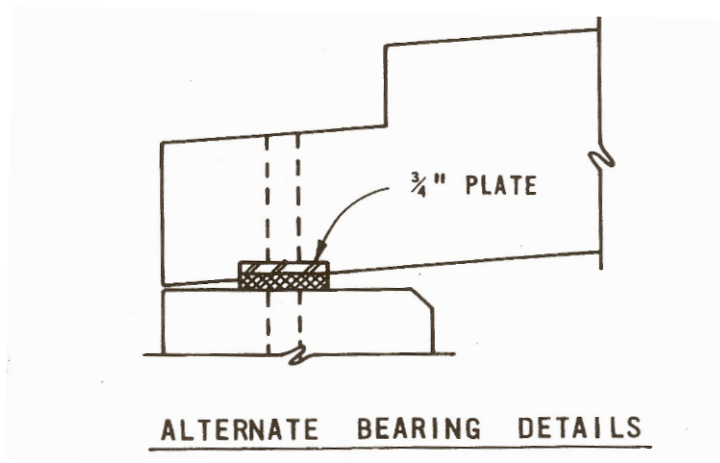


**(b) Alternate bearing details**

**Figure 2-10: End block and alternate bearing details (1976)**

Use of the new bearing conditions stopped in 1977 and the end block design of the box-beam was changed (Figure 2-11).  The end block was changed again in 1979 (Figure 2-12).
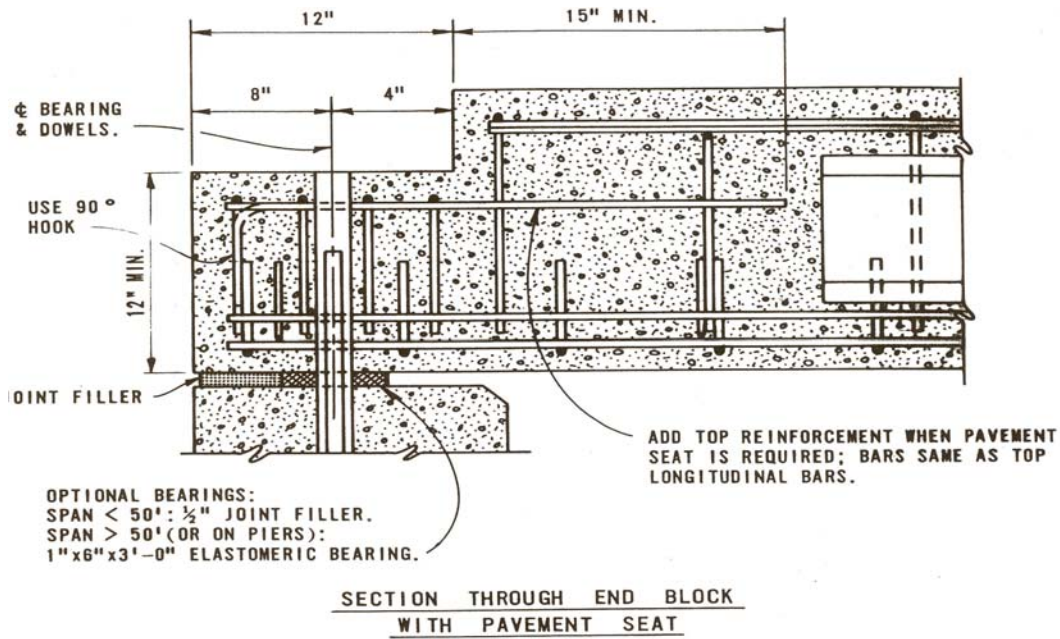
**Figure 2-11: Detailing of end block (1977)**
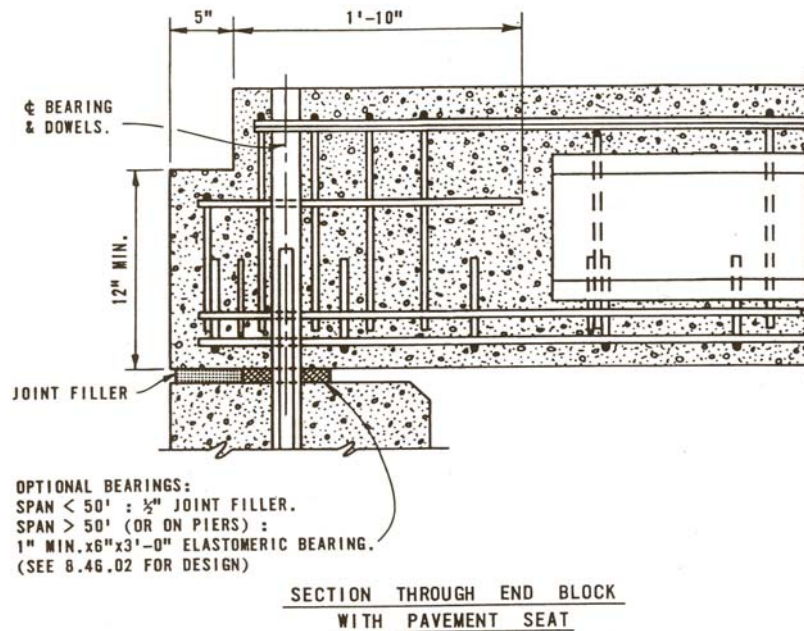


**Figure 2-12:  Detailing of end block (1979)**

In 1983 the transverse post-tensioning force and locations were changed and given in the Table 2-8.  There were also some changes to stirrups and longitudinal reinforcement details.

CENTER FOR STRUCTURAL DURABILITY – Condition Assessment and Methods
of Abatement of Prestressed Concrete Box-Beam Deterioration

23

**Table 2-8: Transverse post-tension force and tendon locations as of 1983 along the beam length**

| Span Length (ft) | Locations | Force/Tendon | |
|---|---|---|---|
| | | HS 20 | HS 25 |
| Up to 50 | 1 at center of span;<br>1 at each end of beam | Span Length 20-36-feet:<br>63 kips<br><br>Span Length over 36-feet:<br>82.5 kips | Span Length 20-36-feet:<br>82.5 kips<br><br>Span Length over 36-feet:<br>104.4 kips |
| Over 50 to 62 | 2 at center of span (11-feet apart);<br>1 at each end of beam | | |
| Over 62 to 100 | 1 at center of span;<br>1 at each quarter point;<br>1 at each end of beam | | |
| Over 100 | 2 at center of span (11-feet apart);<br>1 at each quarter point;<br>1 at each end of beam | | |

In 1985, the shear key dimensions were changed but the available drawings from 1985 did not indicate this particular change. However, post-tensioning tendons were introduced to replace post-tensioning tie rods (Figure 2-13). Post-tensioning forces and the tendon locations along the beam length were also changed in the same year as shown in Table 2-9. The spacing between adjacent beams was increased to 1½ inches and shear keys were grouted to the full-depth.
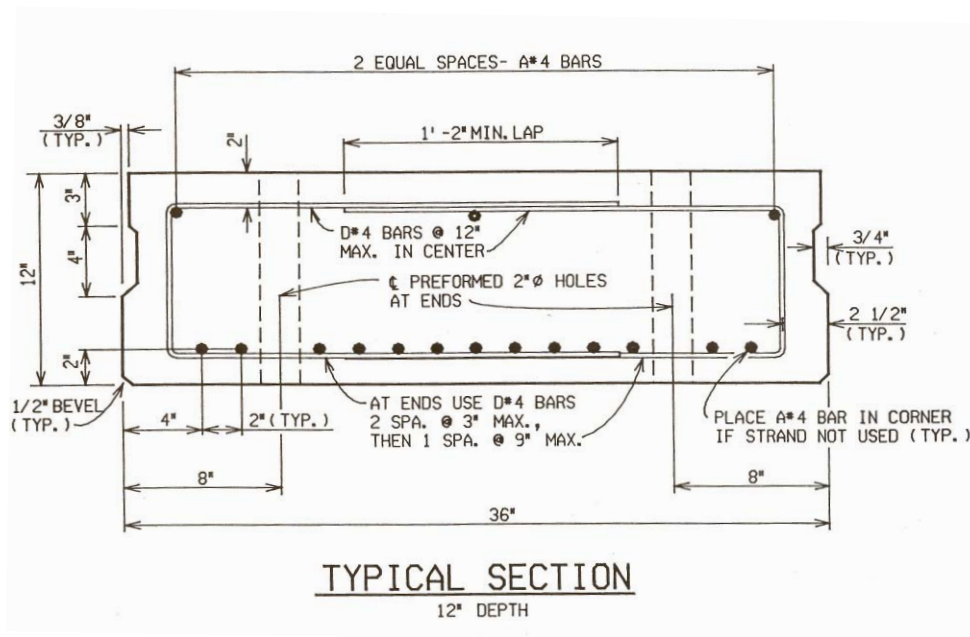


**Figure 2-13: Box-beam section with shear key dimensions (1985)**

**Table 2-9: Transverse post-tension force and tendon locations along the beam length (1985-present)**

| Span Length (ft) | Tendon Locations | Force/Tendon (kips) | |
|---|---|---|---|
| | | HS 20 | HS 25 |
| Up to 50 | 2 at center of span (11-feet apart); 1 at each end of beam. | 82.5 | 104.5 |
| Over 50 to 62 | 1 at center of span; 1 at each quarter point; 1 at each end of beam | | |
| Over 62 to 100 | 2 at center of span (11-feet apart); 1 at each quarter point; 1 at each end of beam | | |
| Over 100 | 1 at each end of beam with 5 equally spaced between | | |

In 1987, in an effort to eliminate longitudinal cracks on the deck surface over the joints between box-beams, the following changes were implemented:

1. To reduce the tendency for the beams to rotate transverse post-tensioned tendons were installed in pairs, top, and bottom, on all decks where the beams are 33 inches deep or deeper.

2. To reduce the shrinkage cracking in the keys, the joints and keyways were filled with type IV grout.

3. The surfacing over the box-beams must be a six-inch thick reinforced concrete slab. Stirrups were projected from the beams into the slab to provide composite design.

As given in Table 2-10 transverse post-tensioning locations along the beam height were specified in 1990.

**Table 2-10: Transverse post-tension tendon locations along the beam height (1990-present)**

| Beam Size | Description |
|---|---|
| 12x36-inch | At each location place 1 tendon 5.5 inches below top of the beam |
| 17x36-inch 21x36-inch 27x36-inch | At each location place 1 tendon at mid depth of the beam |
| 33x36-inch 39x36-inch 42x36-inch | At each location place 2 tendons, 1 at each third point of the beam depth |

In 1993 box-beam sections of 4-feet (48 inches) wide with depths of 21, 27, 39, 42, 48, 54, and 60 inches were introduced (Figure 2-14).

In 2001, bottom flange thickness of the 36-inch wide box-beam was increased from 4.5 inches to 6 inches to provide more cover for double layers of prestressing strands while top flange thickness remains at 5 inches. The top and bottom flange thickness of a 48-inch wide box-beam is 6 inches. The spacing between adjacent box-beams may vary from 1½ to 3 inches.
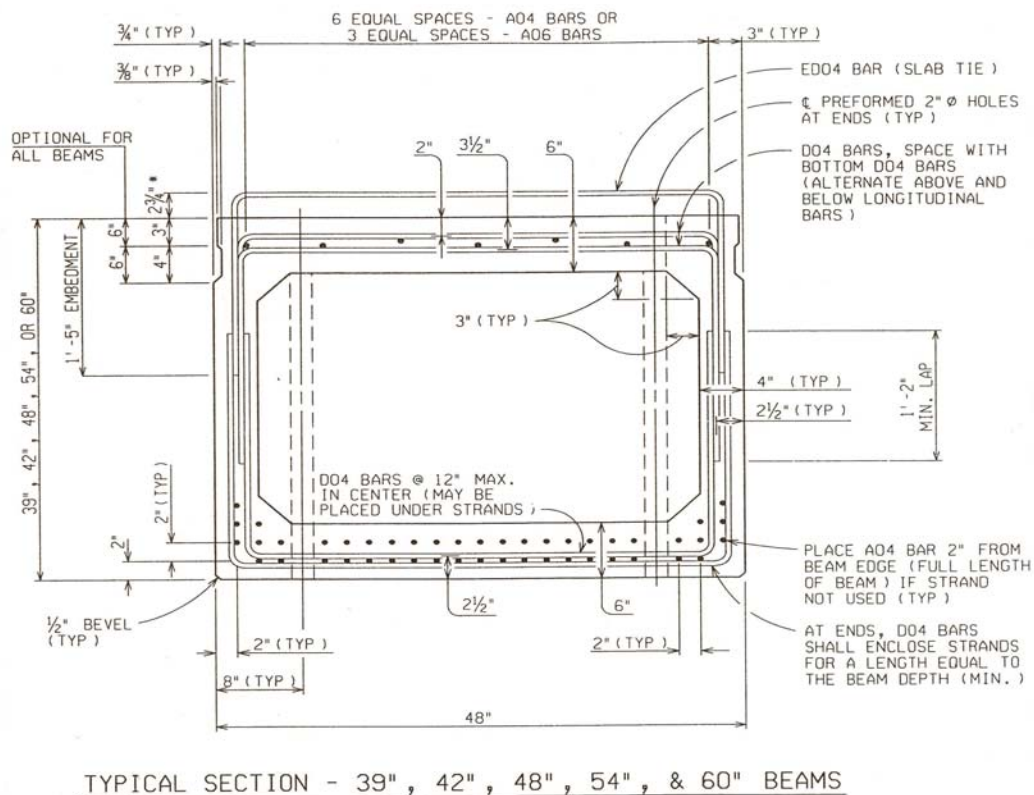


**Figure 2-14: Detailing of typical box-beam section (2001)**

No clear information is available for changes made to the standard box-beam design between 1987 to 1993 and 1993 to 2001. Specifications for the construction of box-beams were updated in 2003, however, the standard box-beam design remains unchanged since 2001.

## 2.5   Durability and Deterioration

There has been great concern about durability, especially in materials for structures that are subjected to harsh environments.  Durability is the ability of concrete to resist weathering action, chemical attack, abrasion, and other service conditions (ACI 1990).  The heightened awareness of the importance of durability is evidenced by the ACI 318 Building Code Requirements for Reinforced Concrete (ACI 1989) that featured a new chapter devoted to the issue of durability.

In a deicing environment, pre- and post-tensioned structures show susceptibility to corrosion at localized points on the structure.  This can occur at end expansion joints separating the deck slab from the approach slab, at joints separating the spans along the length of the bridge, through longitudinal spaces between adjacent box-beams, and at anchorage zones in post-tensioned members.  The actions of traffic and environment lead to joint failure, which allows deicer runoff to pass through the joints onto the pier caps and beam-ends in I-beams, and onto the sides of box-beams.  The ACI 318-89 mandated the latest Post-Tensioning Institute (PTI) standards for improved corrosion protection of unbonded tendons.  Unbonded tendons used in corrosive environments must be completely encapsulated and be further protected with high quality greases.  With an extra layer of protection provided by sheathing, post-tensioned structures are more corrosion resistant than pre-tensioned construction (Whiting et al. 1998).

Environmental conditions are not the only factor behind the potential deterioration of a member.  Durable concrete needs to have a water/cement ratio less than 0.45 and be free of chloride admixtures.  Segregation of the concrete may occur at the bottom of cast members and the resulting 0concrete may lack acceptable durability (Emmons 1994).  Concrete cover over the top of the slab reinforcement must be 2.5 inches, per *AASHTO Standard Specifications 8.22.1* and *AASHTO LRFD 5.12.3*, when exposed to deicers (AASHTO 2002, AASHTO 2004).  The *AASHTO Standard Specifications* (AASHTO 2002) specifies that additional concrete cover beyond the minimum 1.5 inches should be provided for prestressed beams when the contact of deicing agents is unavoidable.

Prestressing steel needs to be cold-drawn wires; quenched and tempered wires are hard and brittle.  Quenched and tempered wires are not approved for use in the United States (Whiting et al. 1993).

CENTER FOR STRUCTURAL DURABILITY – Condition Assessment and Methods
of Abatement of Prestressed Concrete Box-Beam Deterioration

27

In Michigan, the most common environmental conditions that require concrete durability are diurnal thermal cycles, freeze-thaw cycles, exposure to acidic gas (carbon dioxide), and exposure to deicing chemicals (road salt). Other states may experience similar conditions (Enright and Frangopol 2000). It is suggested that concrete deterioration be categorized as dismemberment, dissolution, or erosion (Emmons 1994). Forms of concrete distress can vary widely, including cracking, spalling, delaminations, and minor surface damage (Xanthakos 1996).

### 2.5.1 Observed Distress Types

Boenig (Boenig et al. 2000) conducted inspections and large-scale testing of bridge beams located in Texas which showed premature concrete deterioration. Study of distressed beams indicated direct correlation between premature deterioration and concrete susceptibility due to high cure temperatures, high levels of slowly soluble sulfate, alkali loading of concrete, and reactive aggregates. Cure temperatures are often higher at the solid end blocks and intermediate diaphragms due to the solid mass of concrete at these locations. This may cause these areas to be more susceptible to deterioration. It was found that significant deterioration of susceptible concrete occurred in severe exposure locations. Most damage found during inspections in the Texas DOT project occurred at the beam ends where water could seep through joints and on the exterior faces of outside beams.

Juntunen and Needham studied different types of distress in prestressed box-beams in Michigan and discussed the causes and effects of each (Needham and Juntunen 1997). During this study chloride samples were taken from seven box beam structures and five I-beam structures to determine if the chloride concentration in a representative number of typical prestressed beams is high enough to initiate corrosion in the beams. The procedure for selecting bridges is not described in the report. Based on the investigation of chloride content in box-beam bridges, Needham and Juntunen concluded that the condition of the box-beam bridges on county roads is better than those on state trunklines. The reason is likely due to decreased traffic loads and less chemical deicers applied to county roads. The investigation revealed that chloride contamination is primarily the result of leaky joints and filtration of water through the deck. The study results indicate that the ends of the box-beams exhibit greater deterioration than the interior (Needham

and Juntunen 1997).  The examples of distress types in prestressed box-beams are summarized in Table 2-11.

**Table 2-11: Observed distress types in prestressed box-beams (Needham and Juntunen 1997)**

| Types of Distress | Description |
| --- | --- |
| Long horizontal crack in the web of the beam | The crack is caused by the foam void shifting during fabrication, causing the beam web to be too thin on one side. Restraint shrinkage is likely the cause of horizontal cracking. |
| Map Cracks | The map cracking in the sides of a prestressed box-beam was caused by the foam void shifting during fabrication, causing the beam web to be too thin on one side. |
| Horizontal cracks | The horizontal and frown faced cracks sometimes found in the end of prestressed box-beams are caused by the restraining effect of unreleased strands as the beam shortens from partial prestress and from shear generated by the cutting orders of the strands. |
| Longitudinal deck cracks | |
| Longitudinal cracks at the bottom of the beam | Longitudinal cracks are found running along the bottom of side-by-side box-beam. The shear stirrup did not extend across the bottom flange, thus there was no support for this type of cracking. |
| Shear cracks | Shear cracks in prestressed beams are a serious sign of distress of the beam. The beam may be overloaded or it may not have adequate reinforcement. Sometimes shear cracks turn and run horizontally where box-beam's web meets the bottom flange. |
| Moisture along interior beams and at beam ends | The greater deterioration at the beam-ends is found than the interior of beams due to salt laden water leaking from the joints over the supports. |
| Corrosion stained cracks | Corrosion stained cracks on the bottom flange are found in the locations of beam having prestressing strands. |
| Tendon break | Usually this type of distress is observed at the box-beam-ends due to corrosion of prestressing tendons. |
| Spalling of concrete | Heavily corroded prestressing tendons caused spalling of concrete at the locations of beam having prestressing tendons. |

CENTER FOR STRUCTURAL DURABILITY – Condition Assessment and Methods
of Abatement of Prestressed Concrete Box-Beam Deterioration

### 2.5.2 Cracking

Cracks in prestressed concrete are more critical than for conventional reinforced concrete because the cracks allow moisture and chloride to reach the prestressing strands. Cracks in prestressed beams could indicate that loads are greater than anticipated on the structure, the beam is not properly reinforced, the prestressing strands were released prior to the concrete reaching minimum strength, or loss of prestress has occurred. However, not all cracks in prestressed beams are structural. Some cracks are caused by shrinkage of the concrete, improper curing of the concrete, and some cracks are caused by the procedures used to prestress the beams (Juntunen 2000).

NHI (National Highway Institute) Course No. 13055, *Safety Inspection of In-service Bridges* classifies cracks in prestressed beams as follows:

- Hairline: less than 0.004 inches (0.1mm)
- Narrow: 0.004 to 0.009 inches (0.1 to 0.23mm)
- Medium: 0.010 to 0.030 inches (0.25 to 0.76mm)
- Wide: greater than 0.030 inches (0.76mm)

### 2.5.3 Thermal Distortion

Nearly all Michigan bridges are situated in a location that allows fascia beams to be exposed to uneven (diurnal) solar heating. Like many materials, concrete expands when heated and shrinks when cooled. Having a temperature differential on an element such as a prestressed concrete box-beam would cause expansion on the outward-facing side and induce weak-axis bending stresses. Fixity of the top flange may cause an out-of-plumb condition for the beam web and induce additional stress into the member. A partially fixed beam end, such as one created by a frozen bearing may impose additional stress at the beam end. When stress build-up is relieved, tension cracks, shear cracks, or buckling may result (Emmons 1994). The coefficient of thermal expansion of the concrete and freedom from restraint affect the amount of thermal distortion related distress.

### 2.5.4 Freeze-Thaw Deterioration

Without entrained air, the cement matrix surrounding the aggregate particles may fail when it becomes critically saturated and frozen (ACI 1992). Freeze-thaw deterioration is

CENTER FOR STRUCTURAL DURABILITY – Condition Assessment and Methods
of Abatement of Prestressed Concrete Box-Beam Deterioration

31

a function of porosity, moisture saturation, number of freeze-thaw cycles, air entrainment, member surface, and aggregate quality (Emmons 1994). An important fact to consider regarding freeze-thaw damage is that concrete which is dry or contains only a small amount of moisture is essentially not affected by even a large number of cycles of freezing and thawing (Kosmatka and Panarese 1988). Evidence of freeze-thaw deterioration is usually in the form of small surface disintegration (Emmons 1994). Freeze thaw damage is resisted by proper structure design to minimize exposure, low water-cement ratio (w/c), appropriate air entrainment, quality materials, adequate curing, and special attention to construction practices (ACI 1992).

### 2.5.5   Corrosion-Induced Deterioration

Corrosion of prestressing steel is one of the most destructive deterioration mechanisms for prestressed concrete bridges in the United States (Whiting et al. 1993). An improved understanding of the influence of corrosion damage upon structural performance would assist owners and operators of structures to plan strategic, cost-effective remedial treatment (Cairns and Millard 1999). Corrosion can be generally defined as the deterioration of a substance or its properties because of a reaction with its environment (NACE 1970).

Numerous references were reviewed to gain an understanding of how steel reinforcement and prestressing steel corrode inside the concrete. Two types of corrosion are generally recognized in prestressed concrete: stress corrosion and pitting corrosion (Whiting et al. 1993; Leonhardt 1964). Pitting corrosion is a localized form of galvanic corrosion (Novokshchenov 1989). Pitting corrosion is most prevalent in reinforced concrete and prestressed concrete structures. Concrete carbonation (reaction of carbon dioxide and calcium hydroxide to form calcium carbonate; $CaOH + CO_2(aq) \rightarrow CaCO_3 + H^+$) and chloride ion penetration (from deicing salts) are the two primary causes of pitting corrosion. The presence of sufficient chloride ion with water, oxygen, and a corrodible metal leads to pitting corrosion. Carbonation reduces the alkalinity in the concrete and may lead to hydrogen embrittlement type of stress corrosion (Whiting et al. 1993). Stress corrosion cracking of chloride-laden concrete is unlikely to occur (Moore et al. 1970). Research by Legat et al. showed that corrosion is mainly due to high concentrations of

chlorides and in a few cases the carbonization of concrete (Legat et al. 1996). Detailed discussion of carbonation-induced corrosion and deicer-induced corrosion of reinforcing steel and prestressing steel from an extensive literature search have been included in the earlier published report MDOT RC-1412 *Causes and Cures for Prestressed Concrete I-beam End Deterioration* (Ahlborn et al. 2002).

## 2.6    Tools for Identifying Prestressed Box-Beam Deterioration

### 2.6.1    Inspection /Assessment Techniques

From the suggestion of other researchers (Shanafelt and Horn 1980) and for the purposes of this report, the term *inspection* is used to refer to the physical act of obtaining data on the condition of a structural element. *Assessment* is defined as the process of reviewing or making an interpretation of (inspection) data/conditions, structural analysis, and other decision-making processes.

Both assessment and inspection practices are discussed in this section. As an example, the *Pontis Bridge Inspection Manual* (MDOT 1999) has defined assessment criteria for an inspector to follow for assigning a condition state and potential feasible actions. In contrast, the *Michigan Structure Inventory and Appraisal Coding Guide* (MDOT 2003d), used for National Bridge Inspection Standards (NBIS), allows for greater latitude in assigning condition ratings to a structural element. In this case, assessment is left to the judgment of the bridge inspector.

#### 2.6.1.1    Current Approaches

*FHWA Bridge Inspectors Training Manual 90* (Hartle et al. 1995) is the current standard for inspecting bridges and generally covers bridge mechanics, materials, and inspection practices. Guidelines are established to aid the bridge inspector in defined tasks.

The tools for cleaning, inspection, visual aid, measuring, and documentation that many states use for inspecting prestressed concrete box-beams are covered in Manual 90. Included in this list are chipping hammers, mirrors, and optical crack gauges. Conventional non-destructive evaluation equipment (pachometers, ultrasonic thickness gauge, etc.) is not part of the bridge inspector's equipment (Hartle et al. 1995).

CENTER FOR STRUCTURAL DURABILITY – Condition Assessment and Methods
of Abatement of Prestressed Concrete Box-Beam Deterioration

33

Shanafelt and Horn identified similar tools that aid in the inspection of damaged prestressed concrete beams including a magnifying glass, flashlight, camera, and mirror (Shanafelt and Horn 1980). In addition to physical tools used by an inspector, good eyesight and a critical mind are essential personal qualities.

Photography is one of the technologies included in Manual 90. The Tennessee Department of Transportation (TDOT) Bridge Inspection and Repair Office conducted an evaluation of the feasibility of using digital cameras to replace conventional cameras (FHWA 1997). Digital cameras are greatly enhancing the usefulness of bridge inspections, since state-of-the-art computer programs allow engineers in the office to quickly view the conditions of a bridge at the time the last inspection was performed.

Manual 90 provides inspection procedures for prestressed concrete box-beams. The inspection of a box-beam bridge requires a clear understanding of the beam function. This requires a thorough review of design and as-built drawings prior to the inspection and a realization of the high stress regions of the structure (Hartle et al. 1995).

The following is an excerpt from the Manual 90 basic concrete inspection section (Section 5.4.2):

> *When inspecting concrete structures, note all visible cracks, recording their type, width, length, and location. Any rust or efflorescence stains should also be recorded. Concrete scaling can occur on any exposed face of the concrete surface, and its area, location, depth, and general characteristics should be recorded. Inspect concrete surfaces for delamination or hollow zones, which are areas of incipient spalling, using a hammer or a chain drag. Delamination should be carefully documented using sketches showing the location and pertinent dimensions.*
>
> *Unlike delamination, spalling is readily visible. Spalling should also be documented using sketches, noting the depth of the spalling, the presence of exposed reinforcing steel, and any deterioration or section loss that may be present on the exposed bars.*
>
> *There are many common defects that occur on concrete bridges: cracking, scaling, delamination, spalling, chloride contamination, honeycombs, pop-outs, wear, collision damage, abrasion, overload damage, reinforcing steel corrosion, prestressed concrete deterioration.* (Hartle et al. 1995, pg. 5-13)

Each of these distresses is defined in Manual 90. Cracks can be classified as hairline, narrow, medium, or wide cracks. On prestressed concrete structures, all cracks are significant. When reporting cracks, the length, width, location, and orientation (horizontal, vertical, or diagonal) should be noted. The presence of rust stains or efflorescence or evidence of differential movement on either side of the crack should be indicated.

The manual has an eleven-step inspection procedure for prestressed concrete box-beam bridge structures (Section 9.3.2, pg. 9-25):

- *The top of the beam-ends should be examined for horizontal or vertical cracks. These cracks indicate a deficiency of reinforcing steel. These cracks are caused by the stresses created at the transfer of the prestressing forces.*
- *Investigate the lower portion of the beam, particularly at mid-span, for flexure cracks. This indicates a very serious problem resulting from overloading or loss of prestress.*
- *Examine the sides of the beams for cracks. Adjacent box-beams side surfaces are visible only on the fascias. For interior beams, inspect the bottom chamfers for cracks, which may extend along the sides of the beams.*
- *Inspect beams near the supports for vertical cracks, which may be caused by restricted movement by the bearing assemblies.*
- *Check the bottom of beams for parallel cracks that originate from the bearing location.*
- *Investigate the beam for any evidence of sagging. This indicates a loss of prestress.*
- *Inspect at the end of beams for shear cracks.*
- *Examine between boxes in adjacent box-beam bridges for leakage. Look for reflective cracking in the traffic surface and individual beam deflection under live load. These problems indicate that the shear key between boxes has been broken and the boxes are acting independently of each other.*
- *Check areas damaged by collision. A significant amount of prestressed concrete bridge deterioration and loss of section is due to traffic damage. The loss of concrete due to such an accident is not always serious, but it can be, depending on the amount and the location of the section loss.*
- *Investigate underneath boxes for excessive deflection and misalignment. Movement of a bridge can be either catastrophic or of minor concern, depending on the amount and direction of the movement.*
- *On older bridges, verify that void drain holes are open.*

CENTER FOR STRUCTURAL DURABILITY – Condition Assessment and Methods
of Abatement of Prestressed Concrete Box-Beam Deterioration

35

In terms of assessment, Manual 90 requires that inspectors rate bridge elements, including prestressed concrete box-beams, as a whole, rather than allowing individual locations of distress to lower an element's rating. However, inspectors are expected to modify the condition rating accordingly if an isolated distress influences the load carrying capacity or serviceability of the element (Hartle et al. 1995). Manual 90 does not have a uniform damage severity classification for various concrete distresses. Shanafelt and Horn suggest ranking damage assessment into four categories: minor, moderate, severe, and critical (Shanafelt and Horn 1980).

One recent study revealed significant variability from state to state on assigned condition ratings and field notes. In 1998, the FHWA's Nondestructive Evaluation Validation Center undertook a study to evaluate visual inspection of bridges (Graybeal et al. 2001). The Center performed a series of inspection trials among 49 state departments of transportation bridge inspectors. The bridges used in this study were located in northern Virginia and central Pennsylvania. "The primary data used to evaluate the routine inspections were the National Bridge Inspection Standards Condition Ratings assigned by the inspectors to the primary bridge components (deck, superstructure, and substructure)." In-depth inspections were rated on the inspector's field notes. The study showed a significant variability from state to state on assigned condition ratings and field notes. The Center's recommendations were to revise the condition rating system to increase accuracy and reliability, increase the training of inspectors with respect to methods that identify reoccurring defects, and study the types and sizes of specific defects that will be found in an in-depth inspection.

Other studies have been performed to determine current policies and practices that may affect the accuracy and reliability of visual inspection. A survey of state departments of transportation, a local-level department of transportation, and selected bridge inspection contractors showed how inspection management might influence the reliability of inspections (Rolander et al. 2001).

Effects of the deterioration should be understood through engineering assessments (Shanafelt and Horn 1980). For accidental impact damage of prestressed concrete bridge

beams, Shanafelt and Horn do not recommend field assessment of damage, due to the potential for making premature assessments. More innovative repair techniques appear to be generated by having repair assessments be office-based, away from the field process. However, ideas and alternatives for repair are suggested by the field inspector. Shanafelt and Horn concluded that complex engineering calculations were not required to develop in-place repairs, but that a basic level of calculations should be performed to verify restoration of strength and durability (Shanafelt and Horn 1980). Xanthakos developed procedures for performing a capacity analysis of a prestressed concrete beam, considering compromised prestressing strands (Xanthakos 1996).

Shanafelt and Horn provide recommendations for assessment of exposed, damaged, and severed strands (Shanafelt and Horn 1980). Nearly all states allow beams with one to three severed strands to remain in service. Location of a damaged beam within a structure should be given consideration in the assessment stage. For example, fascia beams may not be loaded to the same levels as internal beams and therefore a greater amount of deterioration may be permitted (Shanafelt and Horn 1985).

### 2.6.1.2 New Approaches

A manual of recommended practice for the inspection, assessment, and repair of deteriorated prestressed concrete bridge beams has been developed within NCRHP Report 280 (Shanafelt and Horn 1985).

A rivet gun chipper is a tool that may be used by inspectors to evaluate the quality of concrete around a prestressing strand (Shanafelt and Horn 1985). Deflection and elastic shortening techniques have been used in the past to estimate tension in exposed prestressing strands.

To evaluate box-beams for a New York State DOT project, engineers used techniques consisting of visual examination, counting broken/deteriorated/corroded strands, and measuring remaining concrete section (Hag-Elsafi and Alampalli 2000).

In addition to a visual inspection, Whiting et al. used a variety of survey techniques for a research project involving the inspection of prestressed concrete bridges (Whiting et al.

CENTER FOR STRUCTURAL DURABILITY – Condition Assessment and Methods
of Abatement of Prestressed Concrete Box-Beam Deterioration

37

1993).  These techniques included half-cell potential measurements, delamination survey, cover measurements, corrosion rate measurements, petrographic analysis, chloride sampling and analysis, and penetrating sealer effectiveness.  Techniques showing results fairly consistent with prestressed concrete I-beam end deterioration included half-cell potential measurements, corrosion rate measurements, and chloride sampling.   The deicer-environment bridges reviewed by Whiting et al. generally had deterioration consisting of cracked and spalled concrete with exposed corroding strand and stirrups (Whiting et al. 1993).

Similar techniques were chosen by Arner and Panganiban and  by Kennedy for the investigation of deteriorating bridge decks (Arner and Panganiban 1986) and (Kennedy 1991).  These techniques included half-cell potential testing, cover measurements, and chloride ion content testing.  Arner and Panganiban suggested that delaminations could affect half-cell potential testing by creating an insulating plane in the concrete (Arner and Panganiban 1986).

Monterio et al. studied a nondestructive method using a multi-electrode electrical resistivity array to determine the position of the reinforcing bars and their corrosion state (Monterio et al. 1998).   This work was performed by measuring the frequency dependence of the complex impedance of the bars along the surface of the concrete structure.  By using this method, the background resistivity of the concrete can also be obtained.  The method uses the direct relation between the complex impedance and the corrosion rate of the reinforcing bars to provide a rapid evaluation of the corrosion rate.  Two advantages of the technique are that the measurements are taken on the surface of the concrete and that the method does not require removal of the concrete to connect the device to the bars.  An experiment was conducted to test and determine the efficiency of the method.  Four types of bars were used in the research which included a clean bar, a bar covered with gold, a painted bar, and a corroded bar.  Zhang et al. conducted similar research and concluded that the surface measurement method is agreed to be an accurate method to investigate different corrosion states of the reinforcement (Zhang et al. 2001).

New tools are available not only for the inspection of original bridge elements, but also for monitoring the performance of these repairs. (Halstead et al. 2000) used strain gauges to monitor potential cross-sectional growth of strengthened columns due to the corrosion of reinforcing steel (expansive process). Linear polarization probes were also included in the instrumentation package to measure corrosion rate of internal reinforcement.

(Broomfield et al. 1999) studied corrosion monitoring using half-cell potential measurement, linear polarization, and macro-cell current measurement methods. Linear polarization, concrete resistivity and other probes have been installed in new structures to monitor durability as well as in existing structures to evaluate rehabilitation strategies such as corrosion inhibitor applications and patch repairs.

Data obtained from nondestructive evaluation (NDE) of structures can greatly enhance the maintenance and management of infrastructure systems. Nogueira has proposed a methodology for a systematic application of NDE methods in periodical bridge inspection (Nogueira 1999).

Tinkey, et al. researched non destructive testing techniques on prestressed bridge beams experiencing distributed damage (Tinkey, et al. 2000). This project was a continuation of the Texas DOT program worked on by (Boenig et al. 2000). The authors concluded that the first damage assessment conducted on a beam should be visual in nature and, if it is determined to be necessary, followed by other forms of non-destructive testing. It was found that Acoustic emission tests performed well for evaluating the amount of distributed damage in concrete. Impact-echo testing showed encouraging results, however the resulting test data was somewhat subject to the interpretation of the researcher. It was recommended that a standard procedure be established for this test method prior to implementation of the test. The final test method employed was short-pulse radar which did not adequately detect distributed damage within the beams studied.

Pascale et al. described an experimental program aimed to assess the performance of fiber optic sensors (FOS) in civil engineering applications (Pascale et al. 1999). This technique has been applied to a reinforced concrete bridge beam externally reinforced by fiber reinforced polymer (FRP) sheets. Pascale et al. recommended using fiber optical

sensors for long term monitoring because of cost and very good repetitiveness (Pascale et al. 1999).

NDE for corrosion detection of embedded or encased steel reinforcement or bridge cables using time domain reflectometry was developed and demonstrated (Liu et al. 2001).

In the paper presented by Titman, wide ranges of applications of infrared thermography are explored, particularly relating to structural investigation situations (Titman 1999). Some guidance is given on optimum timing, environmental conditions, and viewing locations for the various situations.

Settipani has shown that gammagraphy can be used to determine strand location, size, corrosion, and concrete defects (Settipani 1987). This technique has shown to be effective on elements 27 inches and less in thickness. According to Settipani, gammagraphy has a high initial cost compared to other non-destructive evaluation methods, but it provides more comprehensive data and a permanent inspection record (Settipani 1987).

Innovative ways to detect concrete delaminations have emerged in recent years. (Henderson et al. 2000) reported that an instrument named Hollow-Deck is an alternate approach to acoustic impact surveys. The technology used involves frequency analysis of sound waves to identify areas of concrete delamination.

(Ganji et al. 2000) and (Gucunski et al. 2000) have performed similar testing using a portable seismic pavement analyzer (PSPA). With the PSPA, (Ganji et al. 2000) were able to detect delaminations not found by chain dragging on bridge decks. (Gucunski et al. 2000) were able to place delaminations into four severity levels by interpretation of surface waves.

Due to the size of the PSPA and the time it takes to complete a single test, the PSPA appears to show little promise for use in prestressed concrete I-beam end inspection. Hollow-Deck technology appears to be similarly inappropriate for beam end inspection. However, non-destructive testing equipment like the Hollow-Deck and PSPA could be

used as calibration and training tools for inspectors performing acoustic impact (delamination) surveys. (Gucunski et al. 2000)

A useful tool in performing assessments of beam deterioration is the understanding of how distresses may have formed. Juntunen prepared a draft report containing description of observed distress in prestressed concrete box-beams (Table 2-11) (Juntunen 2000).

NDE techniques discussed in this section are summarized in Table 2-12.

**Table 2-12. Summary of NDE Techniques**

| NDE Technique | Purpose/ Investigation | Author and/or Agency |
|---|---|---|
| Rivet gun chipper | Concrete quality around prestressing strands | Shanafelt and Horn 1985 NCRHP Report 280 |
| Visual inspection | PC box-beams and I-beam end conditions | Hag-Elsafi and Alampalli 2000, New York State DOT Whiting 1993 Novokshchenov 1989 |
| Half-cell potential measurements | PC I-beam end and bridge decks deterioration | Whiting 1993 Arner and Panganiban 1986 Kennedy 1991 Broomfield 1999 |
| Cover measurements | PC I-beam end and bridge decks deterioration | Arner and Panganiban 1986 Kennedy 1991 Whiting 1993 |
| Corrosion rate measurements | Corrosion state of PC bridge elements | Whiting 1993 Novokshchenov 1989 |
| Petrographic analysis | PC I-beam end deterioration | Whiting 1993 |
| Chloride sampling and analysis | PC I-beam end deterioration | Whiting 1993 |
| Penetrating sealer effectiveness | PC I-beam end deterioration | Whiting 1993 |
| Chloride ion content testing | Condition state of deteriorating bridge decks | Arner and Panganiban 1986 Kennedy 1991 |
| Surface Measurement Method | Rebar location, corrosion state, and resistivity of concrete | Monterio 1998 Zhang 2001 |
| Strain gages | Potential across sectional growth of strengthened columns | Halstead 2000 |
| Linear polarization | Corrosion monitoring | Broomfield 1999 |
| Macro-cell current measurement methods | Corrosion monitoring | Broomfield 1999 |
| Acoustic emission | Amount of distributed damage in concrete | Boenig 2000 Tinkey 2000 Texas DOT |
| Impact-echo testing | Amount of distributed damage in concrete | Boenig 2000 Tinkey 2000 Texas DOT |
| Fiber optic sensors (FOS) | Performance of FOS in civil engineering applications | Pascale 1999 |
| Time domain reflectometry | Corrosion detection of steel reinforcement or bridge cables | Liu 2001 |
| Infrared Thermography | Wide ranges of applications | Titman 1999 |
| Gammagraphy | Strand location, size, corrosion and concrete defects | Settipani 1987 |
| Hollow-Deck | Concrete delaminations | Henderson 2000 |
| Portable seismic pavement analyzer | bridge decks delaminations | Ganji and Gucunski 2000 |

## 2.7  Effects of Premature Deterioration on Concrete Box-Beam Bridges

Boenig et al. (2000) conducted large-scale testing of bridge beams located in Texas which showed premature concrete deterioration.  The team inspected structures experiencing premature concrete deterioration, tested core samples, and conducted large scale tests of laboratory specimens in an effort to predict the capacity of insitu bridge beams showing various signs of deterioration.

The study found the concrete compressive strength to be strongly correlated to the damage index of a beam.  The damage index was assessed by summing the length times the square of width for all cracks found on the beam.  Core samples were taken at several locations of varying damage and tested to determine compressive strength.  A figure was then produced to correlate damage index to compressive strength.  This method could be used as a preliminary means of estimating the compressive strength of the deteriorated concrete.  The adjusted compressive strength should then be incorporated into ACI equation 11-2 to estimate the shear strength of the beam. If necessary, core samples should be taken from the worst section in a beam to assess the compressive strength in lieu of an estimate based on the damage index (Boenig et al. 2000). However, the Windsor Probe test method recommended as a non-destructive test method by ASTM C803 is more convenient to measure insitu concrete strength.  The Windsor Probe Test System drives a steel probe through a template into the concrete surface where aggregate particles are cracked and compressed. The zone and depth of penetration by the probe are correlated to the psi of the concrete's compressive strength.

Boenig et al. (2000) found that flexural capacity of the distressed beams was not significantly lower than undamaged beams due to the locations of deteriorated concrete. Deterioration was found primarily at the beam ends, little damage was found in the compression chord in the maximum moment region, and strands did not experience slippage.  Deterioration of the beam ends did, however, cause reduction in the shear capacity by 14%.  It may be possible for shear failure of beams due to overloads (Boenig et al. 2000).  The extent of deterioration of the tested beams fall under FHWA rating 4 or box-beam rating D or E (see Table 4.2).  However, the test was performed on beams with

CENTER FOR STRUCTURAL DURABILITY – Condition Assessment and Methods
of Abatement of Prestressed Concrete Box-Beam Deterioration

43

cracks appearing on webs of the beams which are difficult to inspect on in-service bridges due to concealed sides of the beams.

Roche et al. conducted the third part of the Texas DOT study on premature concrete deterioration with a study of prestressed concrete box-beams failing in shear (Roche et al. 2001). This team conducted fatigue tests on two full-scale box-beams with premature deterioration in the concrete due to delayed ettringite formation and alkali-silica reaction. The tests were set up such that the beams would fail in shear. The test data resulted in the formulation of a shear versus load cycles to failure graph which may be used to predict the service life of a concrete box-beam with premature deterioration. The tests found that failure occurred after shear cracks opened due to progressive deterioration and that the failure mode was fatigue of the shear reinforcement in tension and transverse bending and/or debonding of shear reinforcement near the cracks. Shear fatigue failure of the deteriorated concrete beams was found to be unlikely if the level and range of stress in the shear reinforcement is kept below the endurance limit of the steel. Slip of the prestressing strands does not appear to be a cause of shear fatigue failure. The first reason for this is that the end block of prestressed concrete box-beams is solid and extends into the beam a distance greater than the transfer length of the prestressing strand. Secondly, the end reaction on the beam causes a transverse clamping force to pinch the strands and increase the frictional resistance between the strand and the concrete. It is difficult to calculate the nominal shear strength of prestressed concrete beams after diagonal shear cracks appear. Hence, it is conservative to assume that the nominal concrete shear strength of cracked beam equals zero for the purpose of analyzing shear strength of the beam.

The fourth report in the series of research conducted by the Texas DOT, authored by Memberg et al (2002). provided information on damage indices and strand pullout tests. In studying the bond strength between prestressing strands and deteriorated concrete it was found that the mean average bond strength was about 60% that for sound concrete. The capacity of the prestressed beams was found to not be limited by this reduction in bond strength. No bond failure was observed in any of the full-size beam tests conducted in this research. Three mechanisms were found to describe the interaction between

concrete and prestressing strand. Before the strands start to slip, bond between the strands and concrete unite the two materials. After the bond is broken, the interface must rely on friction between the two surfaces and the physical constraint caused by the shape of the strands which must twist out of the concrete. While beams may display cracking on the surfaces, the extent to which the cracks propagate inward cannot be visibly determined. For this reason it is hard to assess the interior damage to a beam and therefore the likelihood that strand pull out may be of concern. Memberg et al. (2002) recommended a procedure for assessing the reduced pullout capacity of prestressing strands with premature concrete deterioration. The procedure requires an inspector to measure the crack widths and lengths. This data is applied to damage indices to determine a reduced pullout capacity.

## 2.8  Repairs to Deterioration of Concrete in Box-Beam Bridges

Vaysburg et al. discussed many items which an engineer must consider while determining the proper material and procedure for making repairs to concrete structures (Vaysburg et al. 2004). The authors discussed the importance of complementing properties between the existing materials and the repair materials. Properties of significance are: relative shrinkage, thermal expansion differential, differences in creep properties, and relative fatigue performance between new and existing material. Differences in stiffness and Poisson's ratio can cause interface stresses due to unequal load sharing and strains between the repair and the original material.

Roche et al. made several recommendations to help reduce the rate of deterioration of distressed box-beams (Roche et al. 2001). Cracks in concrete beams should be sealed to prevent corrosion of the strand and reinforcing steel. The sealant used in wide cracks should be flexible while narrow cracks should be filled with a low viscosity, crack penetrating sealant. Equally important to the sealing of cracks is providing a maintenance program which keeps the cracks sealed. As part of the inspection process, it is recommended that select areas of a deteriorating beam be carefully measured and recorded to determine the rate of deterioration over time.

CENTER FOR STRUCTURAL DURABILITY – Condition Assessment and Methods
of Abatement of Prestressed Concrete Box-Beam Deterioration

45

Memberg et al. found that field observations determined that crack sealants proved ineffective in stopping cracks from further propagation (Memberg et al. 2002). Surface and injected sealants, though not eliminating further deterioration, appeared to slow crack growth. The effectiveness of the sealants is unknown because the rates of deterioration prior to and after treatment were not available.

# Chapter 3:    Pontis Data Analysis and Selection of Bridges

## 3.1   Overview

Bridge management in Michigan is performed using a relational database integrated under a software program called "Pontis" (version 4.2 – updated February 17, 2004). Pontis was developed by the U.S. Federal Highway Administration (FHWA), and is licensed through the American Association of State Highway and Transportation Officials (AASHTO) to more than 45 state highway agencies and other agencies nationally and internationally. Pontis stores complete bridge inventory and inspection data, including detailed element conditions. The Michigan information was analyzed in order to select 15 bridges from across the state for detailed investigations of distress types or deterioration of side-by-side prestressed concrete box-beam bridges.

## 3.2   Pontis Data Analysis

Pontis data analysis of Michigan structures indicates that there are 12,638 bridges in Michigan. Of these 12,638 bridges, Michigan Department of Transportation (MDOT) is the owner and has the maintenance responsibility of 5,797 bridges. Local agencies are responsible for the remaining 6,841 bridges. There are a total of 2,054 side-by-side prestressed concrete box-beam bridges in Michigan. Of these, 236 are on the National Highway System (NHS) thus, under the responsibility of MDOT. Appendix A, Table A-1 contains information on the location and geometrical attributes of these 236 side-by-side prestressed concrete box-beam bridges.

According to the Pontis database, in 1955 the first side-by-side precast prestressed concrete box-beam bridge was built in Michigan. Bridges with year built before 1955 were not originally side-by-side prestressed concrete box-beam bridges. They were most likely of another design type and have been replaced by the side-by-side prestressed concrete box-beams in or after 1955. Therefore, it is logical to use the year reconstructed as the year built for those bridges built before 1955. The year reconstructed was also used as the year built when the bridge superstructure was replaced. The histogram of these 236 bridges built

between 1955 and 2003 is shown in Figure 3-1. An inventory of MDOT owned box-beam bridges is located in Appendix A, Table A-1.

One of the objectives of this project was to select and inspect 15 bridges from the side-by-side prestressed concrete box-beam bridges that are on the NHS. Pontis 4.2 and InfoMaker 9.0 were both used to assist in the selection of bridges. InfoMaker 9.0 was used to query the information needed for selecting bridges for inspection. The Michigan Structure Inventory and Appraisal Coding Guide was used for decoding the information given in the tables. To help aid in the selection of bridges, many queries were performed to obtain the fleet parameters and location attributes of box-beam bridges. The results of the queries are shown in Appendix B.
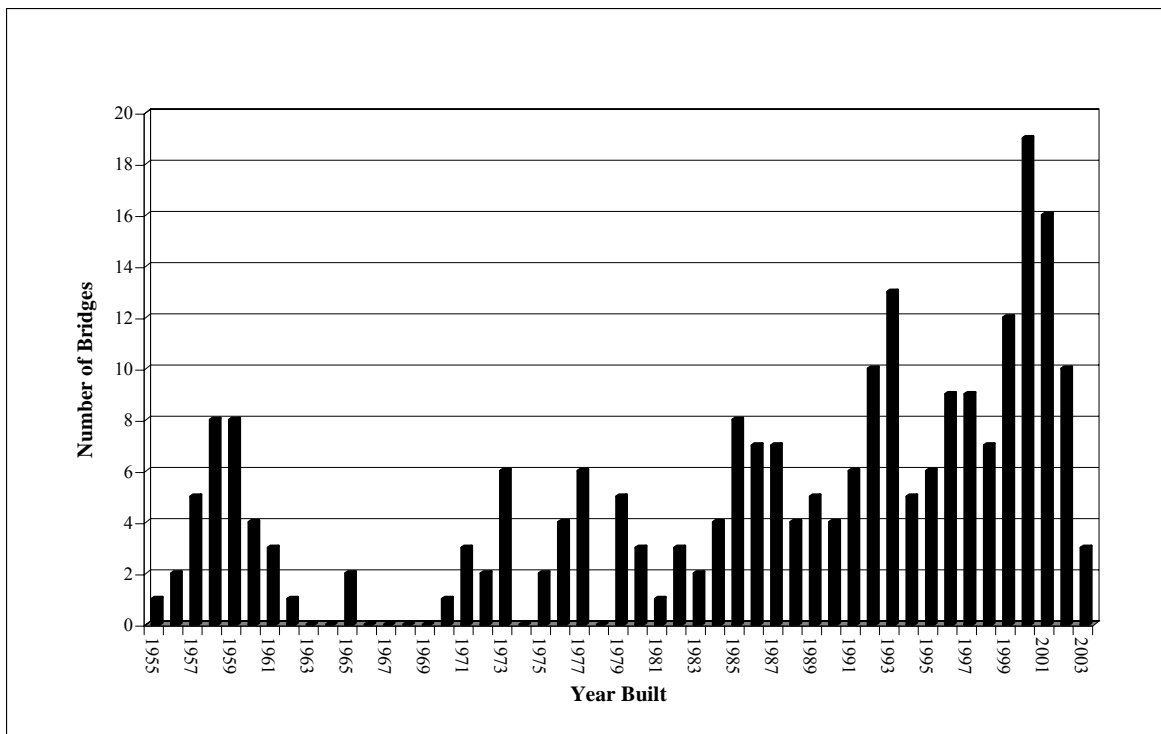


**Figure 3-1: Number of side-by-side prestressed concrete box-beam bridges on the NHS with respect to year built**

The Pontis database stores all of the National Bridge Inventory (NBI) required structure condition data, and the system is used for handling the standard NBI reporting requirements. Structural inventory data (i.e., location, structure ID, length, etc.) can be identified from the

CENTER FOR STRUCTURAL DURABILITY – Condition Assessment and Methods
of Abatement of Prestressed Concrete Box-Beam Deterioration

MDOT safety inspection reports. The safety inspection report is categorized into four major sections, deck, superstructure, substructure, and approach. The four sections are further reduced into elements. Comments on each element condition and element condition ratings are found in the inspection reports.

An inventory level inspection is the first inspection of a bridge and is conducted immediately following construction. After the inventory inspection a routine inspection is conducted on a biennial basis. For the purpose of this study it was assumed that no distress was present on a bridge that had not yet received a routine inspection. When the inspector did not comment on the condition of the bridge in the most recent safety inspection report, previous inspection comments were taken into consideration. The comments taken into consideration only dated back to the last three inspections for each bridge. Special attention was paid to the deck comments, deck ratings, stringer comments, and stringer ratings. The inspection reports were analyzed by viewing each record and counting the occurrences of the following terms: cracked, leaked, corroded, high load hits (HLH), spalled, and no distress. This was completed for both the deck and stringers.

The inspection records for the deck category indicate a total of 136 bridge decks that show no signs of distress. The results are summarized in Table 3-1. The deck comments were further analyzed by counting the occurrences of the following terms: cracked and corroded, cracked without corrosion, uncracked but other distress, and no distress. The percentage of bridges that fell into each category was calculated by comparing with bridges built in the same year. A histogram of the results is shown in Figure 3-2(a). The deck was also categorized into comments found for longitudinal cracking and transverse cracking. Out of 236 comments, there were eight comments for longitudinal cracking and 11 comments for transverse cracking.

The inspection records for the stringer category indicate a total of 127 bridges that show no distress in the stringers. Therefore 109 out of 236 bridges exhibit some sign of distress in the stringers. The results are summarized in Table 3-2. The stringer comments were further analyzed by counting the occurrences of the following terms: cracked and corroded, cracked without corrosion, uncracked but other distress, and no distress. The percentage of bridges

CENTER FOR STRUCTURAL DURABILITY – Condition Assessment and Methods
of Abatement of Prestressed Concrete Box-Beam Deterioration

49

that fell into each category was calculated by comparing with bridges built in the same year. A histogram of the results is shown in Figure 3-2(b). If the stringer was cracked and corroded, it was further categorized into types of cracking. The categories are as follows: longitudinal cracking, transverse or end cracking, cracking caused by leakage between beams, cracking along beam edges, and cracks resulting from spall to steel. It was found that longitudinal cracking and cracks resulting from spall to steel were the most dominant types of cracking. A histogram of the results is shown in Figure 3-3.

**Table 3-1: Inspector comments for the condition of the decks for side-by-side prestressed concrete box-beam bridges**

| Inspector Comments | No. of Bridges |
|---|---|
| Cracking | 66 |
| Leaking | 62 |
| Corrosion | 14 |
| Spalling | 50 |
| Comments are not mutually exclusive and some bridges may have more than one noted distress | |

**Table 3-2: Inspector comments for the condition of the stringers for side-by-side prestressed concrete box-beam bridges**

| Inspector Comments | No. of Bridges |
|---|---|
| Cracking | 74 |
| Leaking | 51 |
| Corrosion | 33 |
| Spalling | 74 |
| High Load Hits | 2 |
| Comments are not mutually exclusive and some bridges may have more than one noted distress | |
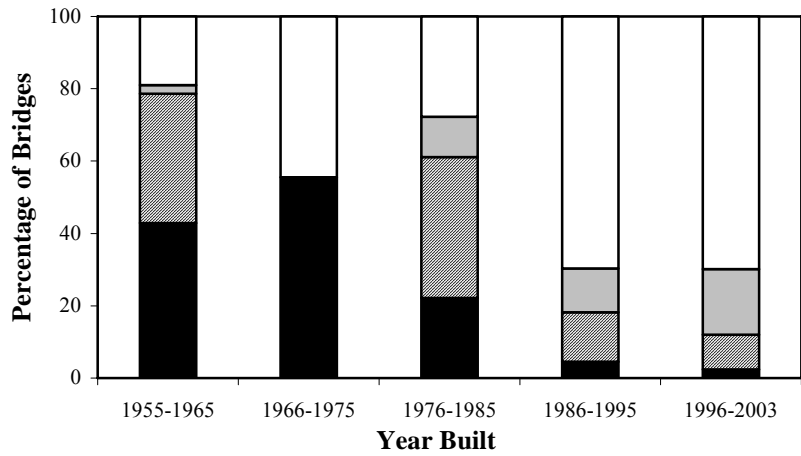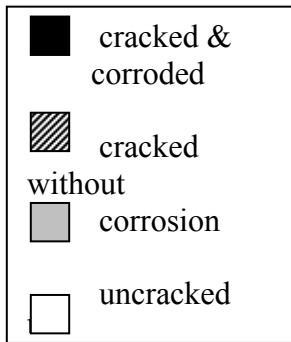
(a)

| 60Year | No. of bridges |
|---|---|
| 1955-1965 | 42 |
| 1966-1975 | 9 |
| 1976-1985 | 36 |
| 1986-1995 | 66 |
| 1996-2003 | 83 |
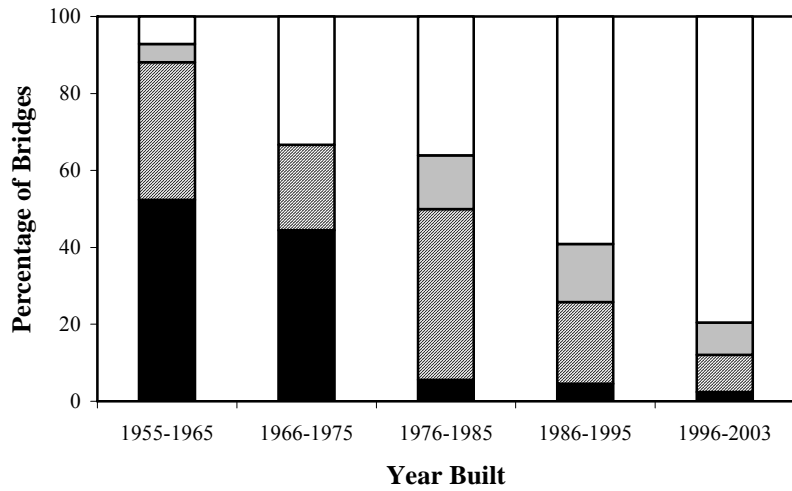


(b)

**Figure 3-2: (a) Histogram of deck conditions and (b) Histogram of stringer conditions**

CENTER FOR STRUCTURAL DURABILITY – Condition Assessment and Methods
of Abatement of Prestressed Concrete Box-Beam Deterioration

51
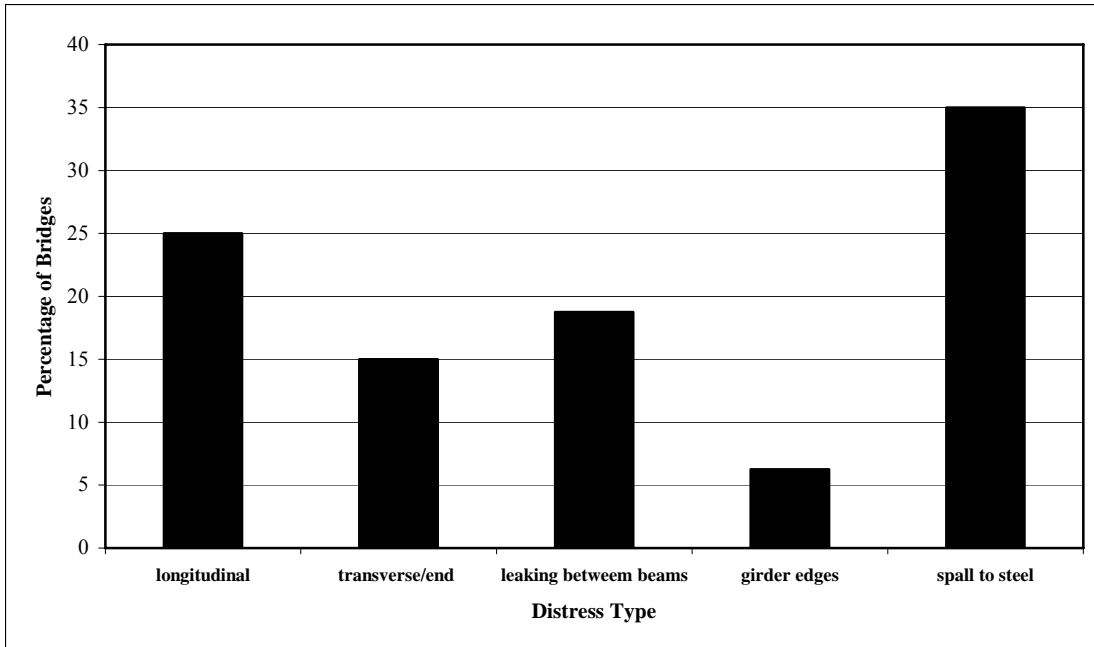
**Figure 3-3: Distress types of bridges with cracked and corroded stringers**

## 3.3 Selection of Bridges for Inspection

In order to select 15 side-by-side prestressed concrete box-beam bridges for inspection, a set of criteria was established. Governing criteria for bridge selection was based on manageable accessibility of the structure. Shoulders or sidewalks must be located on the facility carried and intersecting features. The average daily traffic (ADT) and average daily truck traffic (ADTT) volumes must be moderate in order to regulate traffic.

As discussed in the literature review, significant changes to the design of side-by-side box-beam bridge superstructure have been made in 1974 and 1985. Based on the major changes to their design, the bridges are grouped under those built before 1974 and after 1985; therefore bridges built between 1974 and 1985 are not considered.

The inspection pool is further reduced to single and multi-span bridges with skew angle less than or equal to 30 degrees for bridges built before 1974 and after 1985. Single span bridges built before 1974 were taken into consideration because bridge engineers expressed interest in this category. Single span bridges normally display less problems; therefore, there is an interest in how long these bridges will last. As coded in Pontis, bridges with facility type pedestrian (P), non-motorized traffic (N), miscellaneous (Z), and highway over railway (R)

were excluded. With the above criterion, the previous pool of 236 side-by-side box-beam bridges was reduced to 75. The histogram of the 81 bridges (27 bridges built before 1974, 4 bridges built between 1974 and 1985, and 50 bridges built after 1985) is shown in Figure 3-4.

To help with identifying the bridges for inspection, Table A-2 through Table A-4 found in Appendix A were developed. Table A-2 shows the reduced list of 77 bridges. The pool of 27 bridges built before 1974 and 50 bridges built after 1985 are given in Table A-3 and Table A-4, respectively. Table A-2 includes only the inventory information and deck and stringer ratings. Table A-3 and Table A-4 show deck rating, superstructure rating, and inspection comments on the stringer condition in addition to the inventory information.

The stringer comments from the NBI Inspection Reports of respective bridges given in Table A-3 and Table A-4 were reviewed. The common distresses reported on stringers are grouting or shear key failure, cracks (shear or others), staining, misalignment of beams, signs of corrosion, delamination and spall to steel (STS), and tendon break or damage. These distresses are coded as 0 through 7 respectively (legend is described in the footnote of Table A-3 and Table A-4).

In order to be able to extract the distress progression and mechanisms, it is essential to inspect bridges from new to old. Eight bridges were chosen from the list of 27 bridges built before 1974 and seven bridges were chosen from the list of 50 bridges that were built after 1985. The list of 15 bridges shown in Table 3-3 was presented to the Research Advisory Panel (RAP) members of the MDOT and approved for inspection.

CENTER FOR STRUCTURAL DURABILITY – Condition Assessment and Methods
of Abatement of Prestressed Concrete Box-Beam Deterioration

53
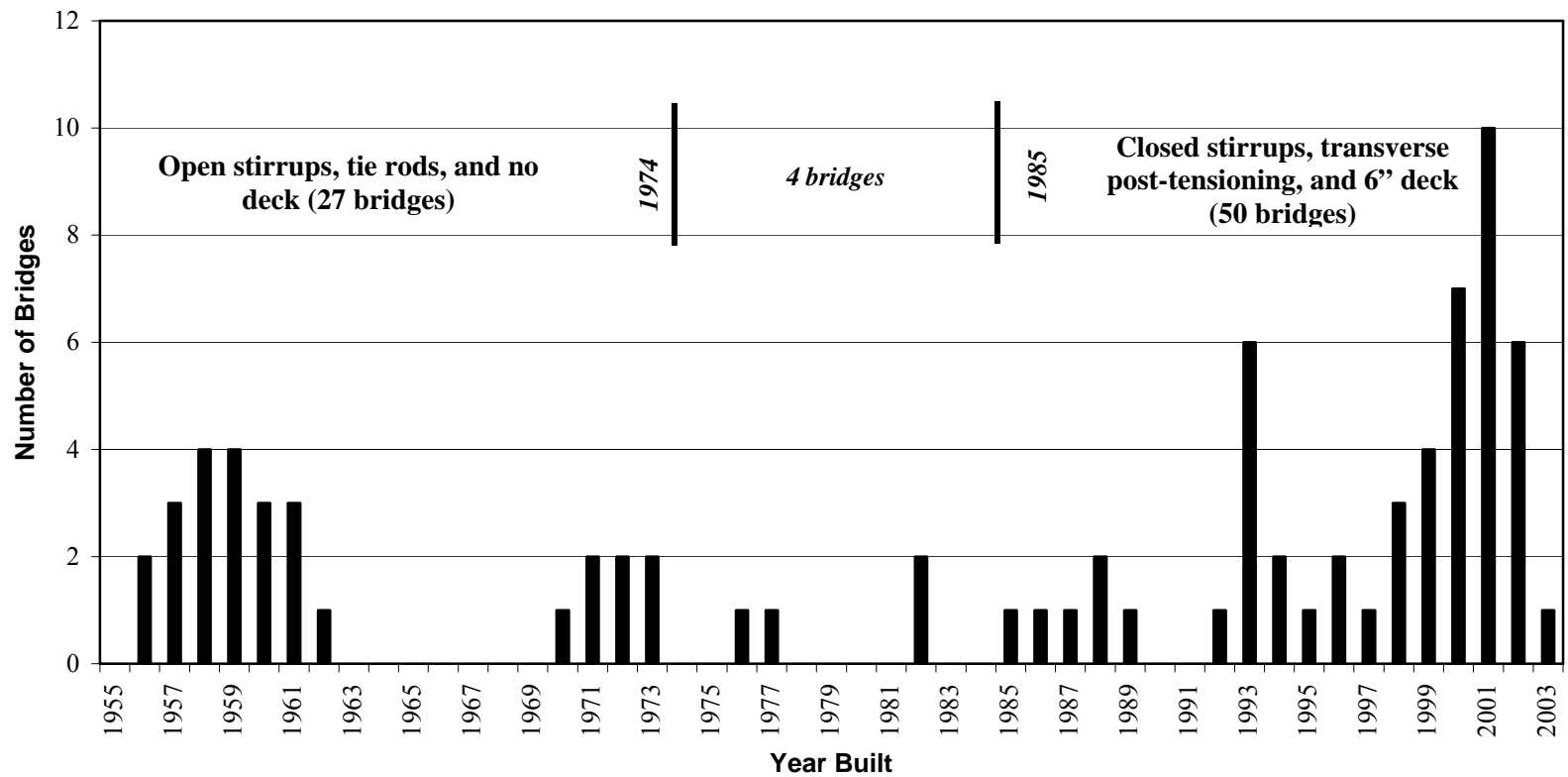
**Figure 3-4:  Number of prestressed concrete side-by-side box-beam bridges (skew < 30 degrees) with respect to year built**

CENTER FOR STRUCTURAL DURABILITY – Condition Assessment and Methods
of Abatement of Prestressed Concrete Box-Beam Deterioration

**Table 3-3: Fifteen side-by-side box-beam bridges chosen for inspection.**

| | Using Pontis Version 4.2 - Feb. 17, 2004 | | | | | | | | | | | | | |
|---|---|---|---|---|---|---|---|---|---|---|---|---|---|---|
| | **SIDE-BY-SIDE BOX-BEAM BRIDGE INVENTORY** | | | | | | | | | | | | | |
| | [skew < 30 degrees; excluding pedestrian (P), non-motorized traffic (N), and miscellaneous (Z), highway over railway (R)] | | | | | | | | | | | | | |
| **Project Bridge #** | **Bridge id.** | **year built** | **district** | **county** | **Feature intersected** | **facility** | **main spans** | **max span (ft)** | **length (ft)** | **skew** | **deck width (ft)** | **ADT** | **ADTT** | **Insp. date** |
| 1 | B02 of 08012 | 1956 | Southwest | Barry | COLDWATER RIVER | M-43 | 3 | 45 | 135 | 24 | 36 | 2400 | 120 | 7/7/2004 |
| 2 | B01 of 32051 | 1957 | Bay | Huron | CASS R | M-19 | 1 | 40 | 40 | 0 | 43 | 1800 | 162 | 6/22/2004 |
| 3 | B04 of 74032 | 1957 | Bay | Sanilac | S FORK CASS R | M-19 | 1 | 40 | 40 | 0 | 43 | 2000 | 160 | 6/22/2004 |
| 4 | B01 of 08032 | 1957 | Southwest | Barry | DUNCAN CREEK | M-37 | 3 | 40 | 110 | 18 | 43 | 10000 | 1000 | 7/7/2004 |
| 5 | S09 of 25031 | 1958 | Bay | Genesee | BRISTOL RD | I-75 | 4 | 51 | 164 | 0 | 139 | 32800 | 2624 | 6/23/2004 |
| 6 | B01 of 32021 | 1958 | Bay | Huron | PIGEON R | M-142 | 3 | 35 | 105 | 0 | 46 | 4200 | 252 | 7/1/2004 |
| 7 | S10 of 38101 | 1958 | University | Jackson | I-94 | DETTMAN RD | 5 | 49 | 208 | 2 | 33 | 54000 | 4320 | 7/17/2004 |
| 8 | S11 of 38101 | 1958 | University | Jackson | I-94 | HAWKINS RD | 4 | 49 | 164 | 0 | 33 | 41000 | 3280 | 7/17/2004 |
| 9 | B02 of 78021 | 1989 | Southwest | St.Joseph | ST. JOSEPH RIVER | US-12 (RELOC) | 3 | 90 | 270 | 18 | 37 | 4300 | 473 | 7/6/2004 |
| 10 | S08 of 41131 | 1993 | Grand | Kent | US-131 | 32ND ST | 4 | 60 | 213 | 4 | 61 | 16925 | 169 | 7/8/2004 |
| 11 | B01 of 53011 | 1993 | North | Mason | LINCOLN R | M-116 | 3 | 51 | 153 | 0 | 47 | 1000 | 60 | 7/9/2004 |
| 12 | S07 of 50011 | 1994 | Metro | Macomb | M-53 | M-59 EB | 2 | 117 | 234 | 0 | 76 | 24000 | 1920 | 7/25/2004 |
| 13 | B01 of 06071 | 1998 | Bay | Arenac | SAGANING CR | M-13 | 3 | 33 | 83 | 0 | 70 | 6400 | 512 | 6/28/2004 |
| 14 | S02-3 of 33045 | 2000 | University | Ingham | PENNSYLVANIA AVE | I-496 EB | 3 | 97 | 165 | 15 | 48 | 28300 | 2264 | 7/18/2004 |
| 15 | S02-4 of 33045 | 2000 | University | Ingham | PENNSYLVANIA AVE | I-496 WB | 3 | 98 | 166 | 15 | 57 | 28300 | 2264 | 7/18/2004 |

Notes:
Table prepared on June 11, 2004.  Please note that Pontis is updated everyday and the data in the tables created in this report reflect version 4.2 of Pontis updated February 17, 2004.

CENTER FOR STRUCTURAL DURABILITY – Condition Assessment and Methods
of Abatement of Prestressed Concrete Box-Beam Deterioration

55

This page intentionally left blank

# Chapter 4:    Inspection and Load Rating Procedures

Proper identification and timely maintenance are essential to preserve Michigan's box-beam bridges.  This report provides the tools needed to properly locate and identify deterioration through the Inspection Handbook.  Repair and maintenance options may be determined through repair option flowcharts, Appendix E.  Finally, changes in the load rating due to distressed or recently reconfigured bridges are required, and suggestions and sample calculations are provided to aid in this task.

Through intensive study and inspection, thirteen types of degradation were identified and ranked.  These are described in detail in the "Prestressed Box-Beam Inspection Handbook," Appendix C.  The handbook developed for prestressed box-beam inspection has been designed to serve as a supplement to the *Pontis Bridge Inspection Manual* (MDOT 1999) and should serve as a guide to aid bridge inspectors and engineers while assessing the condition of box-beams in Michigan bridges for the purpose of scoping or damage evaluation inspections.  The level of detail in the inspection handbook may be greater than needed for routine biennial inspections.

Inspection forms were created to aid in the inspection process and to help ensure that relevant data is collected and organized in a matter useful to a design engineer responsible for assessing the need for repairs.  These forms are located in Appendix D.

A detailed set of flowcharts are provided in Appendix E to further evaluate the inspection results and provide suggestions for repairs to the damaged structural components.   The structural significance of repairs to future bridge inspections are provided in repair matrices located in Appendix F.  Deterioration that compromises the structural integrity of the bridge must be further assessed to determine the bridge load rating in the distressed state.

Bridge load ratings are a necessary step in the bridge maintenance program.  *The Manual for Condition Evaluation of Bridges*, (AASHTO 2003b) is used to provide a bridge load rating to be submitted to the National Bridge Inventory (NBI).  This reference is further supplemented by the *Bridge Analysis Guide* (MDOT 2003a).  Load ratings are required

CENTER FOR STRUCTURAL DURABILITY – Condition Assessment and Methods
of Abatement of Prestressed Concrete Box-Beam Deterioration

57

following construction of a bridge and at any time in which the structure has changed from the previous load rating. A new load rating is required each time the structure has been modified, either through additional construction, maintenance, or degradation. A sample calculation of a load rating both before and after damage is provided in Appendix G to illustrate the changes which occur in a load rating due to degradation.

## 4.1  Common Forms of Deterioration

Michigan typically uses box-beams to produce side-by-side box-beam bridges. These bridges are constructed by laying box-beams adjacent to each other. Shear keys between beams are then grouted full depth and transverse post-tensioning is applied to unite the beams into a single system, which behaves as an orthotropic plate. A reinforced concrete deck is cast above the beams to provide a wearing surface, protect the beams from the elements and to supplement the shear keys and post-tensioning with load transfer between beams. Older bridges may have been constructed with an asphalt wearing surface above the box-beams. In the late 1980's a six-inch reinforced concrete slab was specified to reduce the chances of reflective cracking along the joints which exposed the beams to salt laden water from above. Two main types of deterioration are found in box-beam bridges; loss of continuity between beams, which affects the behavior of the bridge system, and deterioration of individual box-beams.

Reflective cracking of the deck above the joints between box-beams is a serious problem as it allows penetration of deicing chemicals through the deck and between the beams. Reflective cracking of the deck may be a sign of failure in the shear keys between adjacent box-beams and/or loss of force in the transverse post-tensioning strands. The purpose of the shear keys and the transverse post-tensioning is to tie all the beams in the system together. This causes the beams to behave conjointly with proper load transfer between any two adjacent box-beams. Reflective cracking of the bridge deck infers differential movement between beams. Should this happen, the bridge system may no longer behave as designed and overloading of individual elements may occur.

Deterioration of individual box-beams comes in many forms. The visual symptoms usually consist of cracks and/or spalls. These areas are of concern because they may

allow salt-laden water to penetrate into the structural member and cause further deterioration of both the concrete and steel reinforcement. Corrosion of the reinforcement greatly impacts the capacity of the structure, not only does it cause loss of a key component in a prestressed system, but corroding steel may expand three to six times the original volume and cause further loss of concrete section due to cracking and spalling (Teng 2000).

## 4.2 Inspection Handbook

Inspections of Michigan Bridges are scheduled on a biennial basis. More frequent inspections may occur if damage has been indicated during a scheduled inspection or following a damage inducing event, such as a vehicular high-load hit. There are five basic levels of a bridge inspection identified in the *Bridge Inspector's Reference Manual* (FHWA 2002), and identified in Table 4-1 along with a brief description.

**Table 4-1: Types of bridge inspections**

| Type of Bridge Inspection | Description |
|---|---|
| Inventory | Initial inspection of a bridge, data is collected for use in the first load rating. All structural inventory and appraisal data is collected. This inspection serves as a baseline of structural condition for future comparison to distressed locations. |
| Routine | These are the typical inspections conducted on a bridge, usually on a biennial basis. The intent is to determine if there are any changes from the inventory inspection. |
| Damage | The purpose of this inspection is to determine the extent of structural damage resulting from either environmental or human actions. It is usually conducted to determine the need for emergency load restrictions and/or repairs. |
| In-Depth/Scoping | This is a very detailed and specific hands-on inspection to identify any deficiencies not readily detectable using routine inspection procedures. |
| Special | Special inspection of a bridge is conducted to monitor a known or suspected deficiency. A particular problem is monitored and thus this type of inspection is not typically comprehensive enough to provide sufficient information on the whole bridge. |

An inspection handbook has been developed as part of this project and is located in Appendix C. The inspection handbook has been written to provide guidance on typical forms of deterioration specific to prestressed concrete side-by-side box-beam bridges in

CENTER FOR STRUCTURAL DURABILITY – Condition Assessment and Methods
of Abatement of Prestressed Concrete Box-Beam Deterioration

59

Michigan. The handbook may be used for any of the above inspections, however, the content of the handbook will be most helpful when conducting an in-depth / scoping or damage evaluation level inspections.

Thirteen kinds of deterioration are identified in the inspection handbook. The types of distress are ranked according to their level of structural significance by a condition rating specific to this project. The condition nomenclature determined by the Federal Highway Association (FHWA) for the National Bridge Inventory (NBI) is provided to help correlate between the two systems. The grades of deterioration provided in this handbook were developed by the authors and are specific to prestressed box-beams and therefore contain more box-beam-specific detail than the NBI condition ratings. Table 4-2 summarizes the condition rating assigned to Michigan prestressed concrete box-beam bridges.

Table 4-2: Summary of condition states for Michigan prestressed concrete box-beams

| Box-Beam Rating | Description of Possible Conditions Present | FHWA Rating | FHWA Description |
|---|---|---|---|
| A | 1. No cracks or staining | 9-8 | Excellent to very good condition |
| B | 2. Map cracks<br>3. Hairline cracks | 7-6 | Good to satisfactory condition |
| C | 4. Spalling or delamination<br>5. Narrow cracks w/ water or corrosion<br>6. Water stains at joints<br>7. Longitudinal cracks on deck | 5 | Fair condition |
| D | 8. Medium cracks w/o water<br>9. Evidence of displacement between beams | 4 | Poor condition |
| E | 10. Medium cracks w/ water or corrosion | 4 | Poor condition |
| F | 11. Wide cracks w/ water or corrosion | 4 | Poor condition |
| G | 12. Spalling w/ exposed or corroded reinforcement<br>13. Shear or flexure cracking | 3-2 | Serious to critical condition |

The purpose of the inspection handbook is to aid the inspector by illustrating typical forms of distress in box-beam bridges and help reduce the likelihood of overlooking

items which may be needed for additional analysis of the structure.  The inspector should record his/her findings on the inspection report forms located in Appendix D.  The information will then be used by an engineer to determine the need for repair.  A repair flowchart has been created to aid the engineer in this task.

## 4.3  Inspection Report Forms

Specialized inspection worksheets and forms have been developed for use during in-depth / scoping or damage assessment inspections of Michigan box-beam bridges. The level of detail attained in these forms may exceed the intended scope for inventory and routine levels of inspection.  These forms and worksheets are located in Appendix D. Examples of how to properly record information on both of these forms are also located in the appendix.

## 4.4  Repair Option Flowchart

The flowcharts found in Figures E-1 through E-6 of Appendix E may be used by the scoping engineer to asses the proper repairs for distress identified by the field inspector. Figure E-1 is a general flowchart used to identify the likely cause of deterioration.  Two outcomes are available, material related distress and structural related distress.  The material related distress suggests that chemical reactions or other non-mechanical processes are at work within the beam material, causing deterioration.  The root of the problem must be identified and remedied prior to attempting a traditional fix on the structure.  Failure to differentiate between material and structural deteriorations may result in suboptimal performance of the repair.

A flowchart for material related distresses is found in Figure E-2.  This flowchart has been reproduced from *Guidelines for the Detection, Analysis, and Treatment of Materials-Related Distress in Concrete Pavements* (Van Dam et al., 2002).   The flowchart steps through a process to determine the severity of damage and the need for repair.  Limited or minor damage may require no more than regular monitoring.  Damage that lessens the strength of the material may require a load rating analysis and upgrades to the superstructure to maintain design vehicular loads.  There are many forms of material related distress and because of this, a single testing procedure to identify the cause of

deterioration may not be available. For this reason it is suggested that a design engineer familiar with this topic be consulted when a material related distress is suspected.

Figures E-3 through E-6 are used for assessing repair options for various forms of structural degradation. Figure E-3 is a general structural distress flowchart and may be used to determine the need for additional analysis or repairs. A user of this flowchart is directed to one of three other flowcharts depending upon the type of distress identified. Figure E-4 is for minor damage to the beams, Figure E-5 is used for moderate to major damage of the beams, and lastly for deck damage see Figure E-6.

The intent of these flowcharts is to determine the proper repair for the identified distress. Many of the repairs may be made following the Michigan DOT *Standard Specifications for Construction* (MDOT 2003c). A design engineer may be required to design repairs for material related or severe forms of distress. There may also be unique site or project specific conditions for which an engineer may be required, even for more common distress issues.

## 4.5  Repair Lifespan Matrices

The *Michigan Design Manual, Bridge Design* (MDOT 2003b) Appendix 12.09.02 contains a bridge deck repair matrix. This matrix may be used to assess the available repair options for life expectancy and structural improvement to the deck system of the bridge. A copy of this has been included in Appendix F, along with a matrix to consolidate available repair options, life expectancies, and structural benefits for box-beams. This information will be useful in determining the best repair for a given bridge situation. For example, if the year of replacement is known, a lower cost repair could be selected that will perform well for that period. The box-beam repair matrix has been included to illustrate the usefulness of such a design aid. Additional development is needed and it is expected that phase II of this project will help fill in the blanks left empty during phase I.

## 4.6  Load Rating Calculations

Bridge load ratings are used by bridge owners to assess the structural integrity of their bridges and are reported to the NBI.  Every bridge has a load rating on file and this record exists from the time the bridge was constructed.  Damage and deterioration of the structural members of the bridge are incorporated into the load rating, and structural repairs may be required if a load rating falls below accepted standards.  A load rating reflects the current condition of the bridge and is conducted both before and after repairs are made.  Unlike the condition evaluation of a bridge, the load rating of a bridge is controlled by the weakest member within the structure.  It is, therefore, important to recognize and document forms of distress and their locations while conducting an inspection.

### 4.6.1  Overview of Prestressed Concrete Load Rating Procedures in Michigan

Load ratings are calculated according to the *Manual for Condition Evaluation of Bridges, 2003 interim* (AASHTO 2003b), and supplemented by the requirements of the *Bridge Analysis Guide* (MDOT 2003a).  The *Bridge Analysis Guide* (MDOT 2003a) has been used internally by MDOT for several years and will be released outside of the department shortly.  AASHTO, or federal level, load ratings are based on the HS20 truck load.  The federal level load ratings are divided into two sections, an inventory level and an operating level.  The inventory level reflects a frequent live load applied to a bridge.  The operating level is meant to reflect live loads less frequently applied.  The difference between these two is achieved through various load factors.  Only the federal load ratings are reported to the NBI.  The *Bridge Analysis Guide* (MDOT 2003a) requires additional operating ratings using the 3 categories of Michigan legal-load trucks to produce the Michigan level rating, because Michigan allows heavier trucks than the federal government.  MDOT requires that a load rating consider live loads from 28 vehicles under 3 categories; 1-unit, 2-unit, and 3-unit trucks.

Load ratings may be performed using Allowable Stress Design (ASD), Load Factor Design (LFD), or Load and Resistance Factor Design (LRFD).  The sample load ratings (Appendix G) were computed according the guidelines for Load Factor Design because

many bridges currently in service have been designed according to LFD and the LFD method for load rating is required for values reported to MDOT for submittal to the FHWA NBI. MDOT maintains a database of load ratings for all publicly owned bridges within the state. The bridge owner must report load ratings to MDOT for placement within the database. This database is shared with the NBI. A similar approach to that outlined in the appendix may be used for LRFD and ASD load rating analysis, although neither of these are acceptable to MDOT or the NBI.

Load rating a prestressed concrete box-beam requires six conditions for the inventory rating and three conditions for each of the trucks analyzed under the operating rating. Each ratings requires a strength check of the member, both flexural and shear, and a service limit check. The inventory rating requires a service level check of concrete tension, concrete compression, and prestress steel tension. The operating rating only requires that the prestress steel tension be checked. The equations and an explanation of their terms may be found in the *Manual for Condition Evaluation of Bridges, 2003 interim*. The *Bridge Analysis Guide* (MDOT 2003a) contains simple-span reaction tables for each of the legal-load vehicles. One vehicle from each category, 1, 2, or 3-unit configurations is selected, which produces the smallest reaction (moment or shear) to vehicle weight ratio, as determined from the tables. This vehicle is considered the "controlling" vehicle and should be used to determine the Michigan operating rating. A load rating factor of 1.0 indicates that the live load vehicle used for the rating is equal to the load that will cause the flexural, shear, or service capacity to be met. A value less than 1.0 indicates that the strength or service capacity has been exceeded and a load posting may be necessary for the bridge.

The *AASHTO Standard Specifications, 17th Ed*. (AASHTO 2002) allows for using transformed section properties when designing prestressed concrete beams. Although this provision is not normally used by MDOT, a small side study was conducted to determine the effect of using transformed section properties in the load rating calculations. For the control case (A-1, Table 4-3), both gross and transferred section properties were used. The resulting load ratings remained unchanged for the flexure and shear strength ratings and increased slightly for the service load condition when using

transformed section properties. A six-percent and four-percent increase were found for the inventory and operating rating factors, respectively. Other cases may vary slightly, but it is conservative for MDOT to continue to use gross section properties for load ratings.

Posting of a bridge is at the discretion of the bridge owner. Michigan bridges are usually posted as a result of a load rating that indicates that one or more of the Michigan legal load vehicles exceeds the operating level rating. Several vehicles may exceed the calculated live load capacity of a particular bridge. One of these trucks will produce the lightest posting load rating. The simple-span reaction tables in the *Bridge Analysis Guide* (MDOT 2003a) are used to determine which of these trucks control. Of the trucks which exceed the live load capacity, the vehicle with the largest value for reaction (moment or shear) to weight should be used. Because the vehicle with the largest ratio is used instead of the smallest ratio, two different vehicles are used in calculating the operating rating and the posted load. A bridge owner may decide to post limits on a bridge based on the inventory rating of the bridge. Doing so may increase the life of the bridge.

Load ratings are typically reported as a weight due to the differences in weight of the Michigan legal-loads and the HS-20 truck. Reporting the maximum weight allowed is done by multiplying the calculated load rating factor by the weight of the truck that produced this value. Without this step, a load rating factor would always have to be presented along with the vehicle used for the calculations. Federal load ratings are reported in metric tons. Michigan load ratings are completed in U.S. customary tons. For the purpose of comparison, the values presented in this report are in U.S. customary tons.

### 4.6.2   Parameters Influenced by Deterioration

The equations for load rating of prestressed concrete beams require knowledge of material and cross-sectional beam properties. Those properties that have been affected by distress must be changed and a new load rating must be calculated.

Four properties are directly influenced by deterioration: compressive strength of the concrete, moment of inertia, cross-sectional area of the beam, and the cross-sectional area of the prestressing steel. The compressive strength of the concrete is the only property directly related to material related distress. The cross-sectional area of the beam, moment of inertia, and total area of prestressing strand are all related to the physical condition of the box-beam. Changes to the cross-section of the beam also result in different values for centroid and eccentricity of the prestressing strands. All of these components must be updated to reflect a beam in a distressed state. These properties are used directly in the calculation of the service level stresses for both the inventory and operating ratings and are used by the strength ratings to determine the moment and shear capacity of the beam.

Parameters such as applied loads do not need to be reassessed unless the location or type of deterioration indicates that load patterns may change. For example, if load transfer mechanism deterioration lessens the load sharing capabilities of the side-by side box-beam design, the load distribution will be influenced. If this type of deterioration has occurred, it may be necessary to update the distribution factors for live and dead loads to reflect the current condition of the bridge. This may be done by using an assessment of the amount of damage specific to load transfer mechanisms to vary the distribution factors from the full load transfer condition (as originally designed) to no load transfer between beams (complete deterioration of load transfer mechanisms).

### 4.6.3 Distress in Sample Load Rating

Two example cases were used to illustrate the effect that damage to prestressed box-beams have on load ratings. Example A made use of bridge load rating example #6 contained in the *Bridge Analysis Guide* (MDOT 2003a), which was modified to reflect two levels of damage: loss of cross-section due to spalling of concrete, and a beam with spalling and 3 severed strands. This bridge consisted of 27-inch box-beams spanning 50-ft. Additional details are provided in section 4.6.4. Appendix G contains sample calculations for a load rating of the bridge with box-beams in excellent condition and sample calculations for this bridge after changes are made to the input parameters to reflect a spall and three severed strands. The second example, B, reflects a bridge

typical of those found during the inspection phase of the project.  The span was 57-ft and the strand configuration and stressing levels varied from example A.  An overview of the distress simulated for each of the cases in the two examples may be found in Table 4-3. Corresponding section properties for each of these cases may be found in Table 4-4.

**Table 4-3:  Scenarios studied in load rating**

| Case | Scenario | Box-Beam Rating (Table 4.2) |
|---|---|---|
| **Bridge A** | **Bridge Analysis Guide, Example 6** | |
| A-1 | Control condition | A |
| A-1T | Control condition using transformed section properties | A |
| A-2 | Spalling of concrete, 30 inches$^2$ (5.9%) of section loss. | C |
| A-3 | Spalling of concrete and loss of strand, 30 inches$^2$ (5.9%) of section loss and 30% corrosion of strands. | E, F, G |
| | | |
| **Bridge B** | **Typical Bridge from Phase I Inspection** | |
| B-1* | Control condition | A |
| B-2* | Spalling of concrete, 103 inches$^2$ (20%) of section loss. | G |
| B-3* | Spalling of concrete and loss of strand, 103 inches$^2$ (20%) of section loss and 2 severed strands (6.7%). | G |
| B-4* | Spalling of concrete and loss of strand, 133 inches$^2$ (26%) of section loss and 4 severed strands (13.2%). | G |
| B-5 | Spalling of concrete and loss of strand, 133 inches$^2$ (26%) of section loss and 25% corrosion of strands. | G |
| B-6 | Ineffective load transfer mechanism, 10% increase in load distribution factors | D |
| * Normalized live load capacity is available from the finite element analysis | | |

CENTER FOR STRUCTURAL DURABILITY – Condition Assessment and Methods
of Abatement of Prestressed Concrete Box-Beam Deterioration

67

**Table 4-4: Section properties for each case**

| Case | I beam (in4) | I comp (in4) | A beam (in2) | A comp (in2) | A ps (in2) | y b beam (inch) | y b comp (inch) | Distribution Factor Dead | Distribution Factor Live |
|------|--------------|--------------|--------------|--------------|------------|-----------------|-----------------|--------------------------|--------------------------|
| A-1  | 47,300 | 92,640 | 509 | 701 | 1.519 | 13.57 | 18.48 | 0.0769 | 0.258 |
| A-1T* | 48,406 | 94,894 | 517 | 709 | 1.519 | 13.38 | 18.28 | 0.0769 | 0.258 |
| A-2  | 42,633 | 83,581 | 479 | 671 | 1.519 | 14.33 | 19.24 | 0.0769 | 0.258 |
| A-3  | 42,633 | 83,581 | 479 | 671 | 1.085 | 14.33 | 19.24 | 0.0769 | 0.258 |
|      |        |        |     |     |       |       |       |        |       |
| B-1  | 47,300 | 92,640 | 509 | 701 | 2.40 | 13.57 | 18.48 | 0.125 | 0.252 |
| B-2  | 28104 | 57300 | 405.5 | 597.5 | 2.40 | 16.67 | 21.43 | 0.125 | 0.252 |
| B-3  | 28104 | 57300 | 405.5 | 597.5 | 2.24 | 16.67 | 21.43 | 0.125 | 0.252 |
| B-4  | 22341 | 46966 | 375.7 | 567.7 | 2.08 | 17.73 | 22.38 | 0.125 | 0.252 |
| B-5  | 22341 | 46966 | 375.7 | 567.7 | 2.08 | 17.73 | 22.38 | 0.125 | 0.252 |
| B-6  | 47,300 | 92,640 | 509 | 701 | 2.40 | 13.57 | 18.48 | 0.138 | 0.277 |

Highlighted cells indicate changes from control case (A-1 and B-1), as discussed in 4.6.3
* See section 4.6.1 for an explanation of the transformed section properties

Simulation of the spalled scenarios in both examples A and B were conducted by recalculating the cross-sectional properties of the beam to account for the loss of concrete and/or strand. Deterioration of the load transfer mechanism was simulated by modifying the distribution factors for live and dead load to reflect a 10% reduction in load distribution. This represents extreme degradation because even severe cracks in shear keys have been found to only cause a 10% reduction in load distribution between adjacent box-beams (Miller 1998).

The distress accounted for in the load rating example calculations was assumed at the locations of maximum loading. For example, the concrete spall and severed strand distress condition was assumed to be located at midspan for the purpose of assessing the load rating for flexural strength and service conditions. To estimate the shear rating, the distress was assumed at the location of maximum shear, h/2. Placing the distresses at these locations shows the highest effect that these forms of distress will have on a load rating. For a load rating of an actual bridge the location of the distress, along with the loading effects at that location, would be used to provide a load rating for the structure.

### 4.6.4 Load Rating Sample Calculations

Sample calculations for two of the nine load ratings performed as part of this project are found in Appendix G of this report. The control load rating represents the bridge in excellent condition (Case A-1). This example is reproduced from the *Bridge Analysis Guide* (MDOT 2003a) Example 6. This was done to allow those familiar with the example to better understand the effects of distress and to serve as a check on the calculations. Errors were found in the draft version of the referenced example, however, correction of these showed agreement between the results of Example 6 and Case A-1 of this report. Several calculations, such as prestress losses, were not recalculated in Appendix G. The reader is referred to the *Bridge Analysis Guide* (MDOT 2003a) Example 6 for a full and detailed description of equation references and calculations. The second example shows the effects of a concrete spall and loss of several prestressed strands (Case A-3). Parameters influenced by deterioration and the values used in each case are indicated in Table 4-4. A cross-section and elevation of the bridge used for Example A of the load rating, independent of distress level, is shown in Figures 4-1 and 4-2 respectively.
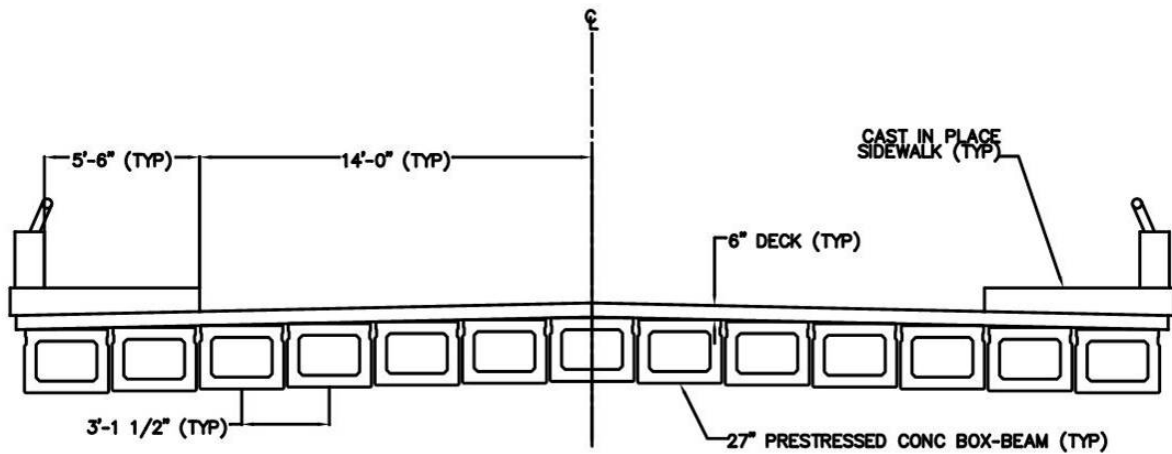


**Figure 4-1: Cross-section: prestressed concrete side-by-side box-beam bridge (Example A)**

CENTER FOR STRUCTURAL DURABILITY – Condition Assessment and Methods
of Abatement of Prestressed Concrete Box-Beam Deterioration

69
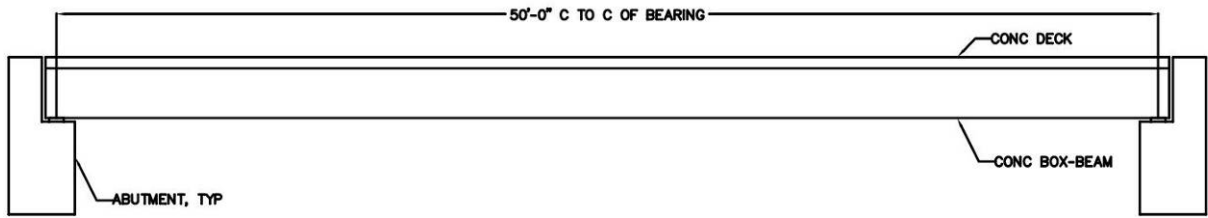
**Figure 4-2: Elevation: prestressed concrete side-by-side box-beam bridge (Example A)**

A cross-sectional view of the beam used for the control condition in Example A is shown in Figure 4-3. This beam was modified by spalls and severed strands as described in Table 4-3, a cross-sectional view of the distressed section of Example A is shown in Figure 4-4.
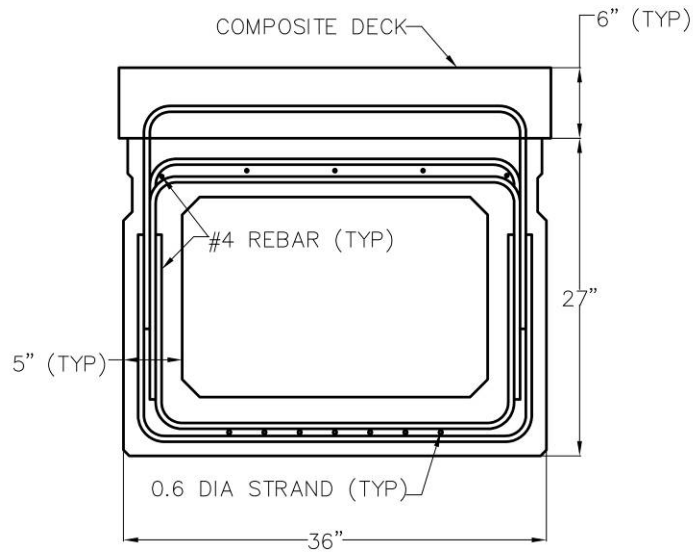


**Figure 4-3: 27-in composite box-beam – excellent condition**
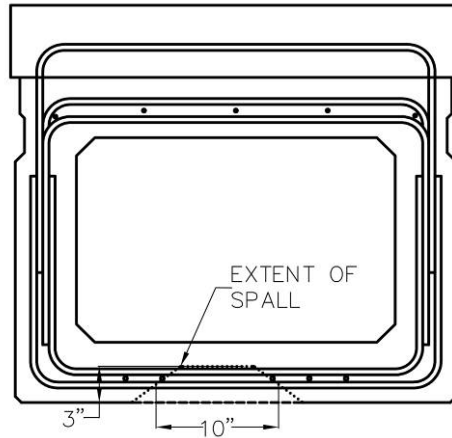
**Figure 4-4: 27-in composite box-beam – spalled concrete and severed strands**

It is important to note that load ratings according to the *Bridge Analysis Guide* (MDOT 2003a), are calculated for HS-20 truck loads even though design may have been conducted using a different live-load (typically HS25 for Michigan designs). MathCAD was used to conduct the load rating calculations because it allowed for a rapid update of input parameters. Specific load rating programs, spreadsheets, or hand calculations could all be modified in a manner similar to that described above.

### 4.6.5   Results of Load Rating Distress Scenarios

Results of the inventory level load rating factor are shown in Table 4-5 (full load rating results are displayed in Tables 4-6 and 4-7). The values presented are the lowest (governing) values from the six equations for inventory level ratings. The controlling equation is also indicated for each of the simulated forms of distress. It was observed that the control conditions provided a satisfactory load rating factor of 1.26 and 1.80 for examples A and B, respectively, and all of the simulated forms of deterioration produced significantly lower load ratings. Repairs may be necessary for any distress which produces an inventory rating factor less than 1.0. The inventory rating is performed using only the HS-20 design vehicle; therefore, comparison may be made using the load rating factor without converting to a corresponding vehicle weight. However, for completeness, the lowest load from Table 4-6 (45 tons) is divided by the HS20 vehicle weight (36 tons)

to obtain a LRF of 1.26.  From the two examples used in this study it is apparent that the force in the prestressing strands is very influential in the final results of a load rating. Example A assumed a prestress force of 177 ksi (after losses), while the force assumed for Example B was 149 ksi.  Variation of this value for each of the examples caused a noticeable change in the resulting bridge load rating factor.  It is therefore very important that the prestress force is known with as much certainty as possible to produce an accurate load rating.

**Table 4-5:  Inventory level load rating factor results**

| Case | Inventory Load Rating Factor (HS-20 Truck) | Controlling Equation |
|---|---|---|
| A-1 | 1.26 | Prestress Steel Tension |
| A-1T | 1.33 | Prestress Steel Tension |
| A-2 | 0.97 | Prestress Steel Tension |
| A-3 | 0.72 | Flexural Strength |
|  |  |  |
| B-1 | 1.80 | Shear Strength |
| B-2 | 1.73 | Concrete Tension |
| B-3 | 1.50 | Concrete Tension |
| B-4 | 1.28 | Concrete Tension |
| B-5 | 0.85 | Concrete Tension |
| B-6 | 1.63 | Shear Strength |

Values for the inventory and operating rating are found in Tables 4-6 and 4-7 for example A and B respectively.  Section 4.6.1 explains the differences between Federal and Michigan Legal levels as well as the differences between inventory and operating ratings. The lowest value for each column controls the load rating for a particular case.

**Table 4-6: Results of load rating for Example A, (U.S. tons).**

| CASE | | Federal Level | | Michigan Legal Level Operating Rating | | |
|---|---|---|---|---|---|---|
| | | Inventory Rating | Operating Rating | 1-unit | 2-unit | 3-unit |
| A-1 | Flexural strength | 49 | 81 | 88 | 142 | 139 |
| | Shear strength | 57 | 95 | 107 | 147 | 172 |
| | Service load | 45 | 328 | 357 | 575 | 562 |
| A-1T | Flexural strength | 49 | 81 | 88 | 142 | 139 |
| | Shear strength | 57 | 95 | 107 | 147 | 171 |
| | Service load | 48 | 341 | 371 | 598 | 585 |
| A-2 | Flexural strength | 49 | 81 | 88 | 142 | 139 |
| | Shear strength | 58 | 97 | 109 | 150 | 175 |
| | Service load | 35 | 279 | 303 | 489 | 478 |
| A-3 | Flexural strength | 26 | 43 | 47 | 76 | 74 |
| | Shear strength | 51 | 85 | 96 | 131 | 153 |
| | Service load | 30 | 279 | 303 | 489 | 478 |
| See 4.6.1 for an explanation of the levels of a load rating analysis | | | | | | |

**Table 4-7: Results of load rating for Example B, (U.S. tons).**

| CASE | | Federal Level | | Michigan Legal Level Operating Rating | | |
|---|---|---|---|---|---|---|
| | | Inventory Rating | Operating Rating | 1-unit | 2-unit | 3-unit |
| B-1 | Flexural strength | 73 | 123 | 131 | 199 | 199 |
| | Shear strength | 65 | 108 | 120 | 158 | 181 |
| | Service load | 67 | 459 | 492 | 747 | 746 |
| B-2 | Flexural strength | 73 | 123 | 131 | 199 | 199 |
| | Shear strength | 70 | 118 | 130 | 172 | 196 |
| | Service load | 62 | 225 | 241 | 366 | 365 |
| B-3 | Flexural strength | 67 | 112 | 120 | 183 | 182 |
| | Shear strength | 68 | 114 | 126 | 166 | 189 |
| | Service load | 54 | 225 | 241 | 366 | 365 |
| B-4 | Flexural strength | 61 | 102 | 109 | 165 | 165 |
| | Shear strength | 67 | 112 | 124 | 164 | 187 |
| | Service load | 46 | 168 | 180 | 274 | 273 |
| B-5 | Flexural strength | 50 | 83 | 89 | 135 | 135 |
| | Shear strength | 63 | 105 | 116 | 153 | 175 |
| | Service load | 31 | 168 | 180 | 274 | 273 |
| B-6 | Flexural strength | 67 | 111 | 119 | 181 | 180 |
| | Shear strength | 59 | 98 | 109 | 144 | 164 |
| | Service load | 61 | 417 | 447 | 679 | 678 |
| See 4.6.1 for an explanation of the levels of a load rating analysis | | | | | | |

Only one deterioration model used in the examples was found to have a live load capacity exceeded by one or more legal-load vehicles. The deterioration model, Case A-3, included a 30-inch$^2$ spall and three severed strands. The weight restrictions were calculated as explained in Section 4.6.1 and are displayed in Figure 4-5 as an example weight limit sign to be posted at the bridge location. It should be noted that these values are different from those reported in the operating rating results of Table 4-7. This is because the vehicle with the smallest moment to weight ratio is used to determine operating ratings. After determining which vehicles exceed the live load capacity of the structure, the vehicle with the largest moment to weight ratio is used to determine the posted load. A significant reduction in weight of a 2 and 3-unit vehicle was found. The maximum legal-load vehicles, as shown in Table 4-8, are the weight limits for all other cases.
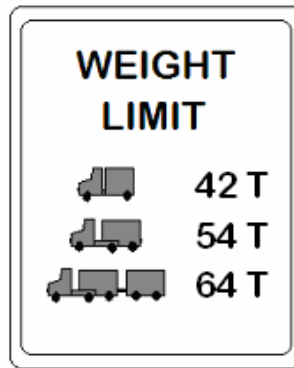


**Figure 4-5: Example of posted Michigan limits from load rating calculations (Case A-3)**

**Table 4-8: Maximum legal-load truck tonnage for Michigan**

| Legal-Load Truck | Max Weight (U.S. Tons) |
|---|---|
| 1-unit | 42 |
| 2-unit | 77 |
| 3-unit | 82 |

### 4.6.6 Load Rating Conclusions

Deterioration of prestressed concrete side-by-side box-beam bridges may produce a significant effect on a bridge load rating. Of the seven deteriorated beam models studied for this report, one indicated that weight limits should be posted for Michigan legal-load vehicles based on the outcome of the operating rating. Even more significant was the impact that deterioration had on the Federal inventory rating of the bridge structures. The inventory rating was greatly reduced due to the presence of deterioration for the cases studied. The shear strength of the beam and the tensile stress in the prestressing strand and concrete were the controlling factors. The *Bridge Analysis Guide* (MDOT 2003a) states that an agency may post a bridge at the inventory rating level in order to extend the life of the structure. A bridge posting is required for one of these bridges due to the operating rating and may be beneficial on other bridges based on their inventory rating.

This page intentionally left blank

CENTER FOR STRUCTURAL DURABILITY – Condition Assessment and Methods
of Abatement of Prestressed Concrete Box-Beam Deterioration

# Chapter 5: Field Inspection

## 5.1 Overview

A detailed field inspection of 15 side-by-side prestressed concrete box-beam bridges was performed. The condition of the box-beams, joints or shear keys, bearings, and deck were documented primarily by visual inspection. In select cases moisture assessment of beam flanges and shear keys were performed by thermographic imaging. Beam condition assessment was the primary focus of the field inspections. The condition data collected was the type, state (level or severity) and location of distresses on the beam. General observations of the pier and abutment conditions were also noted. Photographs depicting varying distress types and severity levels were taken.

In addition to the observations, the analysis of data collected from the field investigation of the 15 bridges and the summary of findings are presented at the end of this chapter.

## 5.2 Inspection Process

### 5.2.1 Documentation Review

Pre-inspection data was obtained from the bridge plans and recent inspection reports. Inspection reports were obtained from Pontis Version 4.2 (February 17, 2004) and bridge plans were obtained from the bridge hard copy files kept at the MDOT Construction & Technology (C&T) Division, Bridge Management Unit. The type of deck and wearing surface, and expansion joint locations are summarized in Appendix H. The inspection templates for documenting condition of bridge deck, beam fascia, beam flange, and shear keys were prepared using the bridge plans. Inspection templates for documenting the deck condition were also prepared.

### 5.2.2 Field Documentation

Field data and the associated photographs were documented on the templates. The completed templates contained the documentation of distress types and severity on the

beams, shear keys or joints, deck, and bearings if any. Inventory information were also incorporated in the templates such as, the bridge ID, location, bridge alignment, dimensions, number of beams, beam ID, etc. The following distress information was recorded on the templates:

- Moisture, efflorescence, and rust stains

- Deposits

- All cracks, their width, length, location, and orientation (horizontal, vertical, or diagonal)

- Spalls, spalled to steel (STS), and broken tendons

- High load hits (HLH) and associated damage on the fascia beams

- Repairs such as concrete patch, crack sealing, and locations

- General attributes such as beam cavity drain holes and stress pockets

- Shear key or joint conditions

- Bearing conditions if accessible

- Deck condition

- Condition of abutments and piers

The collected data were reviewed to ensure completeness. The data documented on the templates were then transferred to CAD drawings for processing. These AutoCAD templates for the 15 inspected bridges are included in Appendix J. A legend describing the symbols used to illustrate distress types is also shown in Appendix J.

A description was provided for each photograph including general location and field of view information. The weather condition at the time of inspection and the precipitation data for the week prior to inspection was researched and documented in order to establish the moisture exposure of the beams.

## 5.3 Inspection Data Review

The weather data for the nearest National Oceanic and Atmospheric Administration (NOAA) weather station was obtained from the National Climatic Data Center (NCDC) (www.ncdc.noaa.gov).

As noted previously that full-depth grouted shear keys in side-by-side box-beam bridges were introduced in 1985. Prior to 1985, partially grouted shear keys were used. Grout in these pre-1985 shear keys was not visible through the joints for inspection. Thus the grout condition column was not included in the inspection templates of the pre-1985 bridges.

The overview of findings and photographs from the inspection of each bridge is presented in Appendix I.

## 5.4 Inspection Data Processing

The field inspection data was documented on templates. The templates also included the bridge ID, location, alignment, dimensions, number of beams, and beam ID for every inspected beam. In addition to the beams, joints and/or shear keys were inspected and signs of distress/deterioration were recorded on the templates. Cracks on the beams were drawn to a rough approximation with respect to their length, location, and orientation. Corrosion, delamination, spall, moisture stain, efflorescence, deposit, and exposed rebar were sketched onto the templates to show approximate areas and locations. The qualitative field data recorded on the templates was converted to quantitative form for analyses.

### 5.4.1 Categorization of Distress and Severity

In analyzing the field data, the common distress types observed in the field were categorized and the severity levels were ranked from least serious to most serious. Table 5-1 displays the categories and severity levels developed based on the field observations. Table 5-2 shows the condition and condition categories for the shear keys, bearings, and drain holes. The index numbers of the severity levels and conditions are the numbers used to formulate the quantitative field data summary table of the inspected bridges. An example from one of the older bridges (S11 of 38101) is shown in Table 5-3 and from one of the newer bridges (S08

of 41131) is shown in Table 5-4. In the tables for the newer bridges the shear key column is added, which is not included in the tables for older bridges built before 1985. As discussed earlier, box-beams with partially grouted shear keys were used prior to 1985. Grout in these shear keys is not visible through the joints for inspection; therefore, there is no shear key condition described for bridges built before 1985.

The length of the crack and the size of the spall were measured and recorded in the crack and spall columns of the tables. A particular crack or spall, is grouped in one of the following locations: upper beam end, lower beam end, upper quarter point, lower quarter point, and mid-span. In the case of spalls, it was also noted in the column along joint/shear key, whether the spall was observed along the beam edges or shear keys. See Figure 5-1 for location definition. The condition summary tables of for all 15 bridges are included in Appendix K.

**Table 5-1: Categories and severity levels of common observed distress**

| Category | Severity Levels |
|---|---|
| **Moisture** | 1. Moisture stains along the beam edges<br>2. Moisture stains or fully moist beam flange<br>3. Efflorescence along the beam edges<br>4. Efflorescence on portions or throughout the beam flange<br>5. Deposits along the beam edges |
| **Crack** | Beam Fascia<br>    1. Shear cracks<br>    2. High load hit (HLH)<br><br>Beam Flange<br>    Locations: beam ends, beam quarter points, beam mid-span<br>    3. Crack<br>    4. Crack leaching efflorescence<br>    5. Crack leaching rust stains |
| **Spall** | Locations: beam ends, beam quarter points, beam mid-span, along joint/shear key<br>    1. Spall<br>    2. Spall to Steel (STS)<br>    3. Patched (repaired) |

**Table 5-2: Conditions noted for shear key, bearing, and drain hole**

| Component | Conditions Noted |
|---|---|
| **Shear Key** | 1. Moisture<br>2. Efflorescence<br>3. Deposit<br>4. Crack<br>5. Spall or missing grout |
| **Bearing** | If the bearings are visible the following were noted:<br>1. Good condition<br>2. Sign of Rusting<br>3. Excessive Movement<br>4. Frozen Mechanisms |
| **Drain Hole** | If there are drain holes, the following were noted:<br>1. Clean<br>2. Moisture<br>3. Efflorescence/deposits<br>4. Rust staining |

CENTER FOR STRUCTURAL DURABILITY – Condition Assessment and Methods
of Abatement of Prestressed Concrete Box-Beam Deterioration

81

**Table 5-3:  Quantitative inspection data table for span 1 of S11 of 38101**

| BM ID | BM FASCIA | | | BM SOFFIT — Crack | | | | | BM SOFFIT — Spall | | | | | | | | BEARING | POPOUT | COMMENTS |
| --- | --- | --- | --- | --- | --- | --- | --- | --- | --- | --- | --- | --- | --- | --- | --- | --- | --- | --- | --- |
| | moist | shear | HLH | bm ends upper | bm ends lower | quarter pts upper | quarter pts lower | mid span | bm ends upper | bm ends lower | quarter pts upper | quarter pts lower | mid span | along joint/ shear key | moist | DH | | | |
| **S11 of 38101 - Year Built 1958** | | | | | | | | | | | | | | | | | | | |
| **Span 1** | | | | | | | | | | | | | | | | | | | |
| EF | | 1 | | 2 | | 2 | | 2 | | | | | | | 5 | | | 5 | 1 stress pocket at mid span, 1 patch (repair) on fascia bm |
| EF | | | | | 2 | | 2 | | | | | | | | | | | | |
| 1 | | | | 1 | | 1 | | 1 | | | | | | | 5 | | | 2 | |
| 1 | | | | 2 | | | | | | | | | | | | | | | |
| 1 | | | | | | 2 | | | | | | | | | | | | | |
| 1 | | | | | | | | 2 | | | | | | | | | | | |
| 2 | | | | | | | | | | | | | | | 5 | | | 7 | |
| 3 | | | | | | | | | | | | | | | 5 | | | 5 | |
| 4 | | | | | | | | | | | | | | | 5 | | | 4 | |
| 5 | | | | | | | | | | | | | | | 5 | | | 5 | |
| 6 | | | | | | | | | | | | | | | 5 | | | 5 | rust stains throughout the bm |
| 7 | | | | | | | | | | | | | 1 | | 1 | 5 | | | 8 | rust stains throughout the bm |
| 8 | | | | | | | | | | | | | 1 | | 1 | 5 | | | 7 | rust stains at upper bm end |
| 9 | | | | | | | | | | | | | | | 5 | | | 8 | |
| WF | 4 | 1 | | 2 | 2 | 2 | 2 | 2 | | | | | | | 5 | | | 4 | |
| WF | | | | | 2 | | 2 | 2 | | | | | | | | | | | 1 spall on fascia bm |
| WF | | | | 2 | | | | | | | | | | | | | | | |
| WF | | | | | | 2 | | | | | | | | | | | | | |
| **Total** | 1 | 2 | | 5 | 4 | 4 | 3 | 5 | | | | | 2 | | 2 | 11 | | | 60 | |

EF – East Fascia, WF – West Fascia, DH – Drain Hole

**Table 5-4:  Quantitative inspection data table for span 4 of S08 of 41131**

| BM ID | BM FASCIA | | | BM SOFFIT — Crack | | | | | BM SOFFIT — Spall | | | | | | | | BEARING | SHEAR KEY | | | | | COMMENTS |
| --- | --- | --- | --- | --- | --- | --- | --- | --- | --- | --- | --- | --- | --- | --- | --- | --- | --- | --- | --- | --- | --- | --- | --- |
| | moist | shear | HLH | bm ends upper | bm ends lower | quarter pts upper | quarter pts lower | mid span | bm ends upper | bm ends lower | quarter pts upper | quarter pts lower | mid span | along joint/ shear key | moist | DH | | moist | efflor | dep | shear crack | MG (spall) | |
| **S08 of 41131 - Year Built 1993** | | | | | | | | | | | | | | | | | | | | | | | |
| **Span 4** | | | | | | | | | | | | | | | | | | | | | | | |
| SF | 4 | | | | | | | | | | | | | | 4 | 3 | 2 | | 1 | 1 | 1 | | 4 stress pockets on fascia bm |
| 1 | | | | | | | | | | | | | | | 4 | 3 | 2 | 1 | 1 | | 1 | 1 | |
| 2 | | | | | | | | | | | | | | | 4 | 3 | 2 | 1 | 1 | | 1 | 1 | |
| 3 | | | | | | | | | | | | | | | 4 | 3 | 2 | 1 | 1 | | 1 | 1 | |
| 4 | | | | | | | | | | | | | | | 4 | 3 | 2 | 1 | 1 | | 1 | 1 | |
| 5 | | | | | | | | | | | | | | | 4 | 3 | 2 | 1 | 1 | | 1 | 1 | |
| 6 | | | | | | | | | | | | | | | 4 | 3 | 2 | 1 | 1 | | 1 | 1 | |
| 7 | | | | | | | | | | | | | | | 4 | 3 | 2 | 1 | 1 | | 1 | 1 | |
| 8 | | | | | | | | | | | | | | | 4 | 3 | 2 | 1 | 1 | | 1 | 1 | |
| 9 | | | | | | | | | | | | | | | 4 | 3 | 2 | 1 | 1 | | 1 | 1 | |
| 10 | | | | | | | | | | | | | | | 4 | 3 | 2 | 1 | 1 | | 1 | 1 | |
| 11 | | | | | | | | | | | | | | | 4 | 3 | 2 | 1 | 1 | | 1 | 1 | |
| 12 | | | | | | | | | | | | | | | 4 | 3 | 2 | 1 | 1 | | 1 | 1 | |
| 13 | | | | | | | | | | | | | | | 4 | 3 | 2 | 1 | 1 | | 1 | 1 | |
| 14 | | | | | | | | | | | | | | | 4 | 3 | 2 | 1 | 1 | | 1 | 1 | |
| 15 | | | | | | | | | | | | | | | 4 | 3 | 2 | 1 | 1 | | 1 | 1 | |
| 16 | | | | | | | | | | | | | | | 4 | 3 | 2 | 1 | 1 | | 1 | 1 | |
| 17 | | | | | | | | | | | | | | | 4 | 3 | 2 | | 1 | 1 | 1 | | |
| NF | 4 | | | | | | | | | | | | | | 4 | 3 | 2 | | | | | | 4 stress pockets on fascia bm |
| **Total** | 2 | | | | | | | | | | | | | | 19 | 19 | | | 16 | 18 | 2 | 18 | 16 | |

SF – South Fascia, NF – North Fascia, MG – Missing grout (spall), dep – deposits (heavy $CaCO_3$ deposits).
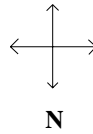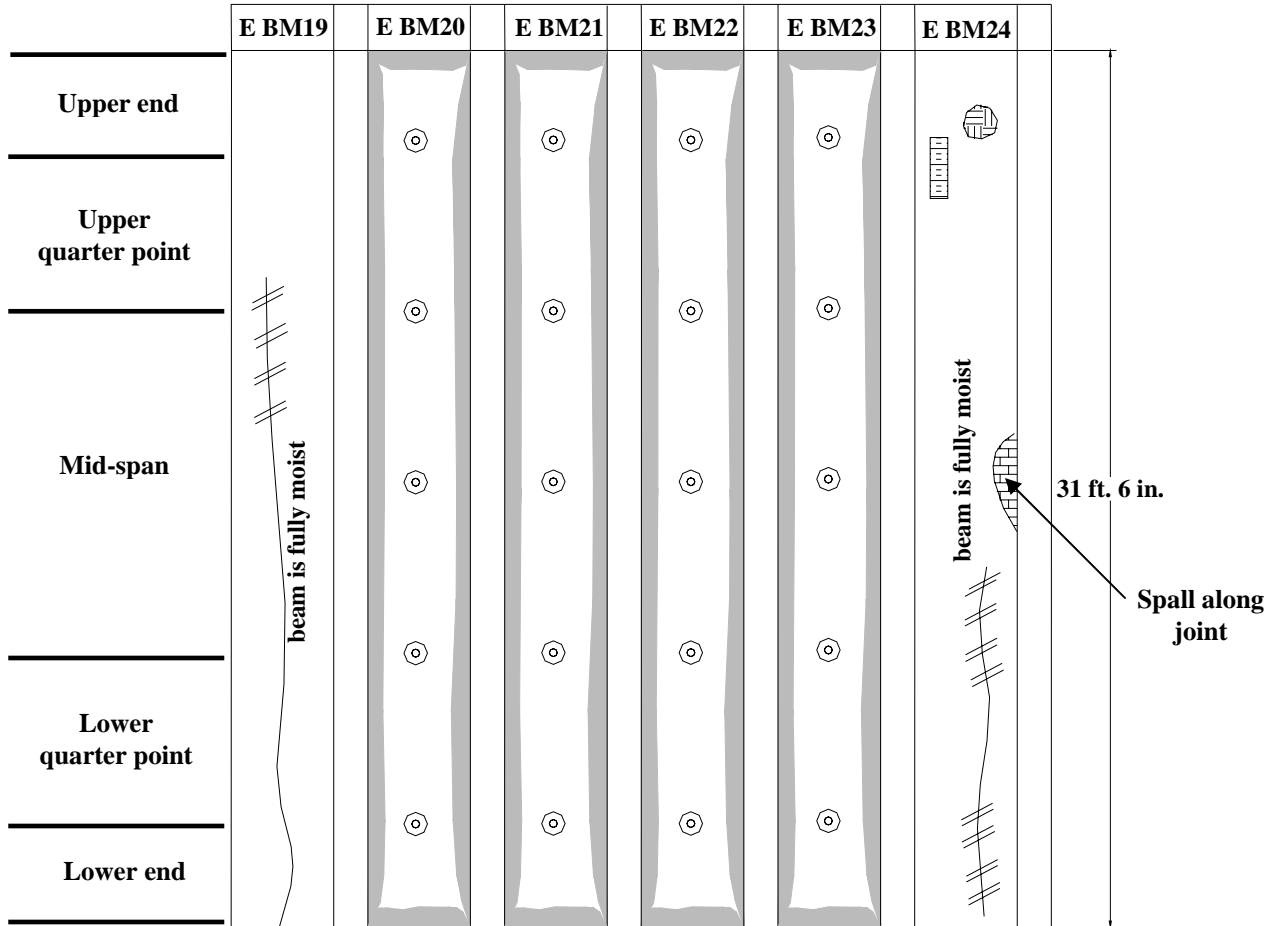
**Figure 5-1: Sample inspection template after processing for field inspection data compilation**

Note: S SP1 – South span 1, E BM – East beam

CENTER FOR STRUCTURAL DURABILITY – Condition Assessment and Methods
of Abatement of Prestressed Concrete Box-Beam Deterioration

83

### 5.4.2  Summary of Quantitative Inspection Data

Upon reviewing the quantitative inspection data, the major distress types can be categorized into three stages:  beam and/or shear key moisture, beam cracking, and spalls.

#### 5.4.2.1  *Beam Moisture Condition*

Prolonged moisture exposure allows water penetration into the concealed sides of the beams. The moisture source appears to be surface water leaking from the deck cracks into the shear keys. Some beams become saturated as observed on the flange.  Also repeated moisture exposure leads to efflorescence along the beam edges, shear keys and occasionally along the beam flanges.  Calcium carbonate ($CaCO_3$) deposits along the beam edges are observed indicating long term moisture exposure.  Figure 5-2 shows the beam moisture conditions for the 15 bridges. Nearly all inspected beams showed prolonged exposure to moisture except for one bridge.
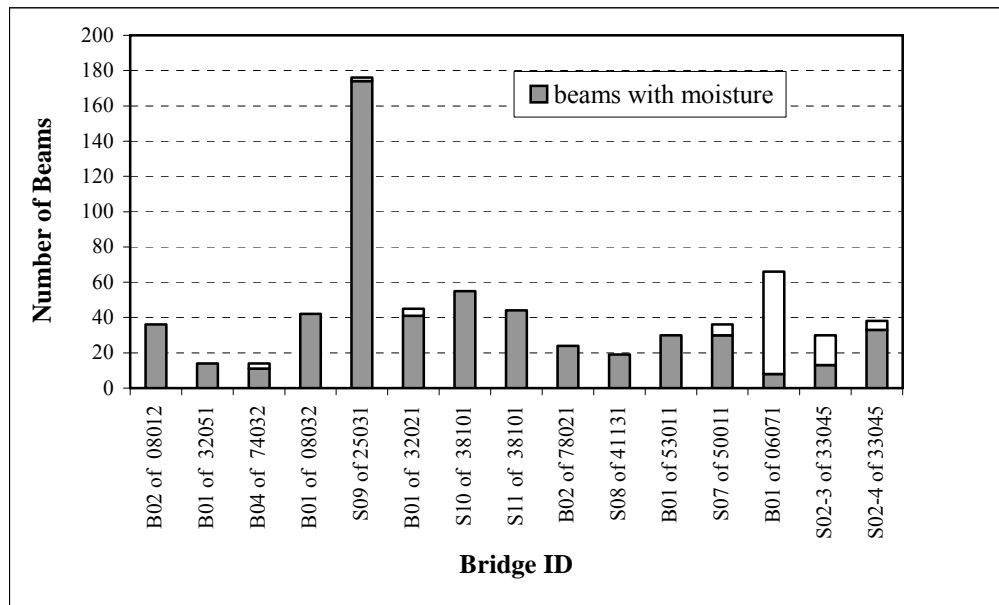


**Figure 5-2:  Observed beam moisture condition of the bridges inspected**

#### 5.4.2.2  *Cracked Beams*

Prolonged moisture exposure initiates tendon corrosion which may cause concrete cracking. An additional mechanism may be beam flange cracking by the outward pressure generated

by the freezing of water collected in the hollow cells. Longitudinal cracking on the beam flanges were common to bridges built before 1985. Beams designed in the 1950's and 1960's did not have stirrups in the bottom flange to control cracking. A summary showing the number of cracked beams of bridges built before 1985 is given in Figure 5-3. All types of cracks observed on the bottom flange were taken into consideration for generating Figure 5-3. For bridges built after 1985, longitudinal cracking was not observed.
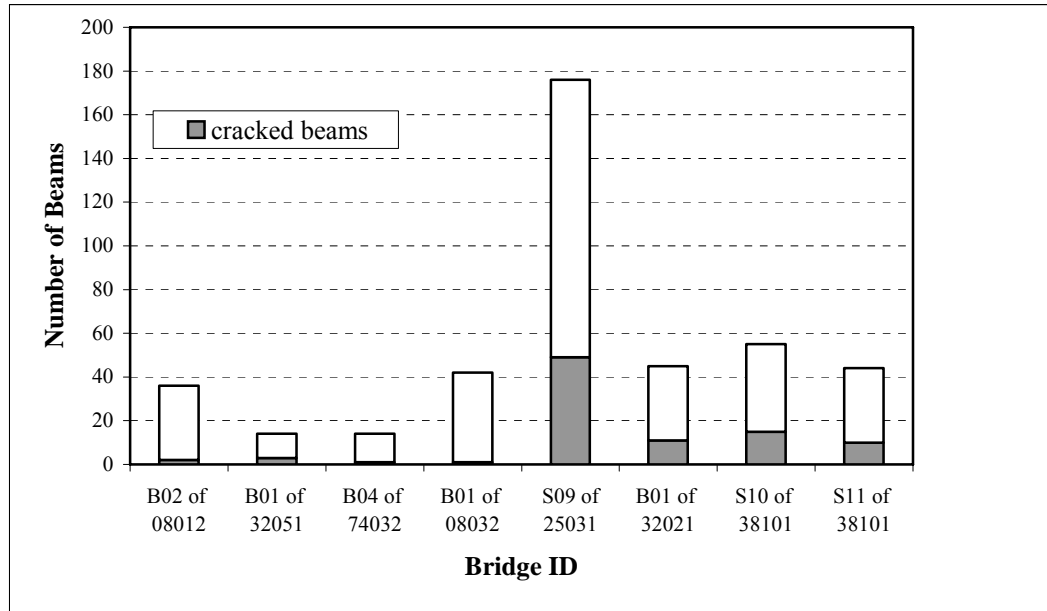


**Figure 5-3: Number of longitudinally cracked beams on bridges built before 1985**

The cracking location along the beam length was documented. Figure 5-4 shows the locations of the cracks along the beam length. As seen in the figure there are no dominant crack locations.

CENTER FOR STRUCTURAL DURABILITY – Condition Assessment and Methods
of Abatement of Prestressed Concrete Box-Beam Deterioration

85
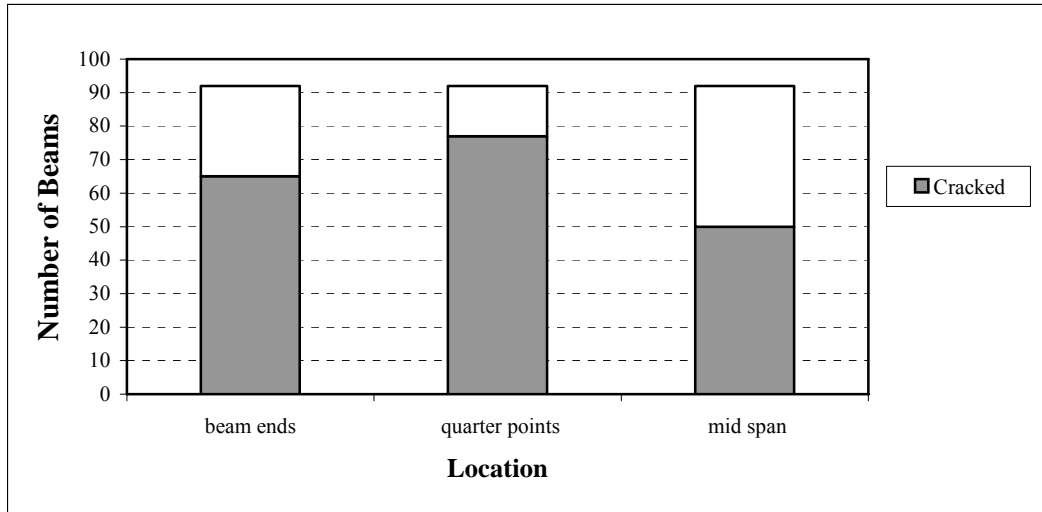
**Figure 5-4: Number of cracks at specified locations along the beam length**

The severity of the cracks was noted for each beam. The three severity levels defined were: only crack, crack with efflorescence, and crack with rust stains. Very few cracks showed rust stains, the majority of the cracks were cracks or cracks with efflorescence. A summary of the severity levels of cracked beams is shown in Figure 5-5.
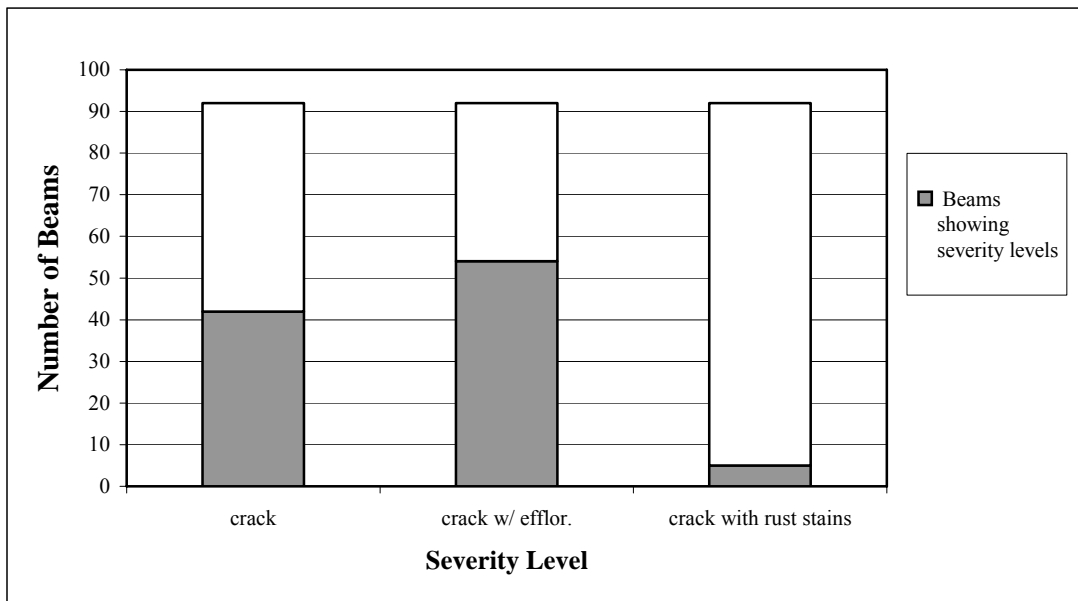


**Figure 5-5: Summary of crack severity levels on beams**

## 5.4.2.3  *Beams with Spalls*

Prolonged moisture exposure initiates tendon and rebar corrosion which will result in delamination, cracking, and spalling of concrete. Corrosion stains were visible along the cracks on the bottom flange. The summary of beams with spalls on bridges built before 1985 is given in Figure 5-6. Concrete spalling was not observed on bridges constructed after 1985. The majority of concrete spalls were concentrated along the beam edges. Tendon breakage was observed infrequently.
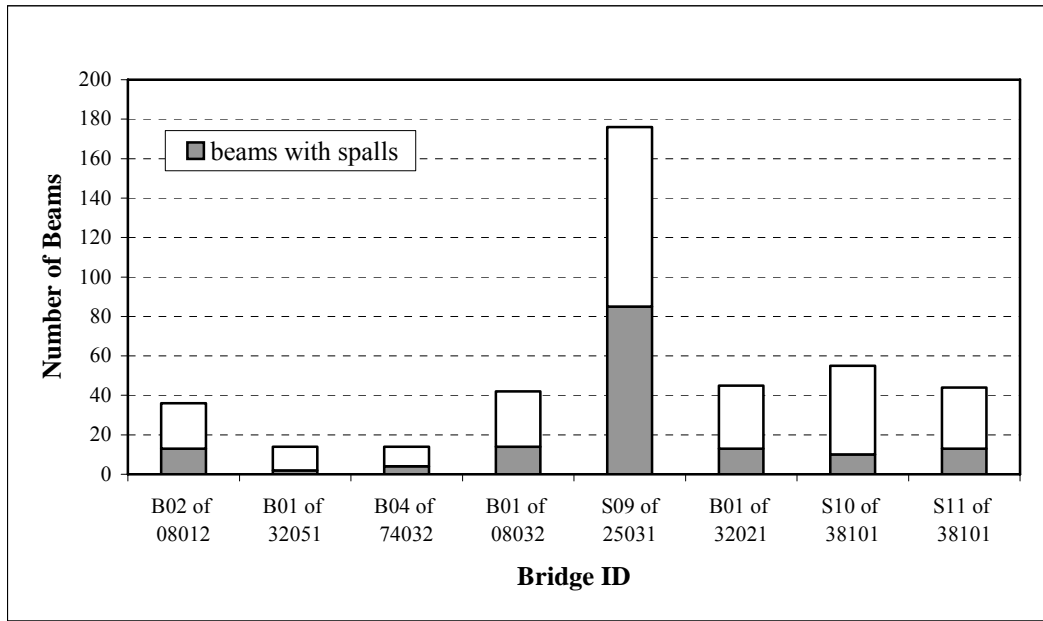


**Figure 5-6:  Summary of beams with spalls for bridges built before 1985**

The spall locations were documented. Beams with spalls at the ends, quarter points, and midspan were documented. Also, spalls along the beam edges or shear key were noted. Figure 5-7 shows the spall locations on the beams. It appears that the spall locations are evenly distributed along the beam length.

CENTER FOR STRUCTURAL DURABILITY – Condition Assessment and Methods
of Abatement of Prestressed Concrete Box-Beam Deterioration

87
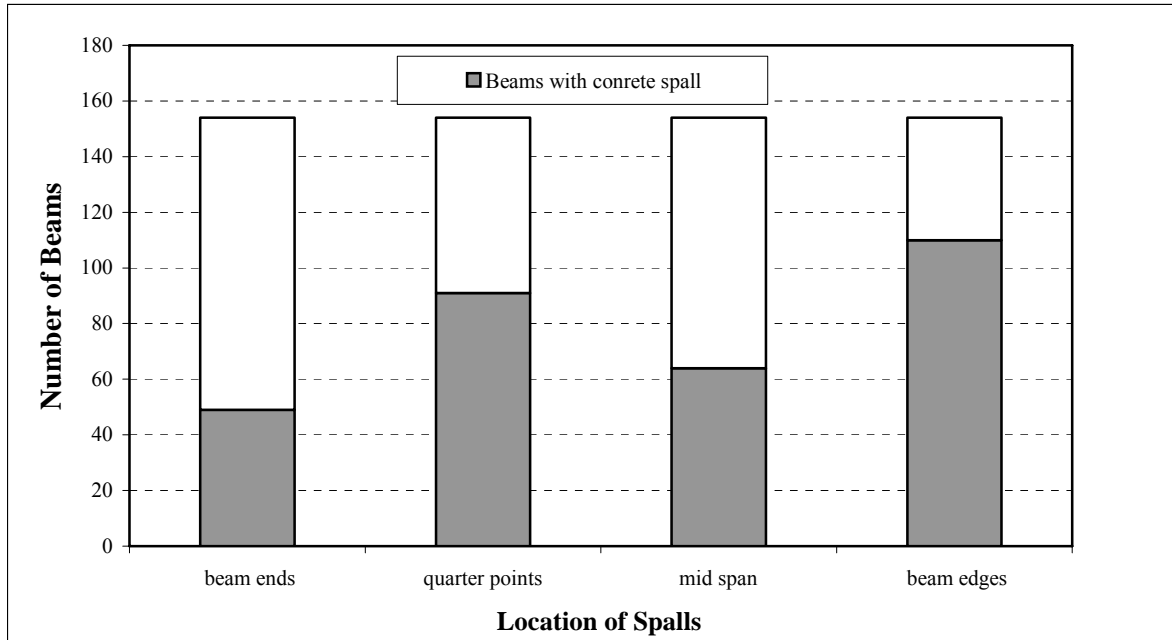
**Figure 5-7: Summary of location of spalls**

The severity of the spalls was noted. Three categories for severity levels were defined: repaired spall, surface spall, and spall to steel (STS). Only a few beams with repairs were documented, STS was apparent on some beams, and surface spalls were observed on many beams. A summary of the severity levels of spalls documented is shown in Figure 5-8.
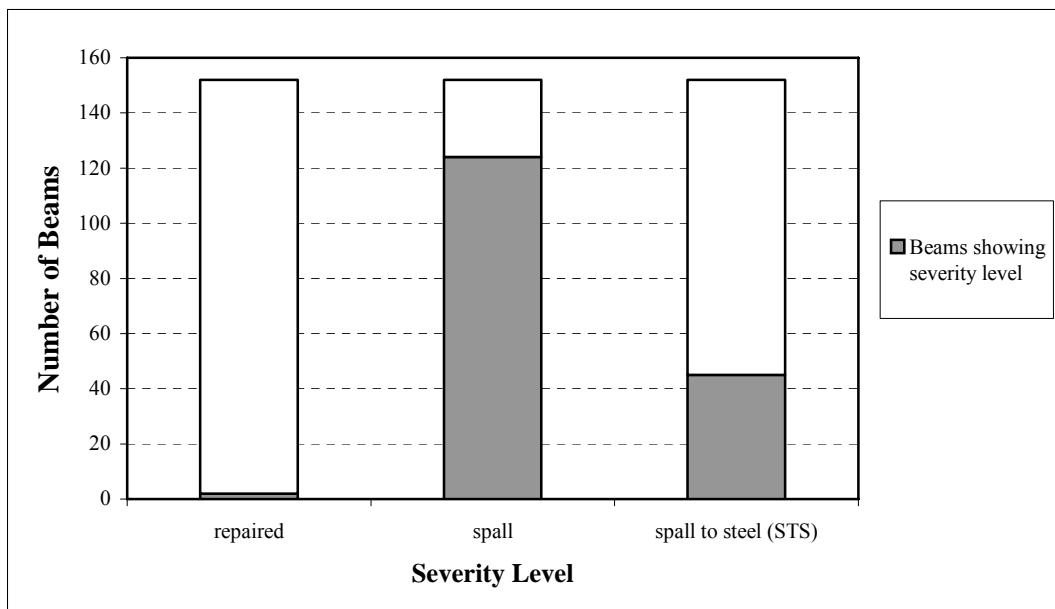


**Figure 5-8: Summary of the severity levels of spalls**

*5.4.2.4 Summary of Shear Key Conditions*

Prior to 1985, partially grouted shear keys were used. The shear key conditions are only summarized for bridges built after 1985 as partially grouted shear keys are not visible from the bottom flanges.

The common types of distress observed in the shear keys were signs of moisture (moisture stains, efflorescence or deposits) and cracked or spalled grout. Figure 5-9 shows the shear key moisture condition. Figure 5-10 shows the shear key cracked/spalled condition. A majority of shear keys show repeated and prolonged moisture exposure. Shear keys of the majority of bridges were cracked or exhibited spalled grout.
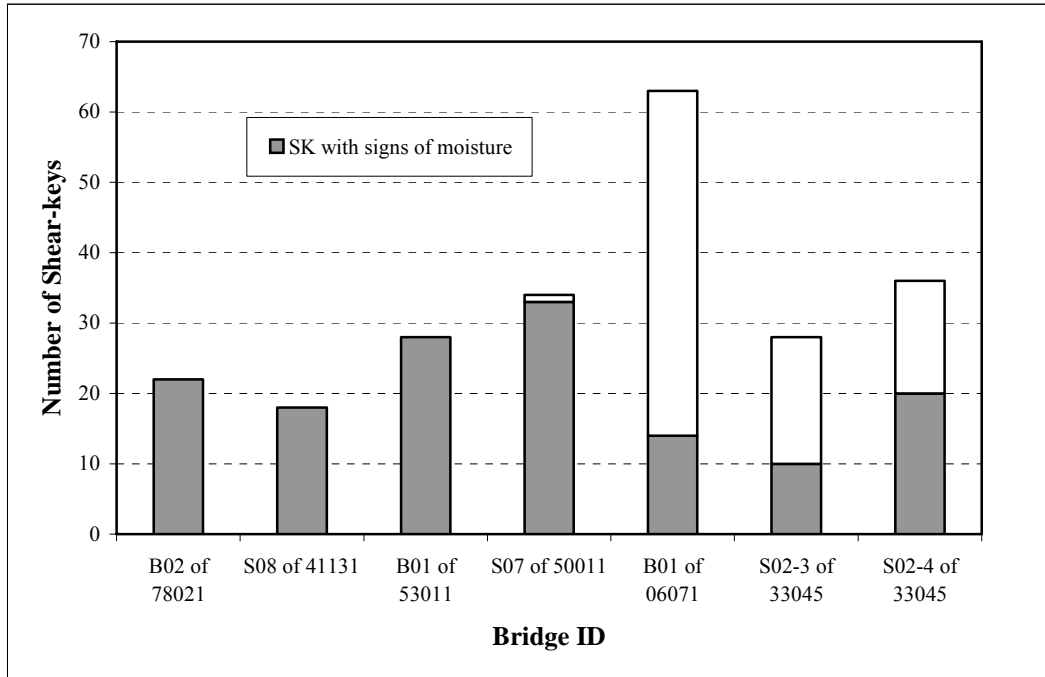


**Figure 5-9: Shear key moisture conditions (bridges built after 1985)**

CENTER FOR STRUCTURAL DURABILITY – Condition Assessment and Methods
of Abatement of Prestressed Concrete Box-Beam Deterioration

89
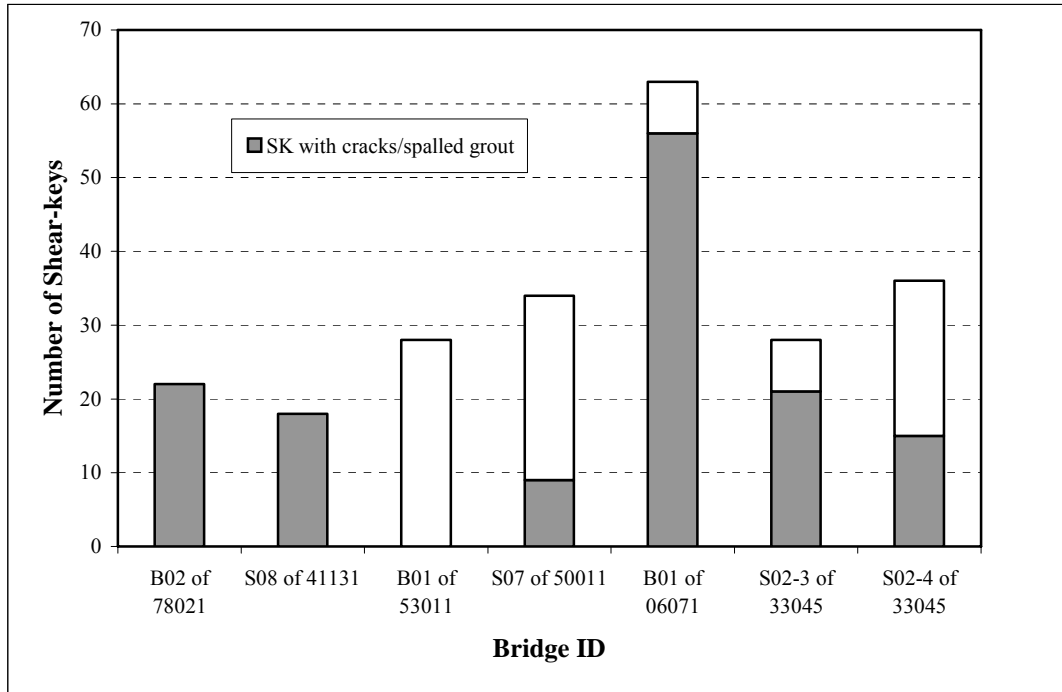
**Figure 5-10:  Shear key cracked/spalled condition (bridges built after 1985)**

## 5.4.2.5   Beam Fascia Conditions

The beam fascia conditions were quantitatively analyzed as shown in the following tables. Table 5-5 summarizes the beam fascia condition of the 15 bridges inspected.  Figure 5-11 to Figure 5-14 illustrate the beam fascia moisture conditions, shear cracks, spalls, and beam fascias with high load hits (HLH), respectively, of the 15 bridges inspected.  Table 5-6 summarizes the condition of the 15 bridges inspected.

**Table 5-5: Summary of beam fascia conditions for the 15 bridges inspected**

| No. | Bridge ID | Year Built | # of beams inspected | Beam Fascia | | | | |
|---|---|---|---|---|---|---|---|---|
| | | | | # of beam fascia inspected | # with shear cracks | # with spalls | # with moisture | # HLH |
| 1 | B02 of 08012 | 1956 | 36 | 6 | 0 | 0 | 6 | 1 |
| 2 | B01 of 32051 | 1957 | 14 | 2 | 0 | 0 | 0 | 0 |
| 3 | B04 of 74032 | 1957 | 14 | 2 | 0 | 0 | 0 | 0 |
| 4 | B01 of 08032 | 1957 | 42 | 6 | 0 | 1 | 4 | 0 |
| 5 | S09 of 25031 | 1958 | 176 | 8 | 4 | 2 | 3 | 2 |
| 6 | B01 of 32021 | 1958 | 45 | 6 | 0 | 1 | 0 | 0 |
| 7 | S10 of 38101 | 1958 | 55 | 10 | 1 | 1 | 9 | 1 |
| 8 | S11 of 38101 | 1958 | 44 | 8 | 4 | 3 | 5 | 3 |
| | **Total (built before 1974)** | | **426** | **48** | **9** | **8** | **27** | **7** |
| 9 | B02 of 78021 | 1989 | 24 | 4 | 1 | 0 | 3 | 0 |
| 10 | S08 of 41131 | 1993 | 19 | 2 | 0 | 0 | 2 | 0 |
| 11 | B01 of 53011 | 1993 | 30 | 4 | 0 | 0 | 4 | 0 |
| 12 | S07 of 50011 | 1994 | 36 | 4 | 4 | 0 | 2 | 0 |
| 13 | B01 of 06071 | 1998 | 66 | 6 | 0 | 0 | 0 | 0 |
| 14 | S02-3 of 33045 | 2000 | 30 | 4 | 0 | 0 | 0 | 0 |
| 15 | S02-4 of 33045 | 2000 | 38 | 4 | 0 | 0 | 0 | 0 |
| | **Total (built after 1985)** | | **243** | **28** | **5** | **13** | **11** | **0** |
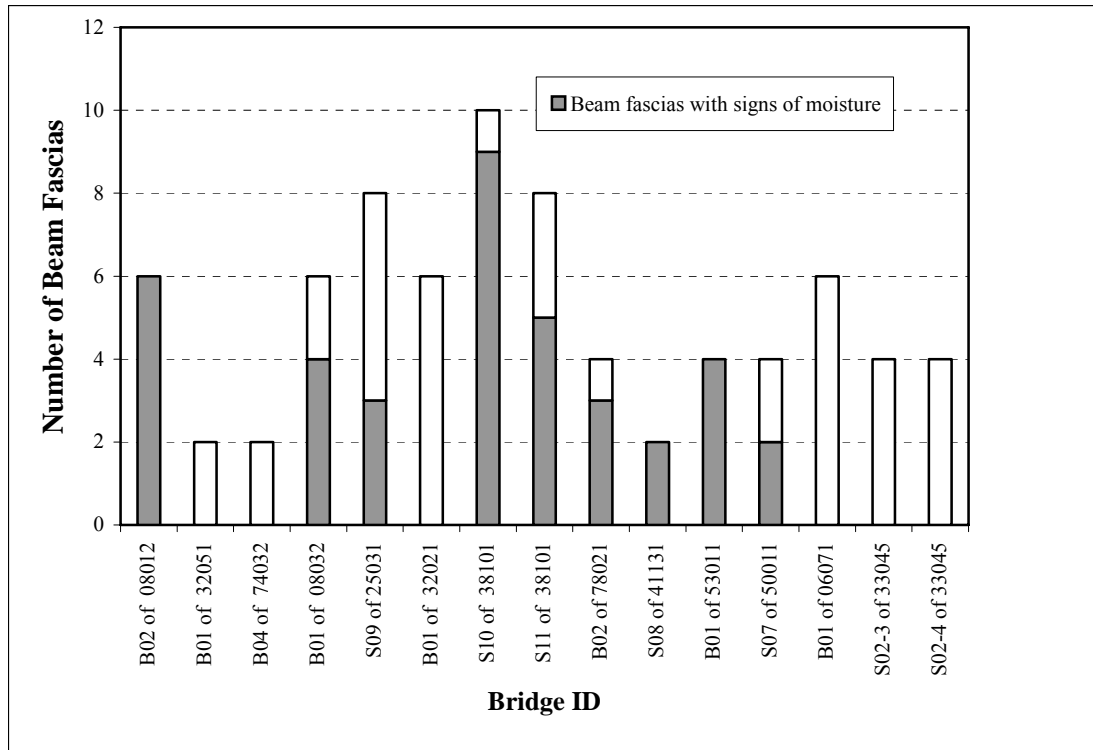


**Figure 5-11: Beam fascia moisture conditions**

CENTER FOR STRUCTURAL DURABILITY – Condition Assessment and Methods of Abatement of Prestressed Concrete Box-Beam Deterioration

91

**Figure 5-12:  Beam fascias with shear cracks**
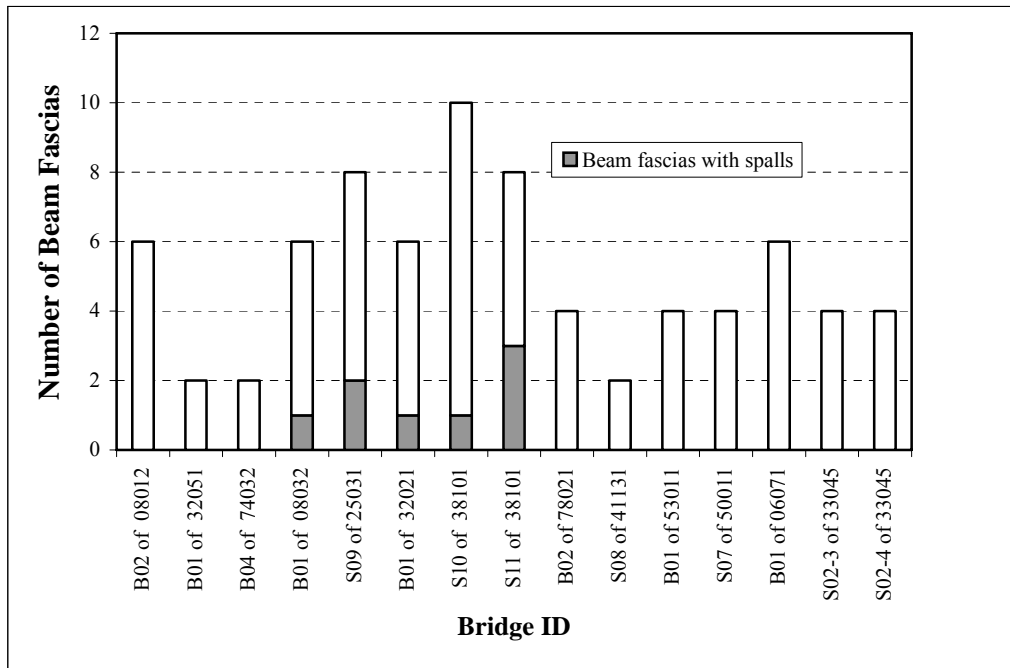


**Figure 5-13:  Beam fascias with spalls**
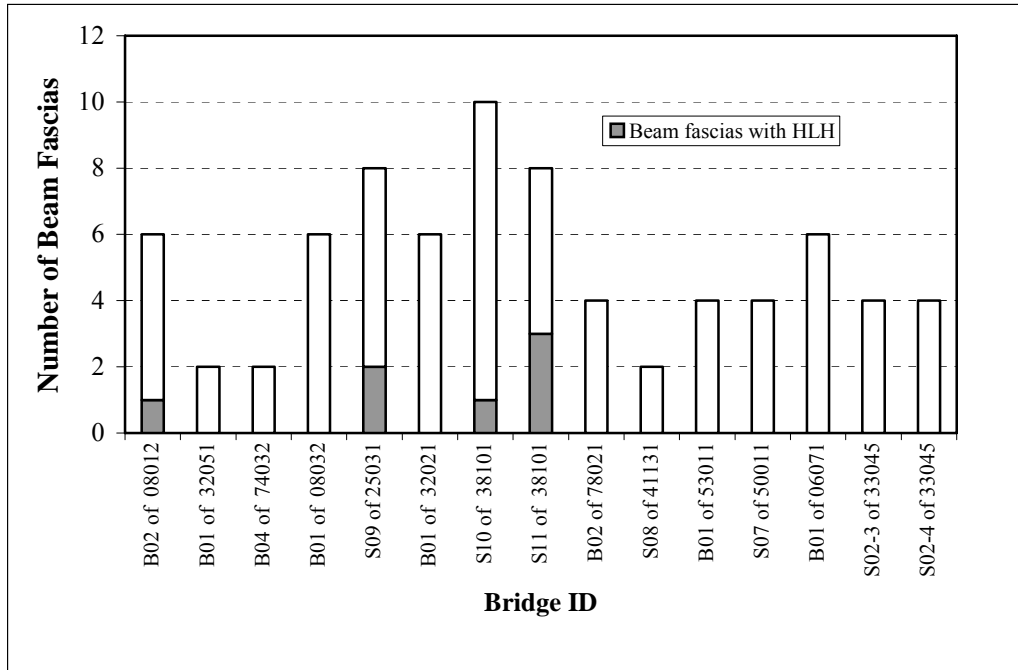
**Figure 5-14: Beam fascias with HLH**

CENTER FOR STRUCTURAL DURABILITY – Condition Assessment and Methods
of Abatement of Prestressed Concrete Box-Beam Deterioration

93

Table 5-6: Condition and condition states of the inspected bridges

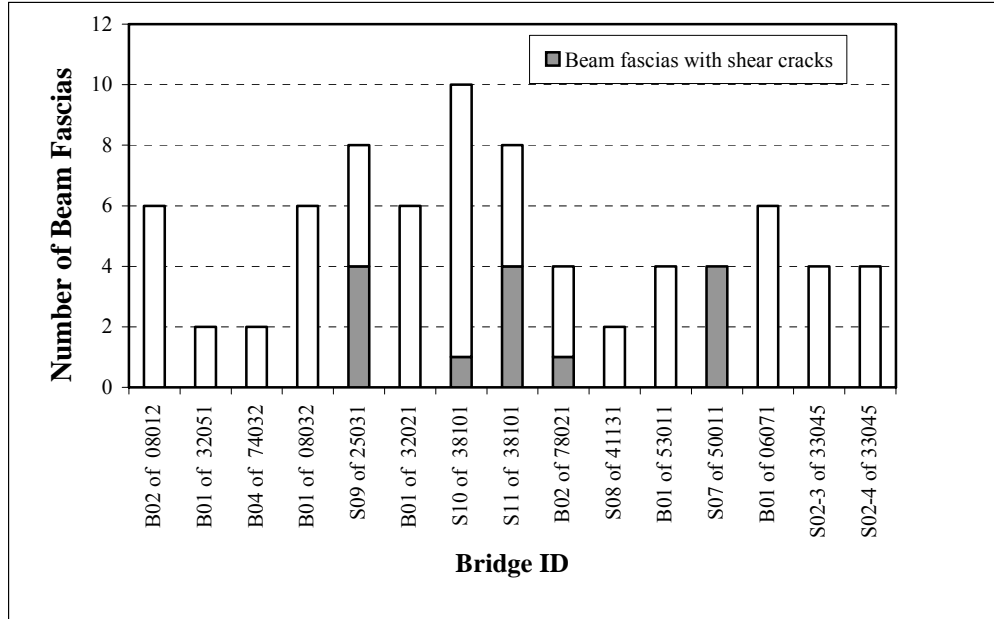| No. | Bridge ID | Year Built | # of bms inspected | Cracks | | | | | Spalls | | | | | | # of bms w/ moist | Shear Key | | | | | Bearing | DH |
|---|---|---|---|---|---|---|---|---|---|---|---|---|---|---|---|---|---|---|---|---|---|---|
| | | | | bm ends | quarter pts | mid span | # of cracks | # of cracked bms | bm ends | quarter pts | mid span | along joint/ sk | # of spalls | # of bms w/spall | | moist | efflor | dep | shear crack | MG | | |
| 1 | B02 of 08012 | 1956 | 36 | 0 | 0 | 2 | 2 | 2 | 9 | 5 | 5 | 11 | 23 | 13 | 36 | not applicable | | | | | rusted | N |
| 2 | B01 of 32051 | 1957 | 14 | 2 | 2 | 1 | 4 | 3 | 0 | 1 | 1 | 1 | 3 | 2 | 14 | not applicable | | | | | not visible | N |
| 3 | B04 of 74032 | 1957 | 14 | 1 | 1 | 1 | 3 | 1 | 0 | 1 | 4 | 2 | 6 | 4 | 11 | not applicable | | | | | not visible | N |
| 4 | B01 of 08032 | 1957 | 42 | 0 | 0 | 1 | 2 | 1 | 3 | 8 | 8 | 3 | 27 | 14 | 42 | not applicable | | | | | rusted | N |
| 5 | S09 of 25031 | 1958 | 176 | 35 | 43 | 24 | 77 | 49 | 36 | 47 | 30 | 72 | 149 | 85 | 174 | not applicable | | | | | rusted where visible | 16 bms (spread box) |
| 6 | B01 of 32021 | 1958 | 45 | 7 | 10 | 6 | 22 | 11 | 3 | 11 | 5 | 1 | 18 | 13 | 41 | not applicable | | | | | rusted | Y |
| 7 | S10 of 38101 | 1958 | 55 | 11 | 11 | 7 | 47 | 15 | 4 | 9 | 4 | 7 | 14 | 10 | 55 | not applicable | | | | | rusted | Y |
| 8 | S11 of 38101 | 1958 | 44 | 9 | 10 | 8 | 39 | 10 | 3 | 9 | 7 | 13 | 22 | 13 | 44 | not applicable | | | | | not visible | 1 bm |
| | **Total (built before 1974)** | | **426** | **65** | **77** | **50** | **196** | **92** | **49** | **91** | **64** | **110** | **262** | **154** | **417** | | | | | | | |
| 9 | B02 of 78021 | 1989 | 24 | 0 | 0 | 0 | 0 | 0 | 0 | 0 | 0 | 0 | 0 | 0 | 24 | 0 | 22 | 0 | 22 | 1 | not visible | Y |
| 10 | S08 of 41131 | 1993 | 19 | 0 | 0 | 0 | 0 | 0 | 0 | 0 | 0 | 0 | 0 | 0 | 19 | 16 | 18 | 2 | 18 | 16 | rusted | Y |
| 11 | B01 of 53011 | 1993 | 30 | 0 | 0 | 0 | 0 | 0 | 0 | 0 | 0 | 0 | 0 | 0 | 30 | 0 | 28 | 0 | 0 | 0 | not visible | Y |
| 12 | S07 of 50011 | 1994 | 36 | 0 | 0 | 0 | 0 | 0 | 0 | 0 | 0 | 0 | 0 | 0 | 30 | 3 | 30 | 2 | 0 | 9 | good condition | Y |
| 13 | B01 of 06071 | 1998 | 66 | 0 | 0 | 0 | 0 | 0 | 0 | 0 | 0 | 0 | 0 | 0 | 8 | 0 | 14 | 0 | 56 | 1 | not visible | N |
| 14 | S02-3 of 33045 | 2000 | 30 | 0 | 0 | 0 | 0 | 0 | 0 | 0 | 0 | 0 | 0 | 0 | 13 | 10 | 0 | 0 | 21 | 0 | not visible | Y |
| 15 | S02-4 of 33045 | 2000 | 38 | 0 | 0 | 0 | 0 | 0 | 0 | 0 | 0 | 0 | 0 | 0 | 33 | 20 | 0 | 0 | 14 | 1 | good condition | Y |
| | **Total (built after 1985)** | | **243** | **0** | **0** | **0** | **0** | **0** | **0** | **0** | **0** | **0** | **0** | **0** | **157** | **49** | **112** | **4** | **131** | **28** | | |

## 5.5 Summary of Bridge Deck and Box-Beam Inspection Results

### 5.5.1 Bridge deck

The original wearing surface of inspected pre-19 bridges was either concrete or bituminous. In most cases the wearing surfaces had been replaced with an overlay of reinforced concrete or latex modified concrete or asphalt. When asphalt is used as the wearing surface a water proofing membrane is often placed over the beams. Longitudinal deck cracking and distressed joints over the abutments and piers were common to all bridges. On most of the pre-19 bridge decks, crack sealants were applied over the longitudinal cracks. Some of the large width longitudinal cracks were sealed; however, significant portions were not watertight. The concrete wearing surface on some of the bridge decks was patched, but cracking along the patch border allowed water penetration into the beams. The asphalt overlay with waterproofing membrane appeared to be an effective means of reducing water penetration. However, when a bridge is on a two-way road, the overlay is generally placed only on one half of the deck while the other half maintains traffic. In all cases inspected, a cold joint formed along the centerline of the deck and allowed water penetration. Expansion joints over the abutments and the piers exhibited extensive distress. The drainage systems of the older bridges were ineffective. This is demonstrated in one structure by scour observed next to the abutment which is an indication of the volume of water that flowed through the joint between the abutment and beams.

Longitudinal cracking was also common in post-1985 bridge decks. Most deck joints exhibited some form of distress or breakdown. In an effort to eliminate the joints over the piers and abutments, the recent practice is to place the deck slab continuous and to design the deck as a continuous member for live loads. After placing the deck slab, construction joints are sawed and sealed at specified locations (usually zero-moment locations) as given in the bridge plans. However, transverse cracking was still observed directly over the piers. In some cases, construction joints were inadequately sawed and cracks propagated within the vicinity of the saw cut joints.

### 5.5.2 Box-Beams

All the pre-1974 bridges showed signs of prolonged exposure to moisture along beam edges and beam bottom flanges. Partially grouted shear keys used in old bridges could not be visually inspected. Overnight rains sometimes helped to identify the leaky joints. Moisture on stub abutments was a clear indication of the volume of water that flowed through the shear keys. Heavy calcium carbonate deposits (efflorescence) signify the amount and length of time of leakage through the joint. The efflorescence on the web of the fascia beam is also due to leakage through the cold joint between the traffic barrier and the deck (Figure 5-15). The leakage from the joints over the piers and abutments lead to bearing corrosion. A maintenance program was initiated to drill drain holes along the beam bottom flanges to drain the water, if any, collected inside the box-beams. The rust stains around the drain holes is an indication of active corrosion.
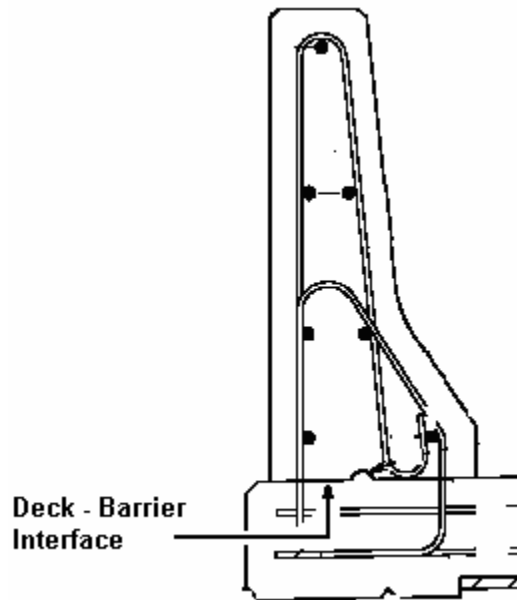


**Figure 5-15: Cold joint between the traffic barrier and the deck (deck-barrier interface)**

The repeated exposure to moisture and subsequently chlorides resulted in initiating and intensifying tendon corrosion, leading to loss of tendon cross-section, concrete cracking, delamination, spall, and finally the breaking of tendons. Delamination, spall and breakage of tendons were concentrated along the beam edges (areas of heavy moisture exposure).

Longitudinal cracking at the box- beam bottom flanges appears primarily due to corroding tendons. An additional mechanism may be beam flange cracking by the outward pressure generated by the freezing of water collected in the hollow cells. Corroded tie-rods, rust stain, and efflorescence were visible at the stress pockets. Exposed and broken tendons were also observed on fascia beams due to high-load-hits.

Full-depth shear keys, 6-inch cast-in-place concrete decks, and transverse post-tensioning tendons were standard details on the bridges that were built during or after 1985. Shear keys of even the very recent bridges, which were built in 2000, were moist and cracked. Grouting of the stress pockets of the fascia beams appeared inadequate. Efflorescence that was visible around the grouted stress pockets indicated a presence of moisture inside the post-tensioning ducts. The *Bridge Design Guide* (2003e) requires the longitudinal joints between beams to be grouted to the full-depth to form a tight and solid joint, yet the spalling of shear key grout upon transverse post-tensioning indicates grout voids. During the inspection it was possible to observe a corroding post-tensioning tendon through a shear key void of a bridge that was built in 2000.

### 5.5.3 Summary of inspection data

The objective of the field inspection was to document the type and progression of identified distress and to study the effects of evolving design procedures on side-by-side box-beam bridge superstructure performance. Nearly all the inspected beams showed prolonged exposed to moisture. The inspection data indicated that leaky expansion and construction joints, and surface water penetrating and leaking through the longitudinal cracking were common to all the bridges, regardless of the age. The precursor to beam distress was often the longitudinal deck cracking. Surface water penetrated through the longitudinal cracks, sometimes getting trapped within the shear keys. The beam sides concealed by the shear key were often saturated. Corrosion initiated when the moisture with chlorides penetrated to the tendons and stirrups. Prior to the 1970's, the box-beams were fabricated using stiffened cardboard to form the internal cavities. With leakage, water collected inside the boxes and initiated tendon corrosion which emanated itself as longitudinal cracks along the beam bottom flanges. A recent preventive maintenance application is now to drill holes at selected

CENTER FOR STRUCTURAL DURABILITY – Condition Assessment and Methods
of Abatement of Prestressed Concrete Box-Beam Deterioration

97

locations along the beam length to drain the trapped water. However, the beams with drain holes still show longitudinal cracking. The cracking progresses to concrete spalls. The majority of concrete spalls are concentrated along the beam edges. The ultimate state of distress, tendon breakage, was observed very infrequently.

# Chapter 6:  Analytical Modeling of a Single Box-Beam

## *6.1  Overview*

### 6.1.1  Objectives of the Analytical Modeling

The objective of the analytical (finite element – FE) modeling was to study the effects of various types and levels of distress on the load capacity of a discrete box-beam.  Two FE models were developed for flexure critical and shear critical beam lengths (see Section 6.2.2 for details of beam length and cross-section geometry selection procedures). Flexure and shear critical truckloads were selected from the group of Michigan legal vehicle loads given in the *Bridge Analysis Guide* (MDOT 2003a).  The load capacities of the box-beams were independently calculated for flexure and shear critical sections.

*Safety, serviceability, economy*, and *aesthetic* are the fundamental objectives of bridge design (Menn 1990).  Safety of the bridge is the single most important consideration. The bridge superstructure capacity assessment is performed with the documented knowledge of the physical condition and loading.  The *Bridge Analysis Guide* (MDOT 2003a) details guidelines for selecting dead and live loads for the capacity assessment of bridge superstructure.  FE modeling and analysis is an accepted and well-established technique used for the load carrying capacity assessment of bridge superstructure and components.

The physical condition of the beams and the remainder of the bridge were documented during the field inspection of 15 in-service side-by-side box-beam bridges.   The inspection data was compiled and analyzed.  Through the data analysis the common girder distress types and levels were identified and are presented in Chapter 5.  In this chapter, the capacities of the box-beams with the documented distress types and levels are evaluated using the finite element (FE) models.   The two FE box-beam models developed and utilized for this purpose are the flexural critical and shear critical span lengths. The box-beam capacities are established from the lowest capacity obtained at the critical sections considering the flexure critical and shear critical beam models and associated critical loads.

### 6.1.2 Bridge Superstructure Behavior

Side-by-side box-beam bridge superstructure is in reality an equivalent orthotropic plate. Plate orthotropy can be due to the geometry or material or both. Timoshenko (1940) described that the orthotropic plate behavior is governed by the Lagrange equation (Eq 6-1).

$$D_x \frac{\partial^4 w}{\partial x^4} + 2H \frac{\partial^4 w}{\partial x^2 \partial y^2} + D_y \frac{\partial^4 w}{\partial y^4} = p(x, y) \tag{6-1}$$

where,     $2H = (D_{xy} + D_{yx} + D_1 + D_2)$  (6-2)

Flexural, torsional, and coupling rigidities of a plate of thickness, $h$, are given below.

$$D_x = \frac{E_x h^3}{12(1 - \upsilon_x \upsilon_y)} \tag{6-3}$$

$$D_y = \frac{E_y h^3}{12(1 - \upsilon_x \upsilon_y)} \tag{6-4}$$

$$D_{xy} = \frac{G_{xy} h^3}{6} \tag{6-5}$$

$$D_{yx} = \frac{G_{yx} h^3}{6} \tag{6-6}$$

$$D_1 = \frac{E_x h^3 \upsilon_y}{12(1 - \upsilon_x \upsilon_y)} \tag{6-7}$$

$$D_2 = \frac{E_y h^3 \upsilon_x}{12(1 - \upsilon_x \upsilon_y)} \tag{6-8}$$

$E_x$, $E_y$, $\upsilon_x$, and $\upsilon_y$ are the equivalent elasticity modulus and Poisson's ratio of the plate in x- and y- directions, respectively. Equation (6-1) is derived by considering the equation of equilibrium (Equation 6-9) of the plate shown in Figure 6-1. Moments and shear forces acting on the plate and the associated stresses and strains can be calculated from equations 6-10 through 6-21 using the deflected shape of the plate ($w$) under a known loading condition ($p(x,y)$) and the flexural and torsional rigidities of the plate.
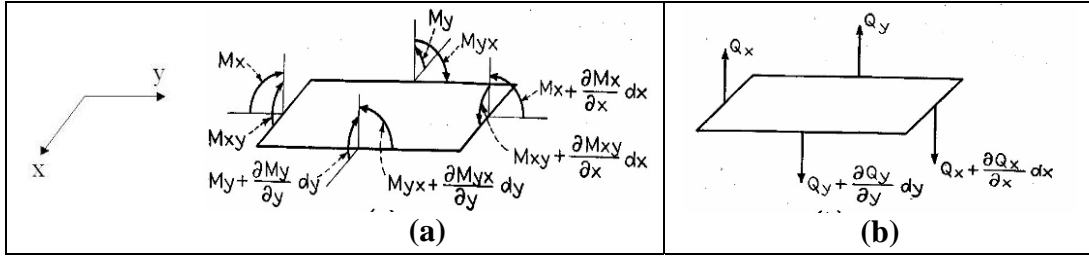
**Figure 6-1: Incremental changes to moments and shear forces acting on the middle plane of an infinitesimal plate element**

$$\frac{\partial^2 M_x}{\partial x^2} + \frac{\partial^2 M_{yx}}{\partial x \partial y} + \frac{\partial^2 M_y}{\partial y^2} - \frac{\partial^2 M_{xy}}{\partial x \partial y} = -p(x, y) \tag{6-9}$$

$$M_x = -\left[ D_x \frac{\partial^2 w}{\partial x^2} + D_1 \frac{\partial^2 w}{\partial y^2} \right] \tag{6-10}$$

$$M_y = -\left[ D_y \frac{\partial^2 w}{\partial y^2} + D_2 \frac{\partial^2 w}{\partial x^2} \right] \tag{6-11}$$

$$M_{xy} = D_{xy} \frac{\partial^2 w}{\partial x \partial y} \tag{6-12}$$

$$M_{yx} = -D_{yx} \frac{\partial^2 w}{\partial x \partial y} \tag{6-13}$$

$$Q_x = -\left[ D_x \frac{\partial^3 w}{\partial x^3} + (D_{yx} + D_1) \frac{\partial^3 w}{\partial x \partial y^2} \right] \tag{6-14}$$

$$Q_y = -\left[ D_y \frac{\partial^3 w}{\partial y^3} + (D_{xy} + D_2) \frac{\partial^3 w}{\partial y \partial x^2} \right] \tag{6-15}$$

$$\sigma_x = \frac{-E_x z}{(1 - \nu_x \nu_y)} \left[ \frac{\partial^2 w}{\partial x^2} + \nu_y \frac{\partial^2 w}{\partial y^2} \right] \tag{6-16}$$

$$\sigma_y = \frac{-E_y z}{(1 - \nu_x \nu_y)} \left[ \frac{\partial^2 w}{\partial y^2} + \nu_x \frac{\partial^2 w}{\partial x^2} \right] \tag{6-17}$$

$$\tau_{xy} = -2Gz \frac{\partial^2 w}{\partial x \partial y} \tag{6-18}$$

$$\varepsilon_x = -z \frac{\partial^2 w}{\partial x^2} \tag{6-19}$$

$$\varepsilon_y = -z \frac{\partial^2 w}{\partial y^2} \tag{6-20}$$

CENTER FOR STRUCTURAL DURABILITY – Condition Assessment and Methods
of Abatement of Prestressed Concrete Box-Beam Deterioration

101

$$\tau_{xy} = -2z \frac{\partial^2 w}{\partial x \partial y} \qquad (6\text{-}21)$$

The orthotropic properties of the side-by-side boxes can be calculated from transverse and torsional rigidities of the deck, box-beam, and shear-key assemblage. These calculations will require approximations and simplifications due to the complicated structural system of the assemblage. Both torsional and transverse rigidities of the bridge are controlled by the method of affixing the box-beams by its sides. Thus, the shear key configuration and primarily the transverse post-tensioning play a primary role. Research reported in the literature on this issue was reviewed and presented below.

### 6.1.3   Orthotropic Modeling of Box-Beam Bridge Superstructure

(Gifford 1961) tested a bridge superstructure of precast hollow adjacent box-beams. Shear keys were provided along the sides of the beams. Varying tie-rod stress levels were applied in the transverse direction, ranging from zero to about two percent of the longitudinal prestress; however, the tie-rod stress levels were not available in the literature. (Gifford 1961) concluded that shear keys were mainly responsible for the distribution of live loads. Also, tie-rods prevented premature failure of the joints due to girder spread under live loads.

A series of experiments were conducted by Jesuś on two scaled down models of 30 feet long and 30 feet wide inverted T-beam bridge (Jesuś 1963). Each model consisted of 12 precast prestressed inverted T-beams positioned adjacent to each other. Transverse connectivity of the beams was established by in-situ concrete placed to a height of ½-in above the stem of the T-beam. After the setting of shear-key concrete the transverse post-tensioning cables were placed at the mid-depth of the beam and stressed. One of the specimens was transversely post-tensioned with the stress level computed by elastic analysis while the other was post-tensioned to about 50 percent of that value. Upon posttensioning the ducts were grouted. Jesuś's conclusions on the effect of transverse post-tensioning magnitude was that a reduction of the transverse stress to 50 percent of the value computed by elastic analysis caused a reduction in the transverse stiffness of the bridge which would increase the live load distribution to the girder (Jesuś 1963).

In a related experimental study, Pama (1964) investigated the impact of varying amounts of transverse post-tensioning on load distribution for two types of bridge superstructures (Pama 1964). One of the structures was the same as the one used by Jesuś (1963). The other structure was built placing I-beams with unsymmetrical flanges adjacent to each other. The space between the beams was filled with concrete placed in-situ to form the shear keys. Transverse post-tensioning calculated from elastic analysis was applied at fractions of ¼, 3/8, ½, ¾, and 1.0 to the inverted T-beam, and 1/16, 1/8, ¼, 3/8, ½, ¾, and 1.0 to the I-beam. Post-tensioning ducts were left ungrouted to allow for the modification of tendon stress levels. The effect of two heavy axles of the AASHTO H20 – S16 truck was simulated during the test. Pama concluded that the transverse post-tension stress limit of 25 percent of the value computed by elastic analysis appeared to be the lower limit at which the structure attains a steady value of torsional stiffness (Pama 1964). However, he recommended conducting more tests with lower transverse stress levels to verify the structural behavior.

A detailed discussion of the use and impact of different shear key configurations, grout materials, and post-tension stress levels on box-beam bridge deck behavior is located in Chapter 2.

### 6.1.4  Live Load Distribution of Side-by-Side Box-Beam Bridge Decks

The finite element models of the box beam with various distresses will be analyzed for live load capacities. In order to associate the capacities of single box beam obtained from the FE analysis to the bridge rating calculations, the live load distributions factors will be utilized. Load distribution factors given in the current bridge design specifications such as *AASHTO Standard Specifications for Highway Bridges* (AASHTO 2002) and *AASHTO LRFD Bridge Design Specifications* (AASHTO 2004) for side-by-side box-beam bridges are summarized below.

#### 6.1.4.1  AASHTO Standard Specifications for Highway Bridges

The live load shear and bending moment for each section shall be determined by applying to the beam the fraction of a wheel load (both front and rear) determined by the following equation:

$$Load\ Fraction = \frac{S}{D} \qquad\qquad (6\text{-}22)$$

where;

$S$ = width of precast member, feet
$D = (5.75\text{-}0.5N_L) + 0.7\ N_L(1\text{-}0.2C)^2$
$N_L$ = number of traffic lanes
$C = K\ (W/L)$ for $W/L < 1$
$\quad = K$ for $W/L > 1$
$W$ = overall (edge-to-edge) width of bridge measured perpendicular to the longitudinal beams, feet
$L$ = span length measured parallel to longitudinal beams, feet
$K = [(1+\mu)\ I\ /\ J]^{\,0.5}$
$I$ = moment of inertia
$J$ = St. Venant torsional constant
$\mu$ = Poisson's ratio for beams
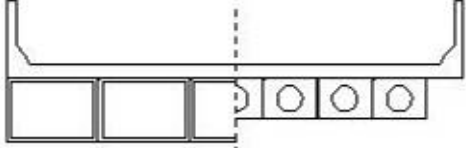
### 6.1.4.2  AASHTO LRFD Bridge Design Specifications

This specification outlines equations for calculating distribution of live loads per lane for moment and shear in the interior beams.  These equations are specified for side-by-side box-beam bridges based on the transverse load transfer mechanism of the bridge deck.  A description of the bridge deck supporting components and the type of transverse connection, deck type, and schematics of the decks are given in Table 6-1.

**Table 6-1:  Box-beam bridge deck configurations**

| Supporting Components | Type of Deck | Typical Cross-Section |
|---|---|---|
| Precast solid, voided or cellular concrete boxes with shear keys | Cast-in-place concrete overlay | **(f)** |
| Precast solid, voided or cellular concrete box with shear keys and with or without transverse post-tensioning | Integral concrete | post tension **(g)** |

*(a ) Distribution factors for moments*

The Equation (6-23) is applicable for both the structural systems (**f** and **g**) if sufficiently connected to act as a unit and valid if;

1. Two or more design lanes loaded
2. $35 \leq b \leq 60$
3. $20 \leq L \leq 120$
4. $5 \leq N_b \leq 20$

$$Load\ Fraction = k\left(\frac{b}{305}\right)^{0.6}\left(\frac{b}{12.0L}\right)^{0.2}\left(\frac{I}{J}\right)^{0.06} \tag{6-23}$$

where;

$b$ = the overall width of the box (inch)
$L$ = span length (ft)
$N_b$ = number of beams
$k = 2.5\ (N_b)^{-0.2} \geq 1.5$
$I$ = moment of inertia
$J$ = St. Venant torsional constant

where;

$$J = \frac{4A_o^{\,2}}{\sum\dfrac{s}{t}}$$

$A_o$ = area enclosed by the centerlines of elements (inches$^2$)
$s$ = length of a side element (inch)
$t$ = thickness of plate like element (inch)

The Equation (6-24) given below is applicable to the structural system **g** (if sufficiently connected to prevent relative vertical displacement at the interface between beams) and valid if;

1. Skew $\leq 45^{\circ}$
2. $N_L \leq 6$

$$Load\ Fraction = \frac{S}{D} \tag{6-24}$$

where;

$S$ = width of precast member (ft)
$D = 11.5 - N_L + 1.4\ N_L\ (1-0.2C)^2$ when $C \leq 5$
$D = 11.5 - N_L$ when $C > 5$
$C = K\ (W/L) \leq K$
$K = [(1+\mu)\ I\ /\ J]^{0.5}$
$N_L$ = number of traffic lanes
$W$ = overall width of bridge (ft)
$L$ = span length (ft)

CENTER FOR STRUCTURAL DURABILITY – Condition Assessment and Methods
of Abatement of Prestressed Concrete Box-Beam Deterioration

105

$\mu$ = Poisson's ratio for beams

*(b) Distribution factors for shear*

The Equation (6-25) is applicable for both the structural systems (**f** and **g**) if sufficiently connected to act as a unit and valid if

1. $35 \leq b \leq 60$
2. $20 \leq L \leq 120$
3. $5 \leq N_b \leq 20$
4. $25,000 \leq J \leq 610,000$
5. $40,000 \leq I \leq 610,000$

$$Load\ Fraction = \left(\frac{b}{156}\right)^{0.4} \left(\frac{b}{12.0L}\right)^{0.1} \left(\frac{I}{J}\right)^{0.05} \left(\frac{b}{48}\right) \qquad \frac{b}{48} \geq 1.0 \qquad (6\text{-}25)$$

### 6.1.4.3 Live Load Fraction on a Beam - Example

The live load distribution factors calculated on the side-by-side box-beam bridge utilized in this report is discussed below (Example B in Section 4.6.3) and summarized in Table 6-2.

*Bridge description*:

The bridge superstructure is composed of eight box-beams. The span length is 57 feet and beam dimensions are 27 inches in height and 36 inches in width. Thickness of both the webs and the bottom flange are 4.5 inches. Top flange thickness is 5 inches. Beams are placed 0.25-inch apart from each other.

**Table 6-2: Distribution of live loads per lane for moment and shear in interior beams**

| Specification | | Distribution of Live Loads per Lane for | |
|---|---|---|---|
| | | **Moment in Interior Beams** | **Shear in Interior Beams** |
| AASHTO Standard | | 0.252 | 0.252 |
| AASHTO LRFD | **(f) & (g)** | 0.245 | 0.403 |
| | **(g)** | 0.254 | - |

According to Table 6-2, there is no significant difference among the distribution factors for moment in interior beams. However, the distribution factors calculated using the AASHTO Standard (2002) for shear in interior beams are significantly different than that

are calculated using the AASHTO LRFD (2004) formulation. The reasons for these differences need to be analyzed.

Current Michigan and AASHTO requirements and published research on transverse post-tensioning force/stress magnitudes and the function of the shear key were presented in Chapter 2. According to the published research and other design guides or specifications, it is apparent that further research is needed to understand the behavior of side-by-side box-beam bridge decks with transverse post-tensioning.

## 6.2 Finite Element Analysis

Finite Element (FE) analysis is a tool that is often used for structural design, assessment of existing structures, researching design parameters and options as well as forensic investigations on structures with distress or damage. In the FE method, the structure/component is divided into finite elements and the behavior of structure is obtained from the behavior of each finite element under the applied loading conditions. A FE analysis gives the global and local response (e.g., stress, strain, displacements, etc.) of the structure at the collection of nodes describing each element and consequently the structure.

The use of FE analysis in this study is for evaluating shear and flexural capacities of distressed box-beams. Side-by-side box-beam bridge designs require a cast-in-place concrete deck, full-depth grouted shear keys, and transverse post-tensioning for the orthotropic action of the bridge superstructure. However, the longitudinal cracking commonly observed on side-by-side box-beam bridge decks may be a result of loss of monolithic action. Spalling of shear key grout, significant water leakage through shear keys, concrete delamination and spall, and corroded and broken prestressing strands are among the documented beam distresses. With these distress conditions and the uncertainty of transverse load transfer among the adjacent beams, superstructure capacity may be limited with the capacity of a single distressed beam. Under this condition, it can be assumed that in the upper bound case a single beam carries as much as a single wheel line load. Hence, two FE models were developed for isolated box-beams considering

CENTER FOR STRUCTURAL DURABILITY – Condition Assessment and Methods
of Abatement of Prestressed Concrete Box-Beam Deterioration

107

flexure critical and shear critical beam lengths determined by the group of vehicle loads established by MDOT (MDOT 2003a).

### 6.2.1 Programs Utilized

#### 6.2.1.1 HyperMesh

HyperMesh is a pre- and post-processing program for finite element analysis. The program assists in analyzing design conditions in an interactive and visual environment (HyperMesh 6.0, 2003).

(a) Pre-Processing

The main advantage of using HyperMesh, as a pre-processor, is the ability to create compatible input files for various finite element analyzers, including ABAQUS.

HyperMesh pre-processing consists of following steps:

- The geometry of the model is created using geometric properties of the structure or the components.

- Finite element discretization (element generation) is performed.

- The complete finite element representation of the geometry is checked for continuity and element quality.

- Boundary conditions, loads and other constraints are applied.

- Material properties and other element properties (post-tensioning, prestressing) are defined.

- The finite element description of the model is exported in the format required by the analyzer, ABAQUS.

(b) Post-Processing

In post-processing, the analysis results are interpreted by completing the following tasks.

- Translating the results from the analysis code's (ABAQUS's) output format into the HyperMesh results format.

- Reviewing and animating the model with deformed shapes.

- Reviewing color contours of element and nodal data results displayed on the finite element model.

- Generating plots, contours, and deformed shapes for reporting and documenting the analysis results.

### 6.2.1.2 ABAQUS

ABAQUS is an FE analysis program. This program has been used in several MDOT funded and other research projects by Wayne State since the late 1980s as described by Ahlborn et al. 2002, Birgul 2001, Yaman 2000, Akbay 1991, and Elzayat 1989. Most recently, in the MDOT project titled, *Causes and Cures for Prestressed Concrete I-Beam End Deterioration* (Ahlborn et al. 2002), ABAQUS and HyperMesh was used to investigate the effects of prestressing tendon arrangements on beam-end cracking and to investigate the effects of nonfunctional bearings on PC-I beam stresses. This FE platform is capable of solving problems ranging from relatively simple linear analyses to the most complicated nonlinear simulations. The program capabilities are described by the element library that can model virtually any geometry and the extensive list of material models that can simulate the behavior of most typical engineering materials such as steel, neoprene, concrete, and geotechnical materials such as soils and rock. General elastic, elasto-plastic, and elastic-viscoplastic behaviors are provided. Both isotropic and anisotropic behaviors can be modeled. User defined materials can also be created with a subroutine interface.

### 6.2.2 Beam Geometry for FE Modeling

### 6.2.2.1 Selection of Beam Cross-Section

The beam geometry for modeling and FE analysis is selected as the most common box-section used among the group of inspected bridges. There are two box-beam configurations: single-cell and double-cell. Both box-beam configurations were used in the bridges that were built before the 1970s. The double-cell sections were discontinued and since 1970 only single-cell box-beams are being used.

Available as-built drawings of 25 bridges were utilized and the box-beam attributes were identified and documented in Table 6-3. The 15 inspected bridges were also included in

CENTER FOR STRUCTURAL DURABILITY – Condition Assessment and Methods
of Abatement of Prestressed Concrete Box-Beam Deterioration

109

this group of 25 bridges. Table 6-3 shows the design date, bridge ID, number of spans, span length and width, beam size (height "h" and width "b"), number of beams per span, and shear reinforcement details. The beam cross-sections are tabulated in Table 6-3 and also shown in a pie chart form in Figure 6-2. Of these 25 bridges the most common box-beam section from Figure 6-2 is identified as the 27x36-inch single-cell. Hence, 27x36-inch box-beam cross-section was selected as the prototype for finite element analysis.

**Table 6-3: Beam types used in side-by-side box-beam bridges**

| Design Date | Bridge ID | No. of Span | Length (ft) | Width (ft) | Beam hxb (inch x inch) | Beams/Span | Remarks |
|---|---|---|---|---|---|---|---|
| 1-9-1992 | B01 of 12022 | 1 | 22 | 50 | 12x36 | 16 (solid section) | Closed stirrups (Figure 2-8 defines solid section ) |
| | | 2 | 22 | 50 | 12x36 | 16 (solid section) | |
| | | 3 | 22 | 50 | 12x36 | 16 (solid section) | |
| 9-1-1993 | B01 of 53011 | 1 | 51 | 47 | 21x36 | 15 | Closed stirrups |
| | | 2 | 51 | 47 | 21x36 | 15 | |
| | | 3 | 51 | 47 | 21x36 | 15 | |
| 4-24-1992 | S08 of 41131 | 1 | 60 | 61 | 27x36 | 19 | No shear details |
| | | 2 | 54 | 61 | 27x36 | 19 | |
| | | 3 | 54 | 61 | 27x36 | 19 | |
| | | 4 | 46 | 61 | 27x36 | 19 | |
| 12-12-1997 | B01 of 06071 | 1 | 25 | 70 | 12x36 | 22 (solid section) | No shear details |
| | | 2 | 33 | 70 | 12x36 | 22 (solid section) | |
| | | 3 | 25 | 70 | 12x36 | 22 (solid section) | |
| 2000 | S02-3 of 33045 | 1 | 33 | 48 | 33x36 | 15 | Closed stirrups |
| | | 2 | 95 | 48 | 33x36 | 15 | |
| | | 3 | 33 | 48 | 33x36 | 15 | |
| 2000 | S02-4 of 33045 | 1 | 34 | 57 | 33x36 | 15 | Closed stirrups |
| | | 2 | 95 | 57 | 33x36 | 15 | |
| | | 3 | 34 | 57 | 33x36 | 15 | |
| 2001 | S10 of 23152 | 1 | 35 | 62 | 33x36 | 20 | Closed stirrups |
| | | 2 | 85 | 62 | 33x36 | 20 | |
| | | 3 | 85 | 62 | 33x36 | 20 | |
| | | 4 | 35 | 62 | 33x36 | 20 | |
| 7-22-2002 | S08 of 50015 | 1 | 40 | 49 | 21x36 | 15 | Closed stirrups |
| | | 2 | 56 | 49 | 21x36 | 15 | |
| | | 3 | 40 | 49 | 21x36 | 15 | |
| 7-22-2002 | S09 of 50015 | 1 | 40 | 49 | 21x36 | 15 | Closed stirrups |
| | | 2 | 56 | 49 | 21x36 | 15 | |
| | | 3 | 40 | 49 | 21x36 | 15 | |
| 12-10-1987 | B01 of 63112 | 1 | 29 | 76 | 17x36 | 24 | Closed stirrups |
| | | 2 | 29 | 76 | 17x36 | 24 | |
| 7-28-1989 | B02 of 78021 | 1 | 90 | 37 | 39x36 | 12 | Closed stirrups |
| | | 2 | 90 | 37 | 39x36 | 12 | |
| | | 3 | 90 | 37 | 39x36 | 12 | |
| 6-9-1994 | S06 of 50011 | 1 | 117 | 84 | 48 x 42 to 48 | 23 | Closed stirrups Tapered beams |
| | | 2 | 119 | 84 | 48 x 42 to 48 | 23 | |
| unknown | S07 of 50011 | 1 | 117 | 76 | 48x48 | 18 | Closed stirrups |
| | | 2 | 117 | 76 | 48x48 | 18 | |

**Table 6-3: Beam types used in side-by-side box-beam bridges (continuation)**

| Design Date | Bridge ID | No. of Span | Length (ft) | Width (ft) | Beam hxb (inch x inch) | Beams/Span | Remarks |
|---|---|---|---|---|---|---|---|
| 6/6/1956 | B02 of 08012 | 1 | 45 | 36 | 27x36 | 12 | No shear details Used tie rods |
| | | 2 | 45 | 36 | 27x36 | 12 | |
| | | 3 | 45 | 36 | 27x36 | 12 | |
| 6/5/1956 | B01 of 32051 | 1 | 40 | 43 | 21x36 | 14 (double cells) | No shear details, Used tie rods |
| 8/16/1956 | B04 of 74032 | 1 | 40 | 43 | 21x36 | 14 (double cells) | No shear details, Used tie rods |
| 7/18/1957 | B01 of 08032 | 1 | 35 | 43 | 21x36 | 14 (double cells) | No shear details, Used tie rods |
| | | 2 | 40 | 43 | 21x36 | 14 (double cells) | |
| | | 3 | 35 | 43 | 21x36 | 14 (double cells) | |
| 3/26/1958 | B01 of 32021 | 1 | 35 | 46 | 21x36 | 15 (double cells) | Open stirrups, Used tie rods |
| | | 2 | 35 | 46 | 21x36 | 15 (double cells) | |
| | | 3 | 35 | 46 | 21x36 | 15 (double cells) | |
| 10/7/1957 | S10 of 38101 | 1 | 31 | 33.5 | 2-21x36, 17x36 | 11 (double cells) | Fascia beams are deep |
| | | 2 | 48.5 | 33.5 | 21x36 | 11 (double cells) | No shear details, Used tie rods |
| | | 3 | 48.5 | 33.5 | 21x36 | 11 (double cells) | |
| | | 4 | 48.5 | 33.5 | 21x36 | 11 (double cells) | |
| | | 5 | 31 | 33.5 | 2-21x36, 17x36 | 11 (double cells) | Fascia beams are deep |
| 6/13/1957 | S11 of 38101 | 1 | 33 | 33 | 2-21x36, 17x36 | 11 (double cells) | Fascia beams are deep |
| | | 2 | 49 | 33 | 21x36 | 11 (double cells) | No shear details, Used tie rods |
| | | 3 | 49 | 33 | 21x36 | 11 (double cells) | |
| | | 4 | 33 | 33 | 2-21x36, 17x36 | 11 (double cells) | Fascia beams are deep |
| 7/16/1958 | B02 of 72022 | 1 | 35 | 61 | 21x36 | 20 (double cells) | Open stirrups, Used tie rods |
| 9/3/1959 | B01-1 of 47013 | 1 | 45 | 49 | 27x36 | 16 | No shear details, Used tie rods |
| | | 2 | 45 | 49 | 27x36 | 16 | |
| 9/3/1959 | B01-2 of 47013 | 1 | 45 | 49 | 27x36 | 16 | No shear details, Used tie rods |
| | | 2 | 45 | 49 | 27x36 | 16 | |
| 6/2/1960 | S01 of 82193 | 1 | 55 | 67 | 27x36 | 22 | Open stirrups |
| | | 2 | 55 | 67 | 27x36 | 22 | |
| 11/9/1956 | S09 of 25031 | 1 | 31.5 | 61 | 2-27x36, 21x36 | 20 | Deep fascia beams on 1 & 4 spans No shear details, Used tie rods |
| | | 2 | 50.5 | 61 | 27x36 | 20 | |
| | | 3 | 50.5 | 61 | 27x36 | 20 | |
| | | 4 | 31.5 | 61 | 2-27x36, 21x36 | 20 | |
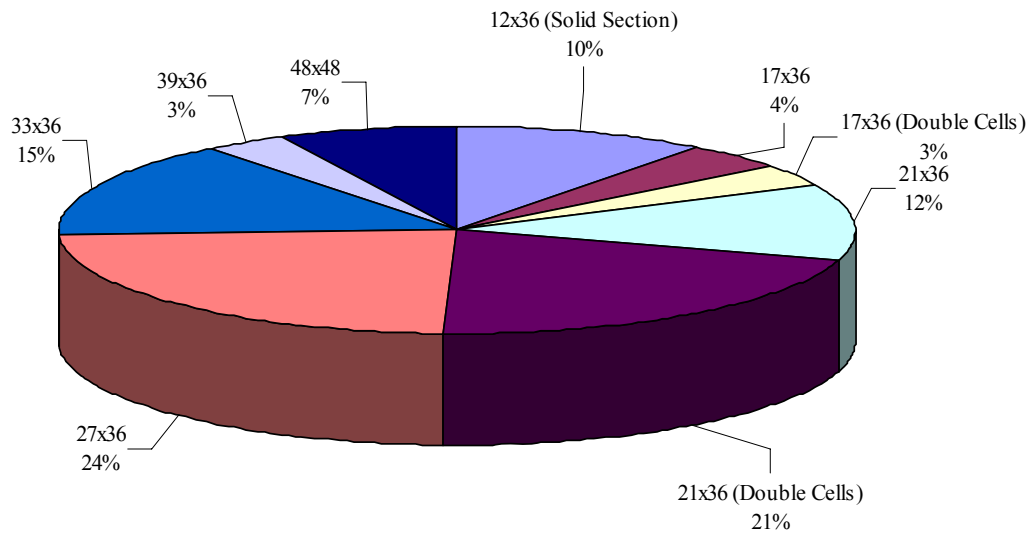
**Figure 6-2:  Beam types used in selected side-by-side box-beam bridges**

### 6.2.2.2   Selection of Beam Length

The span lengths of box-beams were identified from as-built drawings and tabulated in Table 6-4.  In order to evaluate the effects of distress on shear and flexural capacities of the beam, shear critical and flexure critical span lengths were defined.  Table 6-4 shows that the 27x36 box-beam is utilized on spans ranging from 30 to 60-feet.

In identifying the shear critical and flexure critical span lengths of 27x36-inch box-beam, maximum moment, maximum shear, and moment/shear ratios were calculated at various span lengths.  The moment and shear diagrams were constructed using the Michigan legal vehicle configurations given in the *Bridge Analysis Guide* (MDOT 2003a).  Flexure critical span length is identified as the span that has the largest moment value with the highest moment/shear ratio.  Available bridge plans showed design details of a 57-feet long 27x36-inch box-beam.  Span lengths of 57-feet generated the largest moment value with the highest moment/shear ratio under the Michigan legal vehicle loading - truck number 17 (72 ton, 11 axle, Figure 6-3). Hence, a 27x36-inch beam that spans 57-feet is modeled as the flexure critical span length.  The shear critical span length is identified as the span that has the largest shear force value with the lowest moment/shear ratio.  It is preferred to have the shortest span length for shear analysis and the 30-feet span length is selected as the shear critical span length.  The Michigan legal vehicle configuration that exerts the largest shear force value with the lowest moment/shear ratio is identified as

CENTER FOR STRUCTURAL DURABILITY – Condition Assessment and Methods
of Abatement of Prestressed Concrete Box-Beam Deterioration

113

truck number 17 (Figure 6-4). Hence, Michigan legal vehicle loading - truck number 17 (Figure 6-3 and Figure 6-4) is used in the analysis.

**Table 6-4: Number of box-beams used at different span lengths**

| Span Length Range (ft) | Number of Box-Beams | | | | | | | | |
|---|---|---|---|---|---|---|---|---|---|
| | 12x36[+] | 17x36 | 17x36* | 21x36 | 21x36* | 27x36 | 33x36 | 39x36 | 48x48 |
| 20-30 | 92 | 48 | | | | | | | |
| 31-40 | 22 | | 36 | 60 | 179 | 4 | 100 | | |
| 41-50 | | | | | 55 | 100 | | | |
| 51-60 | | | | 75 | | 160 | | | |
| 61-70 | | | | | | | | | |
| 71-80 | | | | | | | | | |
| 81-90 | | | | | | | 40 | | |
| 91-100 | | | | | | | 30 | 36 | |
| 100 up | | | | | | | | | 82 |

+ Solid section
* Double cells

### 6.2.3   Loads and Loading Cases

#### 6.2.3.1   Dead Load

The dead load effect is calculated using nominal dimensions and densities. The dead load factors given in the *AASHTO Standard Specifications* (AASHTO 2002) account for normal variations of material densities and dimensions. *AASHTO Standard Specifications* recommended unit weights of materials and dead load factors were used in the FE analysis. The dead load used for the FE models consisted of the beam self weight and a superimposed dead load. During the field inspection, most of the distresses were observed on the bridges built in 1950's and 1960's. Hence, a bridge that represents a 1950's design was selected for the analysis. This bridge consists of 12-27x36-inch beams and a concrete wearing surface of 3-inch minimum thickness. The cross-sectional area of the beam is 517.5-inches$^2$ (shear keys were ignored in area calculations) with a concrete density of 145 lb/ft$^3$ corresponds to a dead load of 0.521 k/ft. Wearing surface thickness varies due to the crown provided on the profile for drainage. The maximum thickness of the wearing surface was calculated as 4.5 inches for the dead load calculation. As for superimposed dead loads, wearing surface (54 lb/ft$^2$), future wearing surface (25 lb/ft$^2$), railing (11.5 lb/ft), and curbs (519 lb/ft) loads are considered giving a total of 0.326 k/ft

superimposed dead load per beam.  In calculating the dead load per beam it is assumed that the curb and railing loads are equally shared by all the beams (PCI 2003).
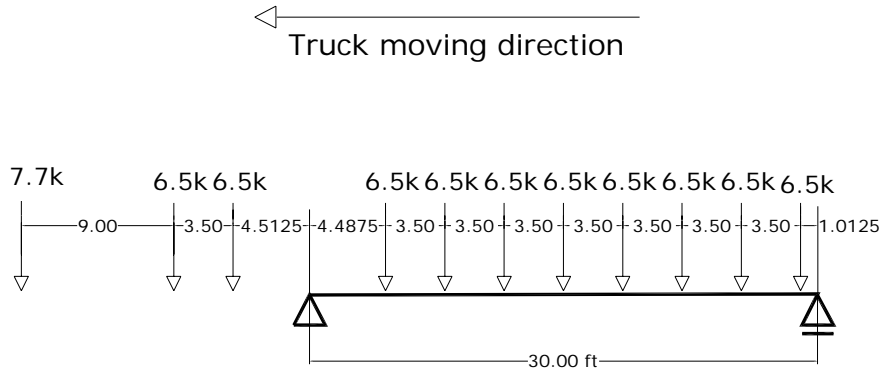
*6.2.3.2   Live Load*

The maximum nominal moving load (live load) effect on a bridge superstructure was calculated using the Michigan legal vehicle configuration.  As discussed earlier MDOT truck 17 generated the maximum moment and shear on the selected spans (Figures 6-3 and 6-4).  The truck load configuration for the flexure critical beam length generated a maximum moment of 608.43 foot-kips at mid span (Figure 6-3 (a) and (b)).  In the case where the documented distresses were located at quarter points of the beam, the truck load configuration is changed in order to generate the maximum moment at the quarter locations of the span.  This load configuration generated a maximum moment of 473.6-foot-kips at the quarter points of the span (Figure 6-4 (a) and (b)).

The truck load configuration for the shear critical model generates a maximum shear of 29.01 kips at a distance d/2 from the support which corresponds to 1.025-feet (Figure 6-5 (a), (b) and (c)).  When analysis is performed under static loading following linear elastic theory, impact and load distribution factors can be used to scale-up or scale-down the final results.  Hence, these factors are ignored during the FE analysis and can be incorporated when the results are being interpreted.

CENTER FOR STRUCTURAL DURABILITY – Condition Assessment and Methods
of Abatement of Prestressed Concrete Box-Beam Deterioration

115

**(a) Wheel line load configuration of Truck 17 generating maximum moment around mid-span**

$M_{max}$=608.43 ft-kips



**(b) Corresponding moment diagram**

**Figure 6-3. Rating vehicle position for FE mid-span critical modeling**



**(a) Wheel line load configuration of Truck 17 generating maximum moment at quarter span**

$M_{max}$=599.35 ft-kips          M=473.6 ft-kips
                                  @ quarter point



**(b) Corresponding moment diagram**

**Figure 6-4: Rating vehicle configuration for FE quarter point critical modeling**

**(a) Wheel line load configuration of Truck 17 generating maximum shear at d/2 distance**



$M_{max} = 208.08$ ft-kips

**(b) Corresponding moment diagram**



$V_{max} = 29.01k$
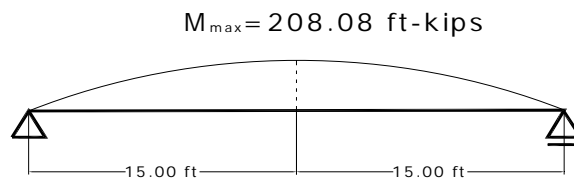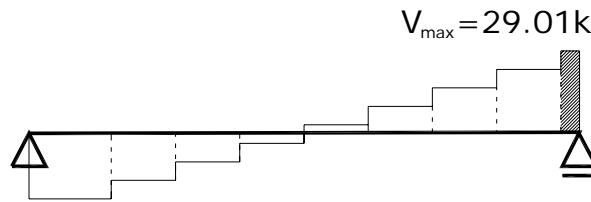
**(c) Corresponding shear diagram**

**Figure 6-5: Rating vehicle configuration for FEA shear critical modeling**

### 6.2.3.3   *Prestressing Load*

The tendons utilized in the model conform to ASTM A-416 (Grade 250).  Strands with a diameter of 3/8-inch and an area of 0.08-inch$^2$ per strand were used.  The material properties of the strands are given in Table 6-5.

**Table 6-5:  Material properties of strands**

| Material Properties | |
|---|---|
| **Ultimate strength** | 20 kips |
| **Ultimate stress** | 250 ksi |
| **Yield strength** | 212.5 ksi |
| **Initial prestressing** | 175 ksi |
| **Modulus of elasticity** | 28,000 ksi |
| **Poisson's ratio** | 0.3 |

In typical prestressed concrete construction the strands are tensioned prior to concrete placement.  Strands are cut after the concrete has reached a predetermined level of strength. Upon cutting the strands, the prestressing force is transferred to concrete through the bond stresses that develop between the tendon and concrete.  Loss of prestressing force is the reduction of tensile stress in prestressing tendons.  Prestressing loss is due to elastic shortening, shrinkage, creep of concrete, and relaxation of tendons. The initial prestress value that was utilized in the analysis is calculated by subtracting the losses due to shrinkage and creep from the initial prestressing stress.  ABAQUS accounts for losses due to relaxation of tendons and elastic shortening.  The final prestressing force after losses was 149 ksi; which also matched the theoretical calculations.

### 6.2.4   Box-beam Geometric and Material Properties

A 27x36-inch cross-section box-beam was used in the modeling of the single beam.  The box-beam is designed according to the 1958 MDOT Bridge Design Manual (MDOT 1958).   The material properties are the modulus of elasticity ($E_c$) of 4000 ksi and Poisson's ratio of 0.2.  The compressive strength of the concrete ($f'_c$) is taken as 5000 psi. Prestressing strands of 3/8-inch diameter and Grade 250 are incorporated in the model. The steel modulus of 28,000 ksi and Poisson's ratio (0.3) defines the material properties of the strands as given in Table 6-5.

The flexure critical model contains a total of 30 strands with a gross area ($A_s$) of 2.4 inches$^2$.  The strand configuration is eight strands at layer one, 18 strands at layer two, and four strands at layer three.  The beam cross-section and tendon geometry are shown in Figure 6-6.
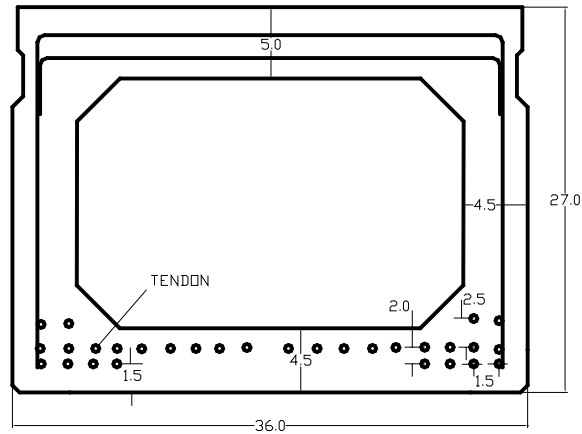
**Figure 6-6: Beam cross-section and tendon geometry for flexure critical model (dimensions in inches)**

The shear critical model consists of a total of ten strands with a gross area of 0.8-inch$^2$. The strand configuration is four strands along layer one, and six strands along layer two. The beam cross-section and tendon geometry are shown in Figure 6-7.
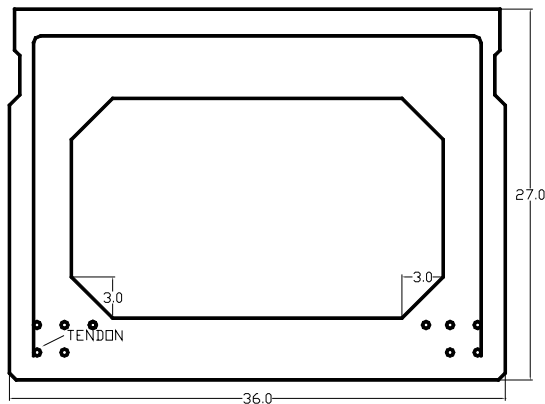


**Figure 6-7: Beam cross-section and tendon geometry for shear critical model (dimensions in inches)**

## 6.2.5    Finite Element Mesh and Connectivity with the Strands

The finite element mesh and element selection was determined based on the mechanics as well as the options and analyses procedures defined by HyperMesh and ABAQUS programs.  Three-dimensional continuum brick elements are used to model the concrete medium.  The continuum element dimensions are uniform in most cases at 1.5x1.5x4.5-

CENTER FOR STRUCTURAL DURABILITY – Condition Assessment and Methods
of Abatement of Prestressed Concrete Box-Beam Deterioration

119

inch. Truss elements are used for modeling the prestressing strands. The spring elements are utilized for modeling the bond between the tendon and concrete medium. The spring elements placed at 4.5-inch increments transfer prestressing force from the strands (truss elements) to the concrete (continuum elements). The transfer lengths that are calculated from *AASHTO Standard Specifications 9.20.2.4* (AASHTO 2002) (50 x tendon diameter) and *AASHTO LRFD Specifications 5.11.4* (AASHTO 2004) (60 x tendon diameter) are 18.75-inches and 22.50-inches, respectively. For FE modeling, the average value of transfer length is taken as 20-inches that conforms with the finite element mesh size used. The spring stiffness was determined by tuning the model until a transfer length of around 20-inches is achieved. The kinematic coupling elements are placed parallel to the springs so that the strand stays in position and can only deform along its axis.

The resulting flexure critical FE model consists of 15,984 eight-node solid continuum elements, 2160 two-node truss elements, 2160 two-node spring elements, and 2160 two-node kinematic coupling elements. And the resulting finite element shear critical model consists of 8,880 eight-node solid continuum elements, 400 two-node truss elements, 400 two-node spring elements, and 400 two-node kinematic coupling elements. The finite element mesh generated for the flexural model is shown in Figure 6-8.
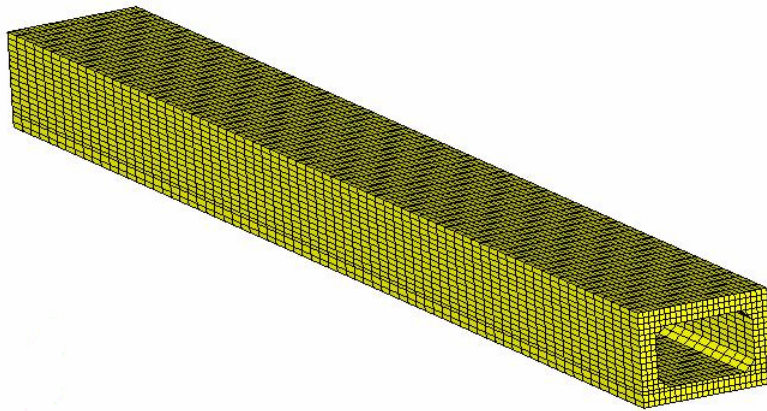


**Figure 6-8: Finite element model of box-beam**
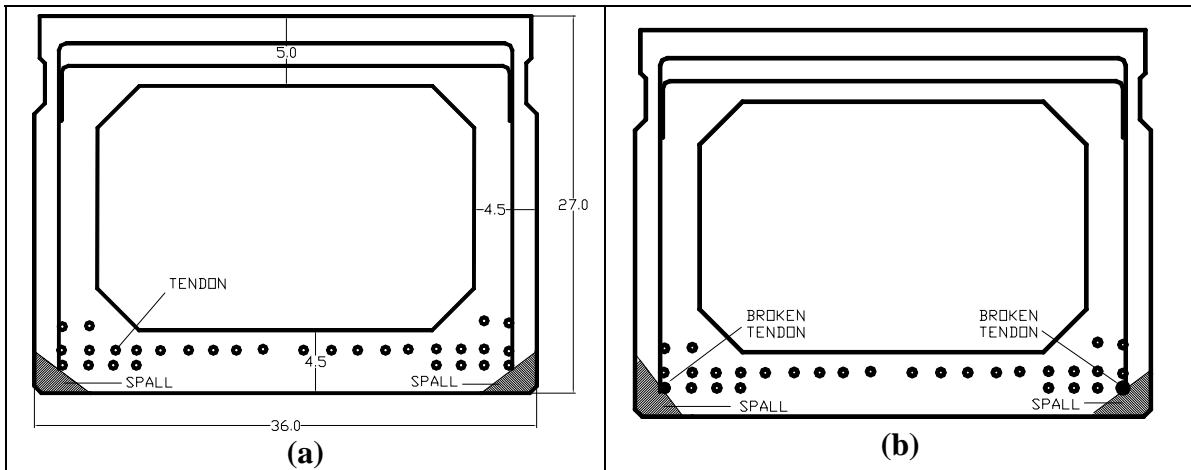
### 6.2.6 The Live Load Modeling

AASHTO Standard Specifications (AASHTO 2002) Section 3.30 defines an area of 10 x 20 inches as the dimensions of the tire contact area. In the analysis, it was assumed that

each wheel load is uniformly distributed over the defined tire contact area. With that assumption, equivalent nodal loads are calculated and applied to the FE model.
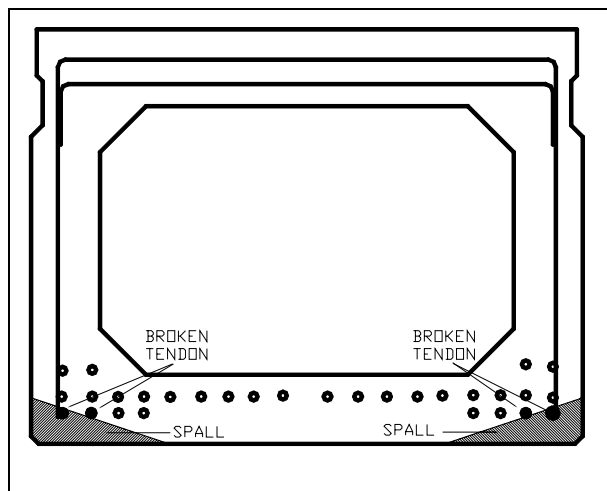
### 6.2.7 Incorporating Beam Distress in FE Models

Distresses commonly observed during bridge inspection were incorporated into the FE models. In the case of the flexure critical model, distresses were incorporated at the mid span and at quarter locations of the model. The length of distress along the beam was taken as 54-inches or 12 elements long. The distress to the concrete was modeled by gradually reducing the elasticity modulus from a depth of distress penetration to the surface. In the case of a broken tendon, the effective distress length was increased by the transfer length where the prestressing force achieved full value. During field inspections distress was observed at nearly every location along the length of the beam. The distress location near the middle and at the quarter locations of the flexure critical beam allowed for representing the critical beam capacities. In the shear critical model, distress levels with a length of 18-inches were incorporated and only at the beam ends.

In these analyses distress was modeled at four different levels. Level one designates the undamaged box-beam. Level two is limited to the concrete section loss due to minor spall along the bottom corners of the box-beam cross-section (Figure 6-9a). Level three designates the spall size as level two but with two broken tendons along the bottom corners of the box-beam (Figure 6-9b). Level four defines a major spall, and includes four broken tendons along the bottom corners of the box-beam cross-section (Figure 6-10). Table 6-6 summarizes the distress levels used in FE models and Table 6-7 shows a visual representation of the distress levels.

CENTER FOR STRUCTURAL DURABILITY – Condition Assessment and Methods
of Abatement of Prestressed Concrete Box-Beam Deterioration

121

**Figure 6-9: Distress level 2 and 3 - (a) concrete spall and (b) spall and two broken tendons**
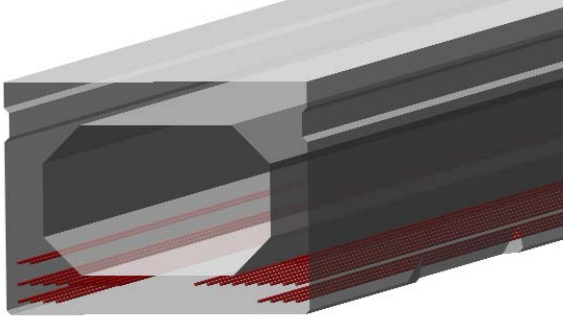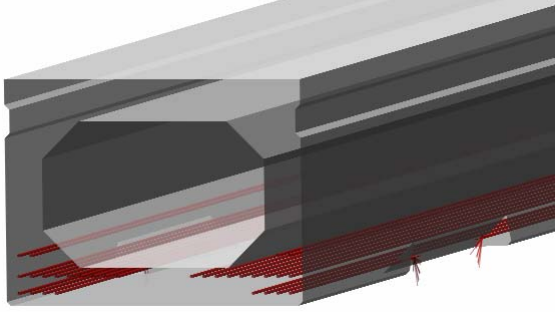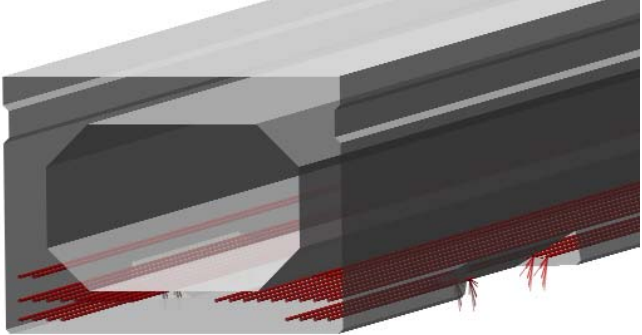


**Figure 6-10: Distress level 4 - spall and four broken strands**

**Table 6-6: Distress level summary in FE analysis**

| Case | Distress Level Summary | Condition State | Figure |
|:---:|---|:---:|:---:|
| 1 | Baseline state; as built properties, no loss of prestressing strand | A | 6-6, 6-7 |
| 2 | Spall along bottom corners of box-beam. Length of spall is 54 inches for flexure critical and 18 inches for shear critical beams. | G | 6-9(a) |
| 3 | Spall along bottom corners of box-beam. Length of spall is 54 inches for flexure critical and 18 inches for shear critical beams. One broken tendon at each spall location. | G | 6-9(b) |
| 4 | Spall along bottom corners of box-beam. Length of spall is 54 inches for flexure critical and 18 inches for shear critical beams. Two broken tendons at each spall location. | G | 6-10 |

**Table 6-7: Distress observed and incorporated in FE models**

| Distressed Levels | Observed During Field Inspection | Finite Element Model |
|---|---|---|
| 2 |  |  |
| 3 |  |  |
| 4 |  |  |

Concrete spalling is modeled by incorporating the effect of partial section loss. This effect was generated in the FE analysis by significantly reducing the elasticity modulus of the concrete elements within the distress zones. Figure 6-11 shows an example of a spall for distress levels two and three. Figure 6-12 illustrates the spall in distress level four.

**(a)**                                          **(b)**
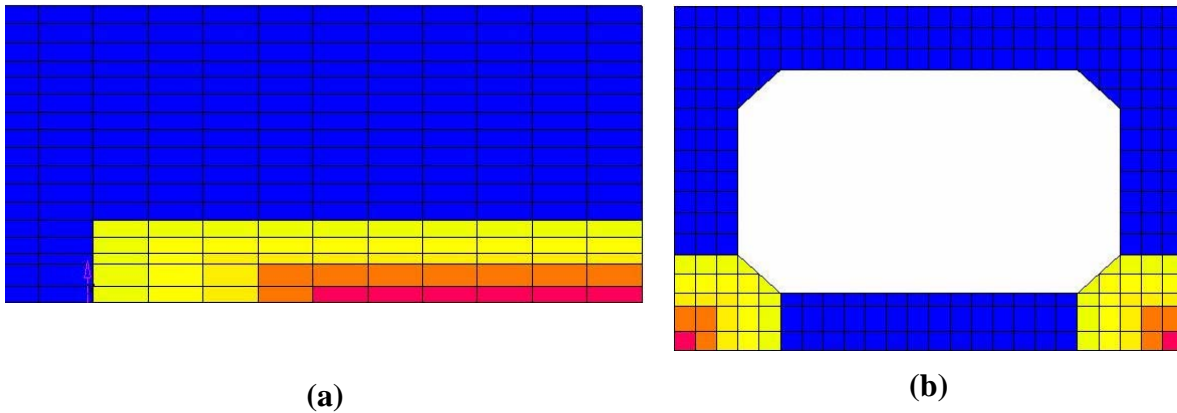
**Figure 6-11:  Finite element model of distress levels 2 and 3: (a) enlarged view of one half of the distress zone along length and (b) section view of the distress zone (note: broken strands are not visible)**

**NOTE:  Yellow (2000, 500, and 25ksi), orange (5ksi), and red (1ksi) represent reduced elastic modulus of the beam (4000ksi in undistressed locations)**



**(a)**                                          **(b)**
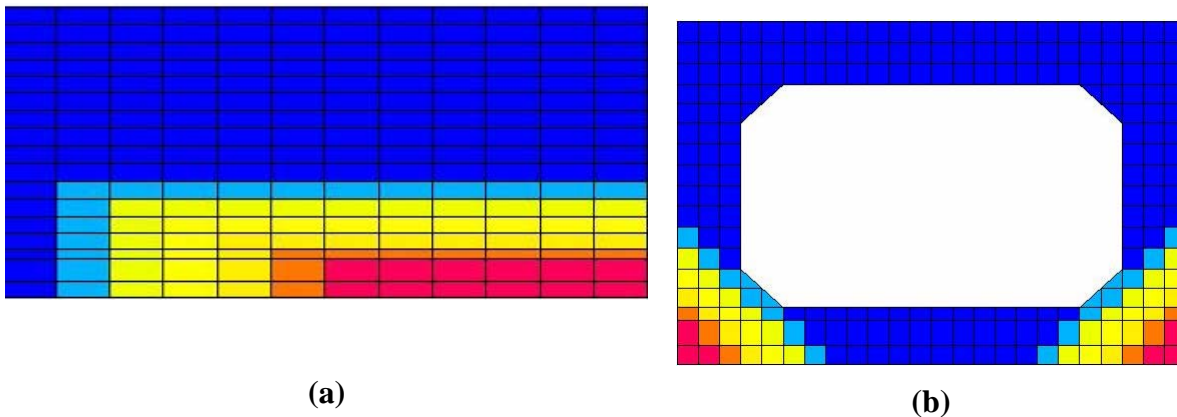
**Figure 6-12:  Finite element model of distress level 4: (a) enlarged view of one half of the distress zone along length and (b) section view of the distress zone (note: broken strands are not visible)**

**NOTE: Light blue (2000ksi),  yellow (1000, 500, and 25ksi), orange (5ksi), and red (1ksi) represent reduced elastic modulus of the beam (4000ksi in undistressed locations)**

### 6.2.8   Prestressed Concrete Box-Beam Load Capacity Criteria

Beam capacities are defined independently for the flexure critical and shear critical beams.  In flexural critical beams, beam live load capacity is defined as the percentage of truck load that generates a maximum tensile stress equal to the allowable tensile stress limit specified in *AASHTO Standard Specifications* (Section 9.15.2.2) and *AASHTO LRFD Specifications* (Section 5.9.4.2) for severe corrosive exposure conditions at or near the bottom fibers ($3\sqrt{f_c'}$).  In shear critical beams, the fracture critical zone is defined between 18 to 27-inches from the support.  Within this zone, principal stresses are

calculated. The beam live load capacity is defined as the percentage of truck load generating a maximum tensile principal stress equal to the tensile stress limit of $3\sqrt{f_c'}$ on the web and within the fracture critical zone.

In both flexure critical and shear critical beams, first the truck position generating the maximum internal stress resultant (bending moment and shear) is established (Figure 6-3 to Figure 6-5). Analysis is performed by incrementally and uniformly increasing the wheel loads while checking the stress within the fracture critical zone. The analysis is stopped when the tensile stress within the fracture critical zone reaches the tensile stress limit. The beam capacity is defined as the percentage of wheel line load applied to the beam during the last loading increment of the analysis.

In the FE analysis, certain assumptions were necessary. The assumptions are grouped under structural behavior and FE modeling.

Structural behavior assumptions are as follows:

1.  Static analysis is performed without impact factors (Section 6.2.3.2).

2.  Small deformation analysis is performed.

3.  Materials remain in an elastic state. Damage and distress is accounted for by cutting tendons and reducing concrete modulus.

4.  Initial prestressing force includes effects from concrete creep and shrinkage. Elastic shortening and relaxation of strands are taken into account in analysis.

FE modeling related assumptions are as follows:

1.  The deformations are only calculated at the nodes. The displacement variations between the nodes are linear.

2.  The bond properties between the tendons and concrete are defined by springs as connection elements.

3.  The tendons are attached to the concrete only at the nodes and only through springs.

4. Using symmetry, only one half of the beam is modeled and analyzed.

5. Self weight is incorporated as a body load, superimposed dead load is applied as a surface load, and the wheel loads are applied as nodal loads that are calculated based on the tire contact area of 10x20 inches defined in *AASHTO Standard Specifications* (AASHTO 2002) Section 3.30.

The allowable tensile stress in a prestressed beam under severe corrosive exposure conditions, due to the combined effects of prestressing, self-weight, and externally applied loads after all losses have occurred, is given as $3\sqrt{f_c'}$ (psi) for tension in the precompressed tensile zone (AASHTO 2004). For the specified compressive strength of 5000 psi, the allowable tensile stress limit for the finite element models is calculated as 212 psi. Flexure critical model capacity is defined when any element axial stress ($f_{zz}$) within the maximum moment region reaches this allowable tensile stress limit. In defining the shear critical model capacity, the stress component of interest within the fracture critical zone is the principal stress three ($f_3 \approx 212 \; psi$).

For the undamaged box-beam (distress level one), the location of the maximum tensile stress occurs near the beam edges at the maximum moment location at mid span. During field inspection, concrete spall was observed along the beam edges. When the distressed beam is considered there is no material at the location where the maximum stress would occur if the material was intact. Therefore, in the case of distressed box-beams, the maximum tensile stress location is uncertain. The reason for this is that the material where the maximum tensile stress is expected no longer exists.

The analysis of a box-beam with quarter point distress is performed with the truck position generating a maximum flexural effect in the quarter location. Under this truck configuration, the bending moment is maximum at about 30-feet from the beam end as shown in Figure 6-3. The quarter point distress may not be critical, as was the case in this analysis, unless the loss of capacity with the distress is significantly high. This is because the undamaged capacity at the location of the maximum moment may be the location where the critical tensile stress occurs.

CENTER FOR STRUCTURAL DURABILITY – Condition Assessment and Methods
of Abatement of Prestressed Concrete Box-Beam Deterioration

127

## 6.3 FE Analysis Results

### 6.3.1 Stress Conventions

The analysis results are presented as contours of primary stress components. The sign convention used in ABAQUS is positive for tensile stresses and negative for compressive stresses. The FE modeling and analysis is performed in three dimensions; therefore six stress components are calculated. A description and coordinate designation of the three-dimensional states of stress are given in Figure 6-13. The variation between the axial stresses on each parallel face of the element in Figure 6-13 generates shear stresses. In forming an analogy with the one-dimensional beam model used in design, $f_{zz}$ is the uniaxial, axial and flexure combined stress, and $f_{yz}$ is the shear stress. Upon reviewing the analysis results, in all cases, stress defined as $f_{zz}$ dominates the other uniaxial stresses. Thus, the critical shear stress is on the y-z plane designated as $f_{yz}$.
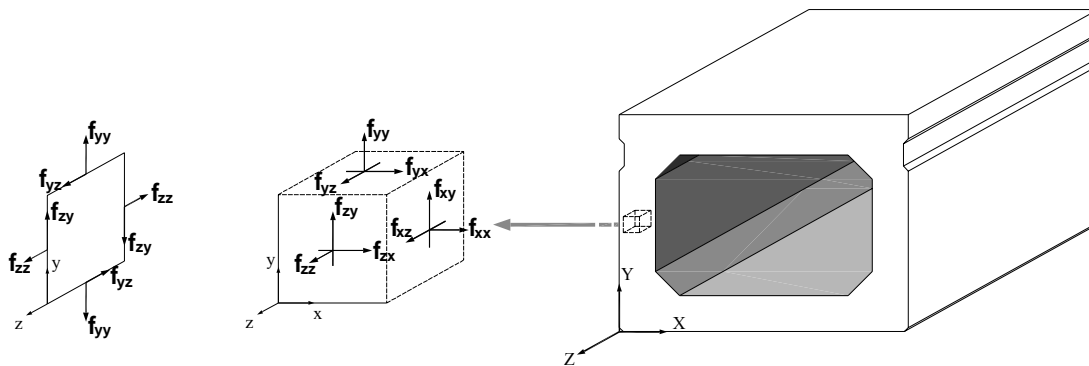


Note: X, Y, Z are the global and x, y, z are the local coordinates

**Figure 6-13:  Stresses and coordinate system used in the box-beam models**

### 6.3.2 Flexural Critical Beam Analysis Results

The uniaxial stresses ($f_{zz}$) obtained from the results of the flexure critical model are shown in Figures 6-14 to 6-17. Figures 6-14 and 6-15 show the undamaged stress trajectories for the models with maximum moment location at mid span and quarter location.

Figure 6-14 shows the flexural contours of the undamaged beam under the truck configuration generating the maximum flexural effect at the mid span. The percentages of wheel line loads that generate the critical tensile stress of around 212 psi are also shown in Figures 6-14 to 6-17.

Figure 6-15 shows the contours of (uniaxial) flexural stress under the truck axle configuration that generates maximum quarter point moments. Figures 6-14 and 6-15 represent the base line for comparison to distressed beams.

Figure 6-16 (a) through (c) and Figure 6-17 (a) through (c) shows the contours of uniaxial stress obtained from the analysis of the beam model with the three damage levels at the mid span and at the quarter locations. Also included in the figures are the percentages of wheel line loads applied to the beam generating the limiting tensile stress of 212 psi. As seen in the figures, near the beam end, the axial stress gradually redistributes and the stress contours become uniform at about the transfer length distance from the end. As expected, the critical tensile stress is obtained at or near mid span for all four distress levels.

**Applied Load = 52.9 % of wheel line load**
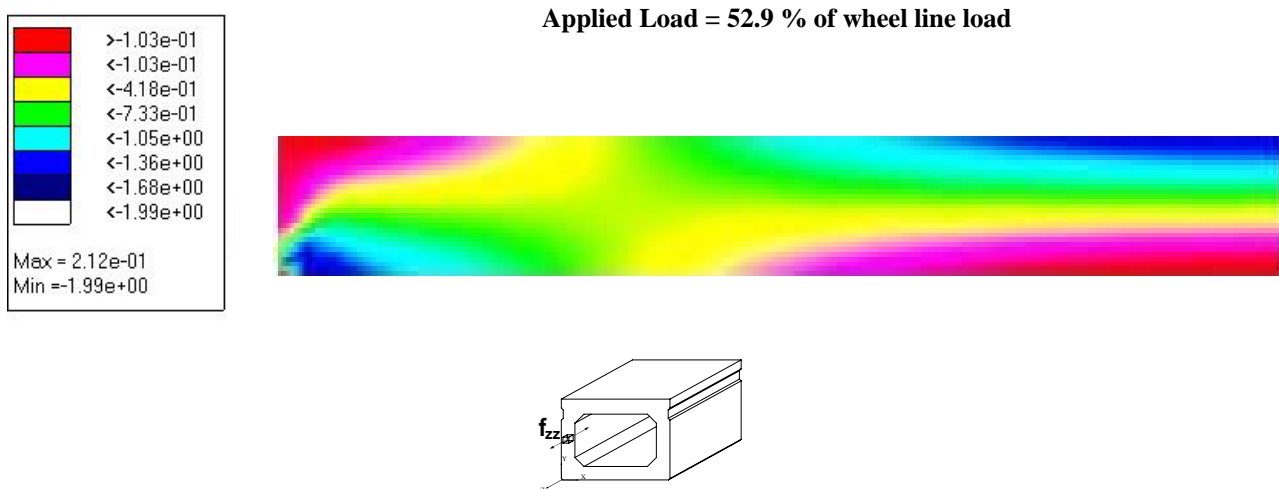


**Figure 6-14: Level 1 – undamaged axial stress ($f_{zz}$) (ksi) trajectory along the length of box-beam for maximum moment at mid span (partial view, supported on left)**

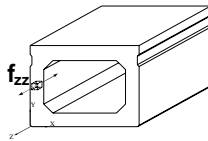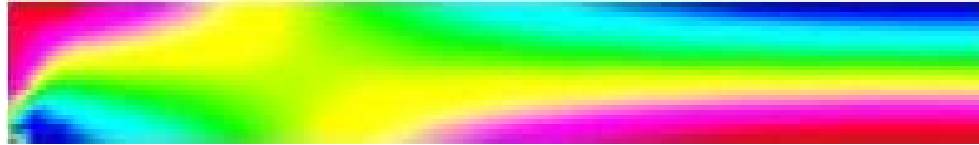**Applied Load = 54.0 % of wheel line load**



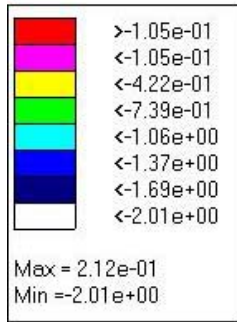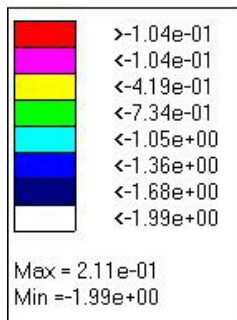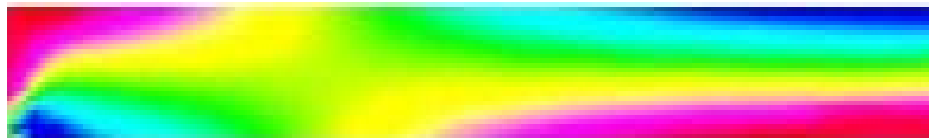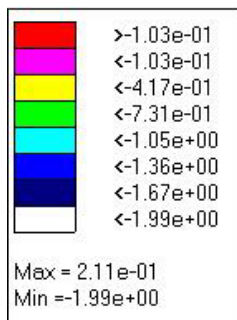**Figure 6-15:  Level 1 – undamaged axial stress ($f_{zz}$) (ksi) trajectory along the length of box-beam for maximum moment at quarter location (partial view, supported on left)**
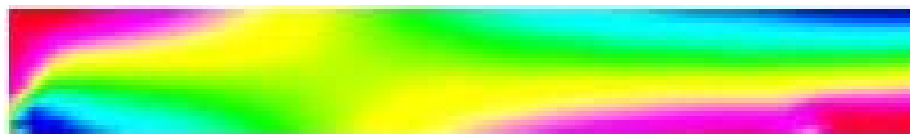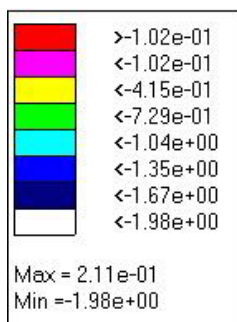
**Applied Load = 55.4 % of wheel line load**



| | |
|---|---|
| >-1.04e-01 | |
| <-1.04e-01 | |
| <-4.19e-01 | |
| <-7.34e-01 | |
| <-1.05e+00 | |
| <-1.36e+00 | |
| <-1.68e+00 | |
| <-1.99e+00 | |

Max = 2.11e-01
Min =-1.99e+00

**(a) Level 2 – spall (partial view, supported on left)**


**Applied Load = 48.4 % of wheel line**



| | |
|---|---|
| >-1.03e-01 | |
| <-1.03e-01 | |
| <-4.17e-01 | |
| <-7.31e-01 | |
| <-1.05e+00 | |
| <-1.36e+00 | |
| <-1.67e+00 | |
| <-1.99e+00 | |

Max = 2.11e-01
Min =-1.99e+00

**(b) Level 3 – spall and 2 broken tendons (partial view, supported on left)**


**Applied Load = 42.5 % of wheel line load**



| | |
|---|---|
| >-1.02e-01 | |
| <-1.02e-01 | |
| <-4.15e-01 | |
| <-7.29e-01 | |
| <-1.04e+00 | |
| <-1.35e+00 | |
| <-1.67e+00 | |
| <-1.98e+00 | |

Max = 2.11e-01
Min =-1.98e+00

**(c) Level 4 – spall and 4 broken tendons (partial view, supported on left)**



$f_{zz}$

**Figure 6-16:  Axial stress ($f_{zz}$) (ksi) trajectory along the length of the box-beam for damage levels 2 to 4 for maximum moment at mid span**


**Applied Load = 56.9 % of wheel line load**

CENTER FOR STRUCTURAL DURABILITY – Condition Assessment and Methods
of Abatement of Prestressed Concrete Box-Beam Deterioration

131

**Applied Load = 56.9 % of wheel line load**

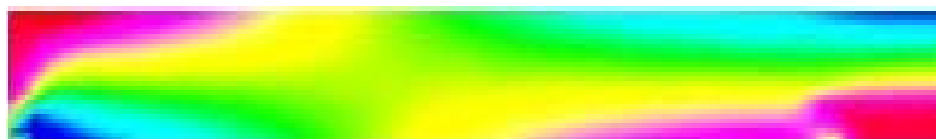**(a) Level 2 – spall (partial view, supported on left)**



**Applied Load = 56.9 % of wheel line load**
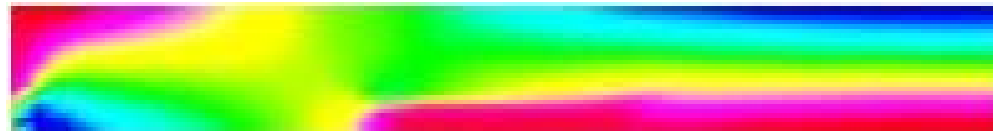
**(b) Level 3 – spall and 2 broken tendons(partial view, supported on left)**



**Applied Load = 58.1 % of wheel line**

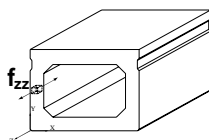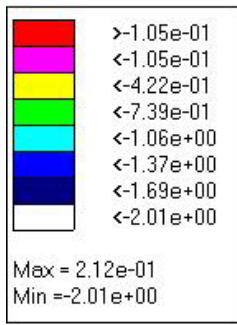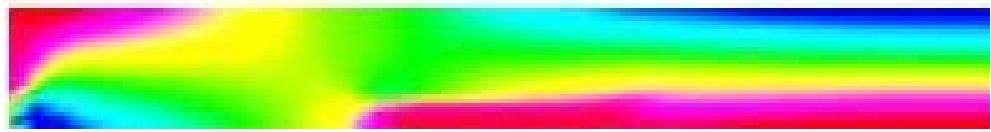**(c) Level 4 – spall and 4 broken tendons (partial view, supported on left)**

**Figure 6-17:  Axial stress ($f_{zz}$) (ksi) trajectory along the length of the box-beam for damage levels 2 to 4 for maximum moment at quarter location**
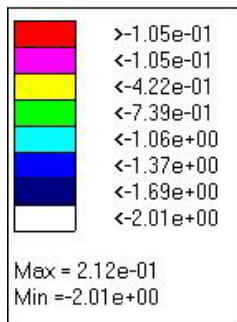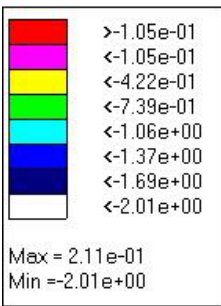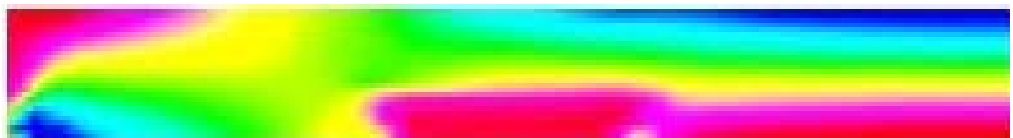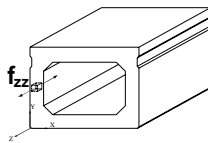
### 6.3.3 Flexural Critical Box-Beam Capacities

The stress and deformation calculations under the dead loads and wheel line loads were performed assuming elastic behavior of both materials (prestressing steel and concrete). The wheel line loads applied to the FE models were scaled to a proportion of the load that would generate the allowable tensile stress of 212 psi. Table 6-8 shows the moment capacities calculated from the sectional stress distribution obtained from finite element analysis. The moment capacities are calculated by taking moments about the neutral axis, after the FE analysis utilizing the uniaxial stress data at the critical cross section. The neutral axis is defines as the location where uniaxial stresses diminish. In the moment calculations the tensile stresses form below the neutral axis contributes to the moment capacity. In order to obtain conservative moment capacities the contribution of tensile stresses below the neutral axis is ignored. This is equivalent to assuming the section to be cracked below the neutral axis. It should be noted that when the tensile stress below the neutral axis is neglected, assuming a cracked section, the resulting moment capacities calculated form sectional analysis will be lower than the equivalent static moment values.

**Table 6-8: Moment capacities for box-beams at various distress levels**

| Beam condition | FE model moment capacity for distress at specified locations | |
| --- | --- | --- |
| | Mid span | Quarter point |
| Undamaged | 601.2 ft-k | 600.9 ft-k |
| Spall | 610.0 ft-k | 600.9 ft-k |
| Spall and 2 broken tendons | 566.8 ft-k | 600.9 ft-k |
| Spall and 4 broken tendons | 527.1 ft-k | 600.5 ft-k |

The girder rating factor is calculated corresponding to each level of distress (Table 6-9) using the bridge rating (load factor) formula in the *Bridge Analysis Guide* (MDOT 2003a). Live load moment capacity of the beam is calculated by subtracting the moment capacities given in Table 6-8 from the static moment generated by the dead loads. From AASHTO (2002) Section 3.8.2, the impact factor for span length of 57 feet is calculated as 0.27. The rating factor of the girder is calculated using the following equation:

$$RF = (C-A_1D) / [A_2L(1+I)] \qquad\qquad (6\text{-}25)$$

$RF$ = the operating rating factor for the live-load carrying capacity

$C$ = the capacity of the member, $M_n$

$D$ = the dead load effect on the member, $M_{DL}$

$L$ = the live load effect on the member, $M_{LL}$

$I$ = impact factor (0.27)

$A_1$ = factor for dead load (1.3 for finite element models)

$A_2$ = factor for live load (1.3 for finite element models)

**Table 6-9: Rating factor for distress levels one through four at mid-span**

| Beam Condition | Moment at Critical Section (ft-kips) | | Rating Factor |
|---|---|---|---|
| | DL + SDL | LL | |
| Undamaged | | 257.2 | 0.36 |
| Spall | 344 | 266 | 0.37 |
| Spall & 2 broken tendons | | 222.8 | 0.33 |
| Spall & 4 broken tendons | | 183.1 | 0.26 |

Note: DL – Dead Load, SDL – Superimposed Dead Load, LL- Live Load

**Table 6-10: Rating factor for distress levels one through four at quarter point**

| Beam Condition | Moment at Critical Section (ft-kips) | | Rating Factor |
|---|---|---|---|
| | DL + SDL | LL | |
| Undamaged | | 256.9 | 0.36 |
| Spall | 344 | 256.9 | 0.36 |
| Spall & 2 broken tendons | | 256.9 | 0.36 |
| Spall & 4 broken tendons | | 256.5 | 0.36 |

Note: DL – Dead Load, SDL – Superimposed Dead Load, LL- Live Load

### 6.3.4 Shear Critical Analysis Results

In the shear stress analysis of the prestressed concrete (PC) box-beam, the critical shear stress location is not obvious. In design, the critical shear is calculated at a cross-section located at a distance equal to the beam depth measured from the support. In PC beams, the critical diagonal tension crack will form at the mid point of the web. (maximum shear stress location is at a distance of at about one half of the beam depth from the support). For the analysis, the PC-box-beam is assumed to reach capacity upon the crack formation. The diagonal tension crack will form by the principal tensile stress reaching the critical tensile stress (212 psi) at about half the beam depth away from the support.

In order to document the shear stress development on the y-z plane, the stress contours were obtained at selected sections along the beam axis as shown in Figure 6-18. Sections *a* through *f* are located at 4.5, 9.0, 13.5, 18.0, 22.5, and 27 inches from the end. The development of shear stresses near the support is viewed at these selected sections. The shear and uniaxial stress contours are shown in Tables 6-11 and 6-12. Each contour starting at a distance of 4.5 inches from the support shows the force transfer to the support in the form of shear and uniaxial stresses. In Table 6-11, shear stresses decrease rapidly from a maximum of 538 psi at 4.5 inches from the support to 249 psi at 13.5 inches from the support. In this length, the area resisting shear gradually increases to the full web area. The decrease in shear stress between 13.5 to 27 inches from the support is more gradual (from 249 psi to 191 psi) as the shear is resisted by the full web (Table 6-12).
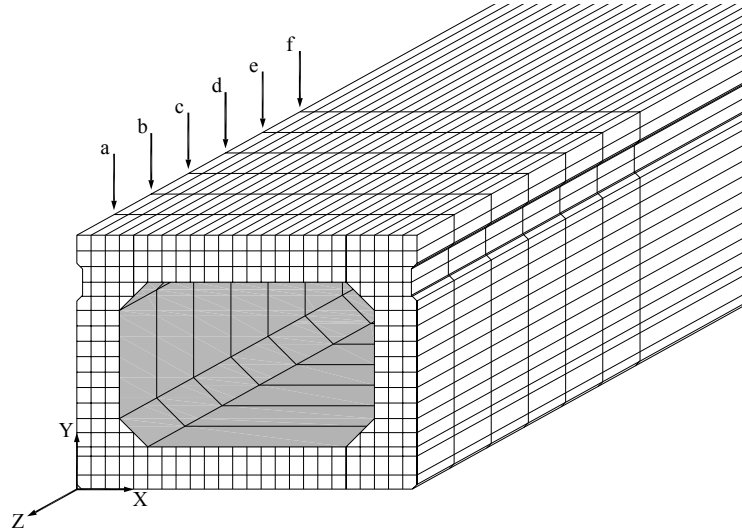


**Figure 6-18:  Sections at which the shear stress distribution is evaluated**

In defining the beam shear capacity the principal stresses are calculated from the shear stress values.  The capacity is defined based on maximum allowable tensile stress ($3\sqrt{f_c'}$ psi) magnitude of 212 psi reached near the beam end and on the web.  The tensile stresses

for the shear critical model are obtained by using the principal stress contours. As shown in Figure 6-19, the principal stresses are calculated by rotating the x-y-z coordinates until the shear stress diminishes. The principal stresses of interest are the tensile (maximum) and compressive (minimum) principal stresses, $f_3$ and $f_1$ respectively. The stress magnitudes on the x-z and x-y planes are small. For that reason, the principal stresses $f_3$ and $f_1$ remain in the y-z plane (refer to Figure 6-13 for definition of y-z plane). Principal compressive stress is $f_1$ and the principal tensile stress is $f_3$.
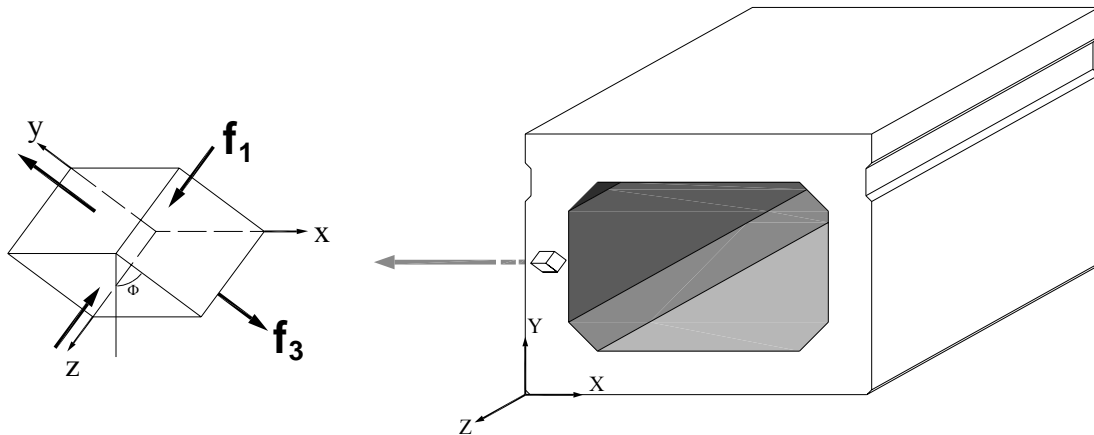


**Figure 6-19: Principal stresses on a finite element**

Figures 6-20 through 6-23 show the uniaxial stress contours for all the four distress states. The contours are plotted on the beam elevation including an enlarged area near the beam end. These figures show the stress path to the support under the live load capacity.

The principal $f_1$ and $f_3$ stress contours of the undamaged beam at cross-sections between 4.5 to 27 inches are shown in Tables 6-13 and 6-14. The principal stress contours for the case of distressed beams are shown for the cross-sections where the tensile stress is about 212 psi. Tables 6-15 through 6-17 show the principal stress contours of beams with end damage levels 2, 3 and 4. In all end damage cases the tensile stress on the web of about 210 psi occurs at 22.5 inches from the support.

**Table 6-11: Axial ($f_{zz}$) and shear stress ($f_{yz}$) (ksi) trajectories for distress level 1 – undamaged (4.5 to 13.5 inches from support)**

| Axial Stress ($f_{zz}$) at Cross-section | Shear Stress ($f_{yz}$) at Cross-section |
|---|---|



**4.5 inches from the support**



**9 inches from the support**



**13.5 inches from the support**
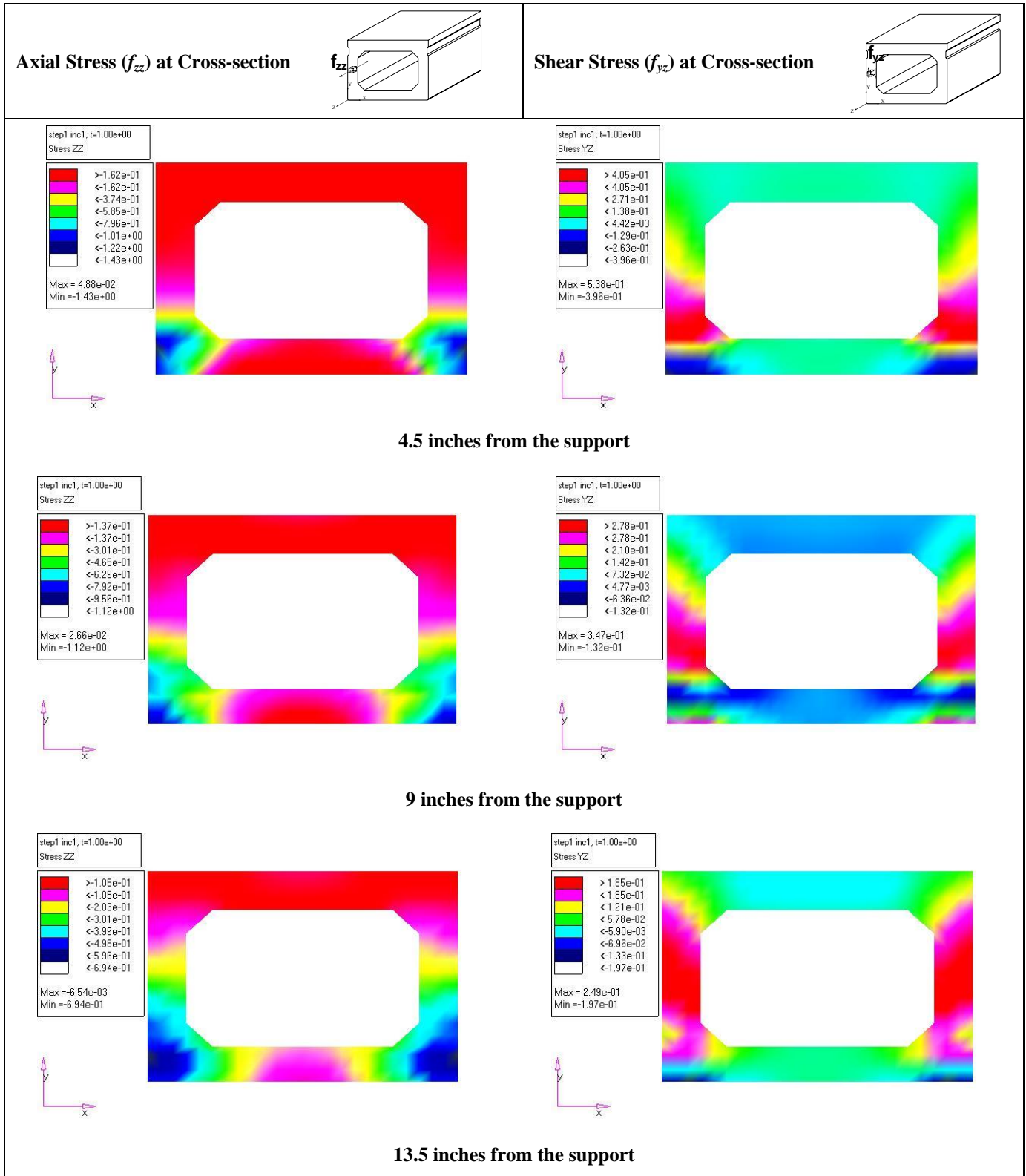
**Table 6-12:  Axial ($f_{zz}$) and shear stress ($f_{yz}$) (ksi) trajectories for level 1 – undamaged (18 to 27 inches from support)**

| Axial Stress ($f_{zz}$) at Cross-section | Shear Stress ($f_{yz}$) at Cross-section |
|---|---|
|  |  |

**18 inches from the support**

|  |  |
|---|---|

**22.5 inches from the support**

|  |  |
|---|---|

**27 inches from the support**
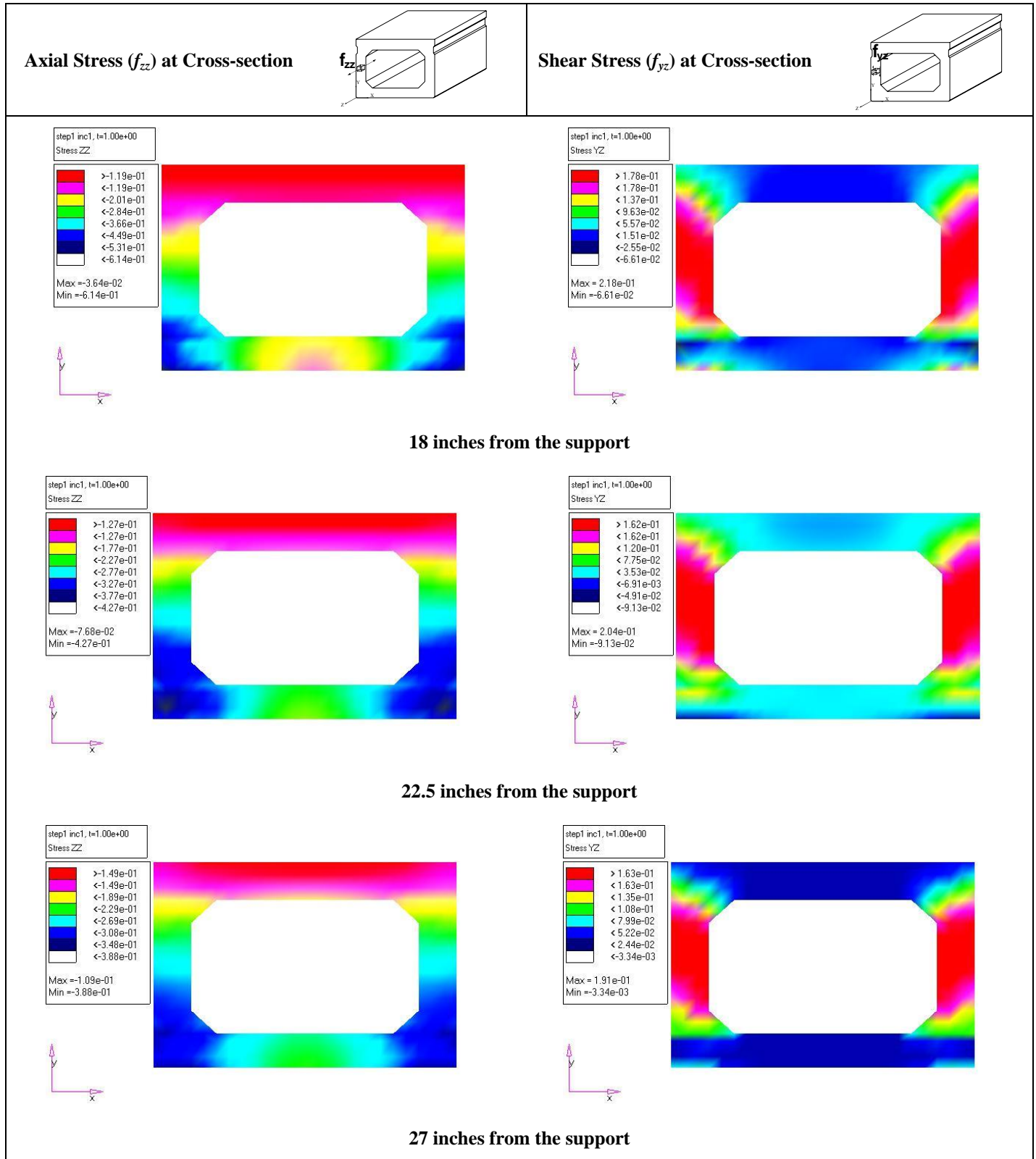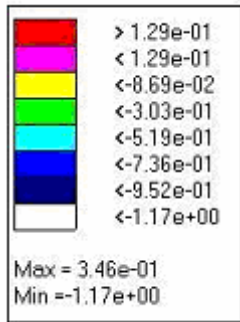
**Axial stress trajectory of full length of box-beam (partial view, supported on left)**
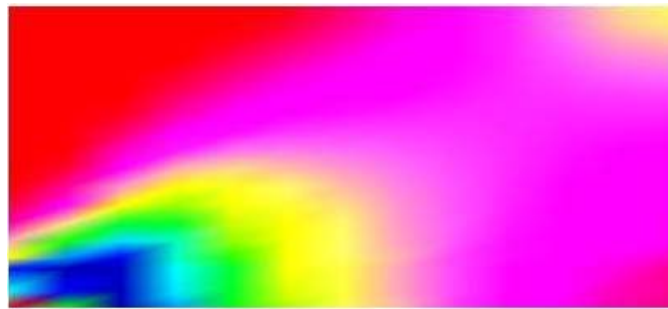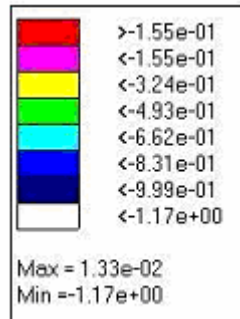


**Axial stress trajectory of enlarged end portion of box-beam**

**(partial view, supported on left)**
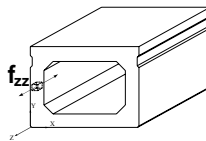


**Figure 6-20: Level 1 – undamaged axial stress ($f_{zz}$) (ksi) trajectory along the length of box-beam**

CENTER FOR STRUCTURAL DURABILITY – Condition Assessment and Methods
of Abatement of Prestressed Concrete Box-Beam Deterioration

139
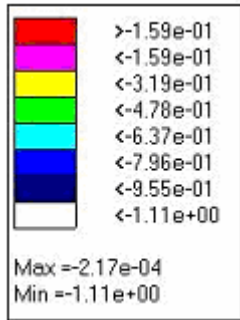
**Axial stress trajectory of full length of box-beam (partial view, supported on left)**
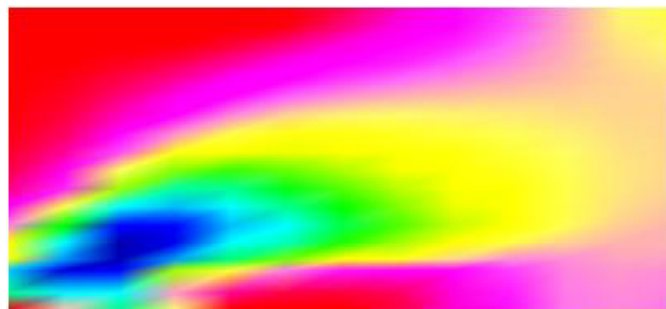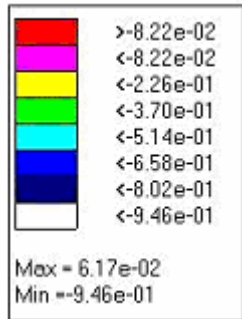


**Axial stress trajectory of enlarged end portion of box-beam**

**(partial view, supported on left)**
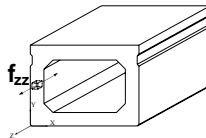


**Figure 6-21:  Level 2 – spall - axial stress ($f_{zz}$) (ksi) trajectory along the length of box-beam**

| > 5.29e-02 |
| < 5.29e-02 |
| <-1.05e-01 |
| <-2.64e-01 |
| <-4.22e-01 |
| <-5.80e-01 |
| <-7.38e-01 |
| <-8.97e-01 |

Max = 2.11e-01
Min =-8.97e-01

**Axial stress trajectory of full length of box-beam (partial view, supported on left)**



| >-1.05e-01 |
| <-1.05e-01 |
| <-2.37e-01 |
| <-3.69e-01 |
| <-5.01e-01 |
| <-6.33e-01 |
| <-7.65e-01 |
| <-8.97e-01 |

Max = 2.69e-02
Min =-8.97e-01
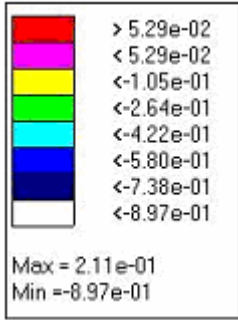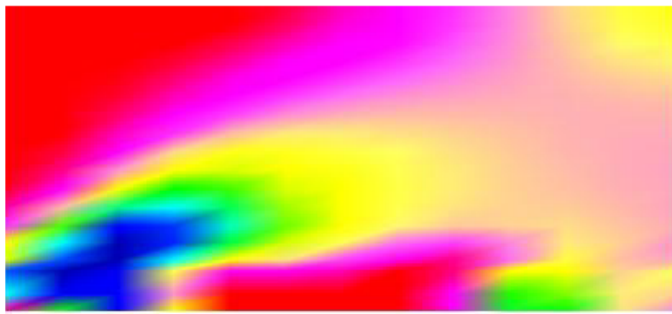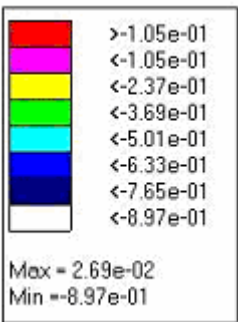
**Axial stress trajectory of enlarged end portion of box-beam (partial view, supported on left)**
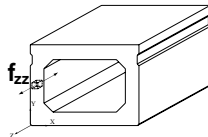


**Figure 6-22:  Level 3 – spall and 2 broken tendons - axial stress ($f_{zz}$) (ksi) trajectory along the length of box-beam**

| | |
|---|---|
| > 1.65e-02 | |
| < 1.65e-02 | |
| <-1.39e-01 | |
| <-2.94e-01 | |
| <-4.50e-01 | |
| <-6.05e-01 | |
| <-7.61e-01 | |
| <-9.16e-01 | |

Max = 1.72e-01
Min =-9.16e-01

**Axial stress trajectory of full length of box-beam (partial view, supported on left)**



| | |
|---|---|
| >-1.04e-01 | |
| <-1.04e-01 | |
| <-2.39e-01 | |
| <-3.75e-01 | |
| <-5.10e-01 | |
| <-6.46e-01 | |
| <-7.81e-01 | |
| <-9.16e-01 | |

Max = 3.16e-02
Min =-9.16e-01
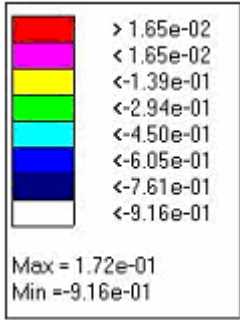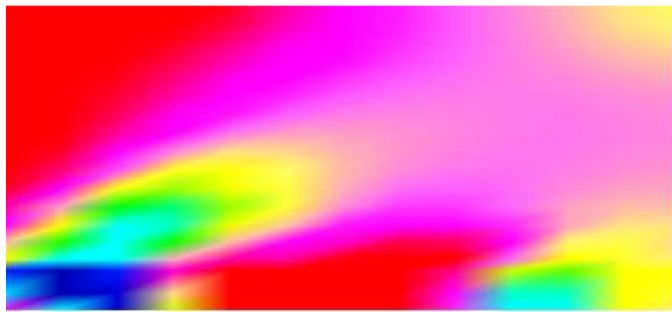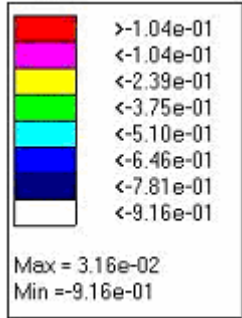
**Axial stress trajectory of enlarged end portion of box-beam**

**(partial view, supported on left)**
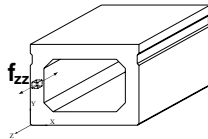


**Figure 6-23:  Level 4 – spall and 4 broken tendons - axial stress ($f_{zz}$) (ksi) trajectory along the length of box-beam**

**Table 6-13: Principal stress 1 ($f_1$) and principal stress 3 ($f_3$) (ksi) trajectories for level 1 – undamaged (4.5 to 13.5 inches from support).**

| Principal Stress 1 ($f_1$) at Cross-section | Principal Stress 3 ($f_3$) at Cross-section |
|---|---|
|  |  |

**4.5 inches from the support**

| | |
|---|---|
|  |  |

**9 inches from the support**

| | |
|---|---|
|  |  |

**13.5 inches from the support**
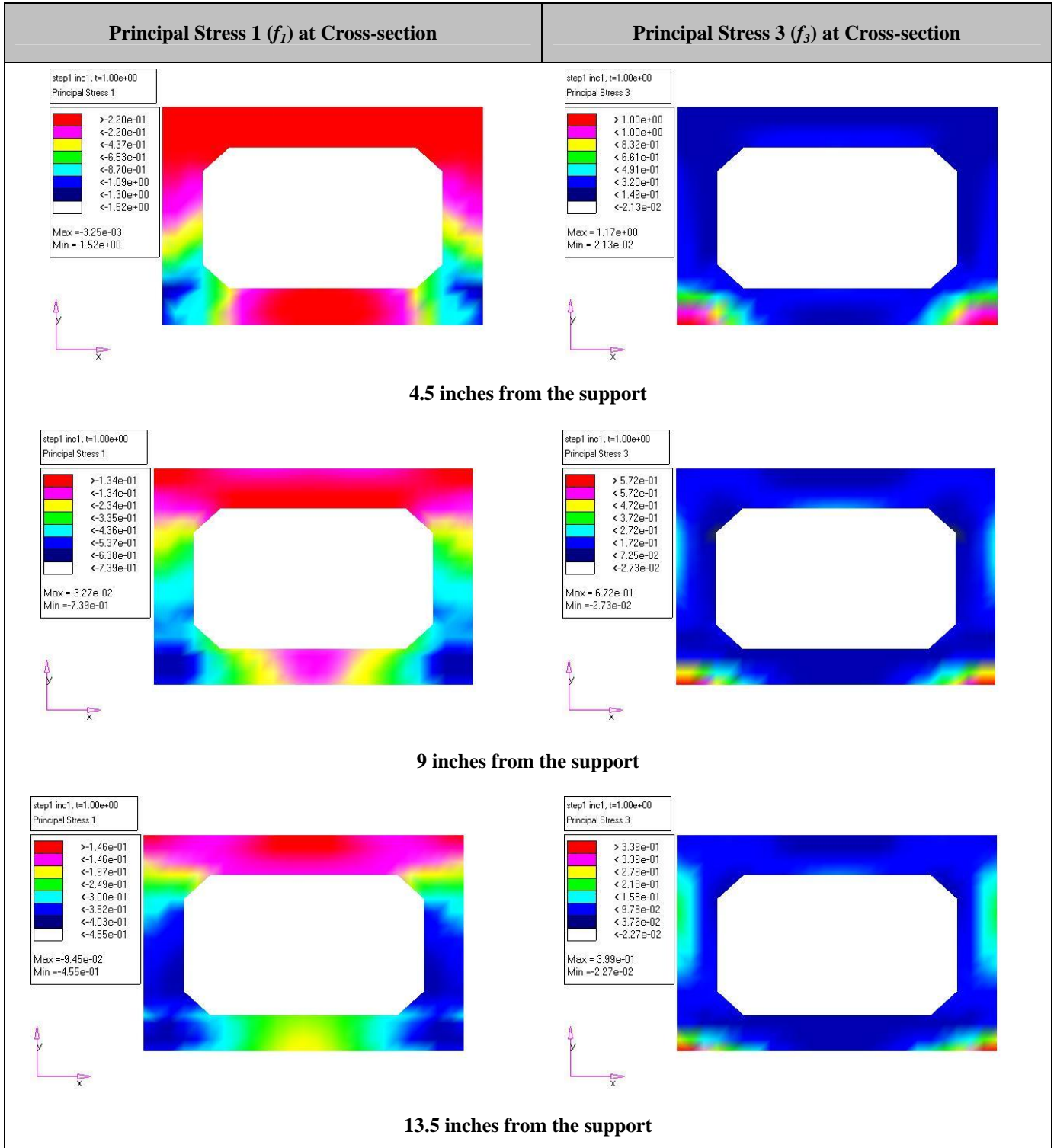
**Table 6-14: Principal stress 1 (*f₁*) and principal stress 3 (*f₃*) (ksi) trajectories for level 1 – undamaged (18 to 27 inches from support)**

| Principal Stress 1 (*f₁*) at Cross-section | Principal Stress 3 (*f₃*) at Cross-section |
|---|---|
|  |  |

**18 inches from the support**

|  |  |
|---|---|

**22.5 inches from the support**

|  |  |
|---|---|

**27 inches from the support**
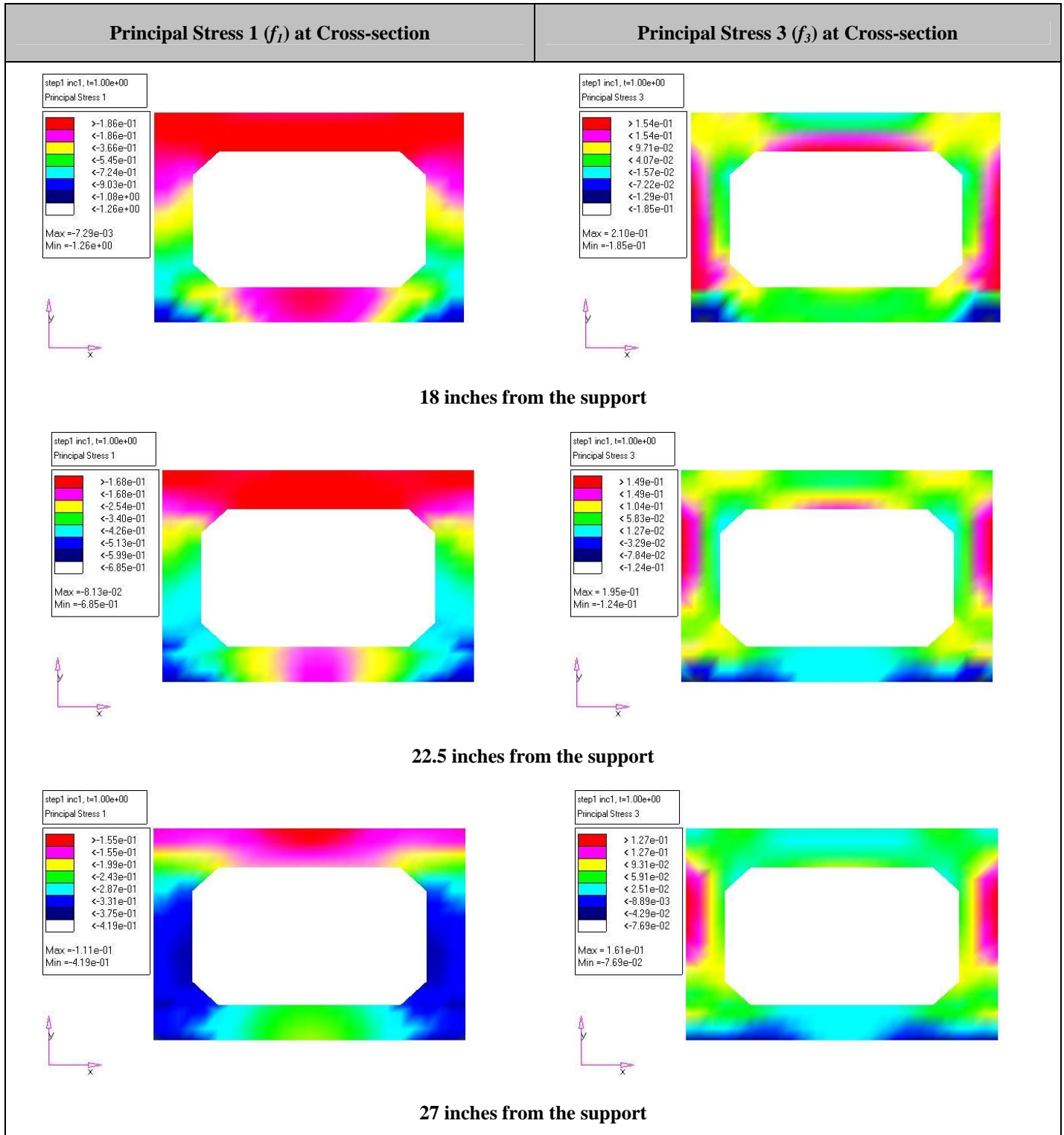
**Table 6-15: Critical principal stress 1 ($f_1$) & principal stress 3 ($f_3$) (ksi) trajectories for distress level 2**

| Principal Stress 1 ($f_1$) at Cross-section | Principal Stress 3 ($f_3$) at Cross-section |
|---|---|
|  |  |
| **22.5 inches from the support** | |
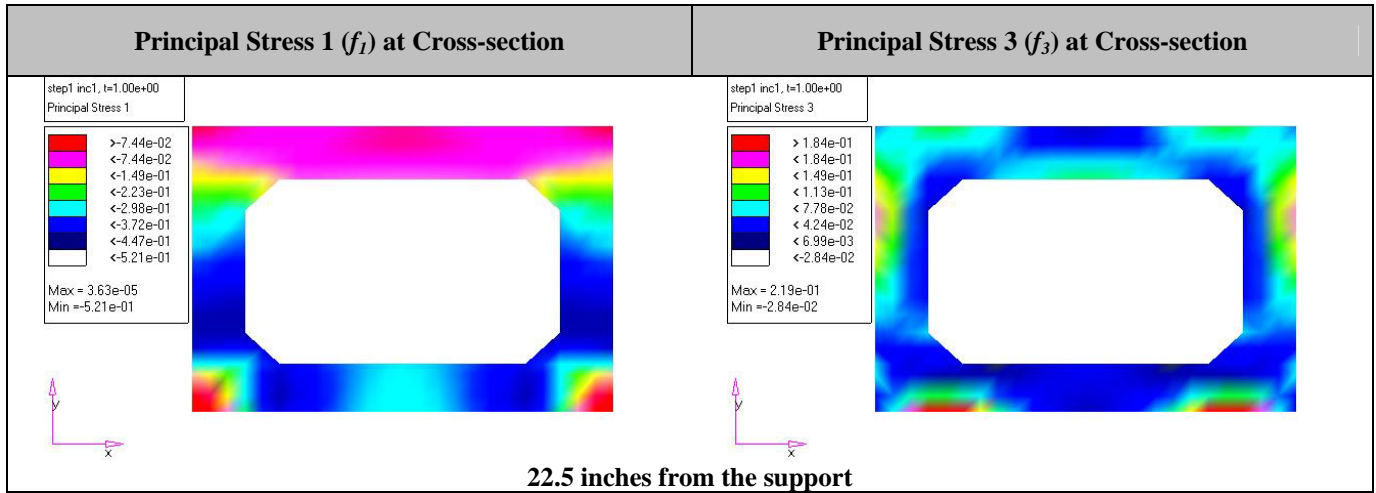
**Table 6-16: Critical principal stress 1 ($f_1$) & principal stress 3 ($f_3$) (ksi) trajectories for distress level 3**

| Principal Stress 1 ($f_1$) at Cross-section | Principal Stress 3 ($f_3$) at Cross-section |
|---|---|
|  |  |
| **22.5 inches from the support** | |
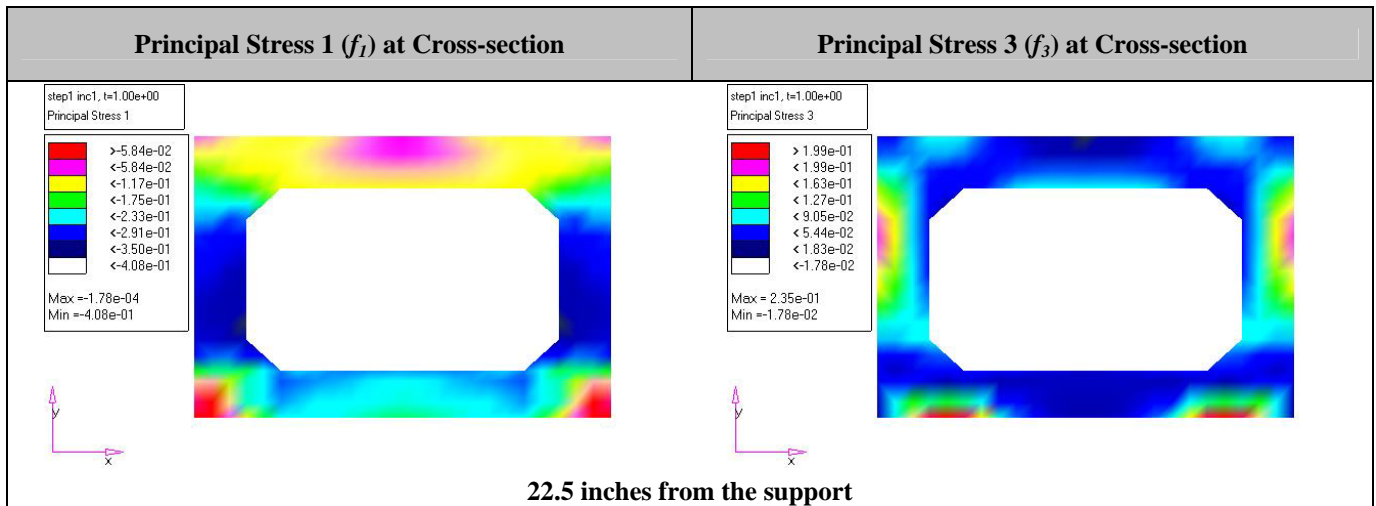
**Table 6-17: Critical principal stress 1 ($f_1$) & principal stress 3 ($f_3$) (ksi) trajectories for distress level 4**

| Principal Stress 1 ($f_1$) at Cross-section | Principal Stress 3 ($f_3$) at Cross-section |
|---|---|
|  |  |
| **22.5 inches from the support** | |
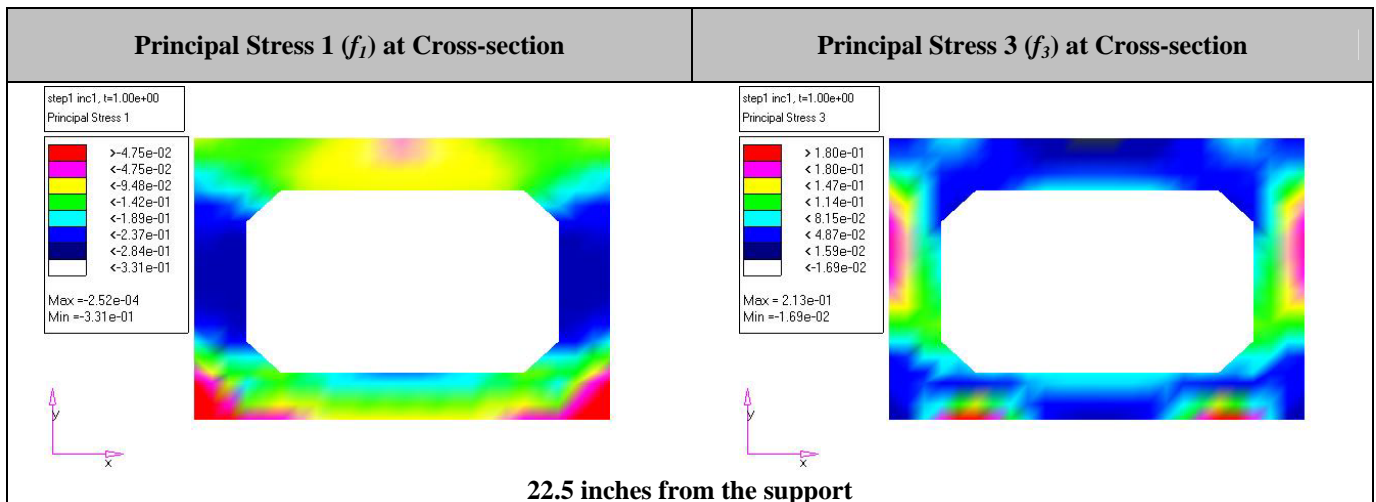
### 6.3.5   Shear Critical Box-Beam Capacities

The rating factor is calculated for each level of distress using the bridge operating rating (load factor) formula in the *Bridge Analysis Guide* (MDOT 2003a) (Table 6-19). The beam shear capacity given in Table 6-18 is calculated from the FE analysis as the cross-sectional shear at the time the principal tensile stress of 212 psi (Section 6.2.7) is reached within the web. The live load capacity in Table 6-19 represents the level of live load at the time shear failure criteria is fulfilled. The difference between the beam capacity and live load capacity is the shear generated by the dead load. When calculating the live load shear, the load distribution factor is taken as one. From AASHTO (2002) Section 3.8.2, the impact factor for span length of 30 ft. is calculated as 0.32 which is greater than 0.3. Hence, the impact factor in Equation 6-26 is taken as 0.3. The rating factor is calculated by the following equation:

$$RF = (C - A_1 D) / [A_2 L (1 + I)] \quad (6\text{-}26)$$

$RF$ = the operating rating factor for the live-load carrying capacity

$C$ = the capacity of the member, $V_n$

$D$ = the dead load effect on the member, $V_{DL}$

$L$ = the live load effect on the member, $V_{LL}$

$I$ = impact factor (0.3)

$A_1$ = factor for dead load (1.3 for finite element models)

$A_2$ = factor for live load (1.3 for finite element models)

The comparison of the rating factors shown in Tables 6-9, 6-10, and 6-12 indicate that flexural capacities (Tables 6-9 and 6-10) will control the beam capacity.

**Table 6-18:  Shear capacity for box-beam**

| Beam Condition | FE Model Shear Capacity (kips) |
|---|---|
| Undamaged | 41.71 |
| Spall | 35.42 |
| Spall and 2 broken tendons | 32.91 |
| Spall and 4 broken tendons | 31.19 |

**Table 6-19:  Rating factor for distress levels one through four for shear**

| Beam Condition | Shear at Critical Section (kips) | | Rating Factor |
|---|---|---|---|
| | DL + SDL | LL | |
| Undamaged | | 29.00 | 0.51 |
| Spall | 12.71 | 22.71 | 0.49 |
| Spall and 2 broken tendons | | 20.20 | 0.48 |
| Spall and 4 broken tendons | | 18.48 | 0.47 |

**DL: Dead Load, SDL: Superimposed Dead Load, LL: Live Load**

## 6.4  Summary and Conclusions

The FE modeling and analysis was performed for a 27x36-inch cross-section box-beam at two beam lengths. The length of 57-feet was determined as critical for flexure under Truck 17 (11 axel truck with total load of 145.4 kips).  Shear critical beam length was established as 30-feet also under Truck 17.  The loads applied on the FE model included beam self weight and superposed dead load totaling 0.847 kip/ft.  The live load was applied in increments until the tensile stress limit of $3\sqrt{f_c'}$ (212 psi) is reached.  The truck load applied on the beam at that time the tensile stress limit is reached is defined as the live load capacity. Flexural capacity is calculated from sectional analysis utilizing the uniaxial stresses obtained from FE analysis.  Shear capacity of the beam is calculated from the truck load generating a principal tensile stress of 212 psi within the fracture critical zone.  The fracture critical zone of the beam is defined at the web and between 13.5 and 27-inches from the support.

The analysis results showed that the beam with the most damage (distress level four) has a flexural capacity equal to 42.5% of the wheel line load and a shear capacity equal to 63.7 %

CENTER FOR STRUCTURAL DURABILITY – Condition Assessment and Methods
of Abatement of Prestressed Concrete Box-Beam Deterioration

147

of wheel line load.  The flexure critical and shear critical beam analysis was performed with the same truck type (Truck 17). Thus, the flexural capacity governs the beam failure.

The rating factor for the individual box-beam was calculated using the formula given in the *Bridge Analysis Guide* (MDOT 2003a).   Strictly speaking, the formulation discussed in the guide is for rating bridges.   However, the beam safety, thus the bridge safety can be evaluated by comparing the normalized live load capacities.  As discussed earlier, the beam flexural capacity is calculated directly from the cross-sectional stresses obtained under the level of wheel line load generating the critical tensile stress. In calculating the capacities, the section is assumed fully cracked and the tensile stress is neglected.  In analytical methods (procedures given in design manuals), it is assumed that the flexural stress distribution across the beam width, at a particular distance from the neutral axis, is uniform.  However, in a 3D box-beam, the stress distribution across the beam width resembles to a parabolic curve giving the maximum stress levels near the beam corners or sides.  The stress distribution patterns used in calculations caused the differences of box-beam ratings calculated from analytical and FE methods. The ratings calculated from FE method is more accurate than that calculated from analytical methods because the FE method is capable of representing the stress distribution on a 3D box-beam model.  The rating factors obtained from analytical and FE methods are shown in Table 6-13. The rating factors were calculated using the load distribution factor of one and impact factors of 0.27 and 0.3 for flexure and shear, respectively.  The distribution factors calculated using the *AASHTO Standard Specifications for Highway Bridges* (AASHTO 2002) and the *AASHTO LRFD Bridge Design Specifications* (AASHTO 2004) were around 0.25.  Hence, even the beam with the most damage (distress level four) provides a reserve capacity of 7% of wheel line load.  This reserve is only available if the shear keys allow the load distribution to adjacent beams.  In the case of non-functional shear key the beam must provide a capacity for 100% of wheel line load.

Table 6-20:  Rating factor comparison calculated from analytical and FE methods

| Beam Condition | Rating Factor | |
|---|---|---|
| | **Analytical Method** | **FE Method** |
| **Undamaged** | 0.41 | 0.36 |
| **Spall** | 0.42 | 0.37 |
| **Spall and 2 broken tendons** | 0.40 | 0.33 |
| **Spall and 4 broken tendons** | 0.36 | 0.26 |

This page intentionally left blank

# Chapter 7: Phase I Conclusions and Recommendations

## *7.1 Conclusions*

Five objectives were identified for Phase I of this project. The first objective was to identify common types of deterioration in Michigan box-beam bridges and to develop inspection techniques for early identification of cracking and strand corrosion at the ends of the beams. This was accomplished through extensive field investigations of 15 bridges located in the lower peninsula of Michigan. The field inspections identified common types and states of deterioration. Cracking and strand corrosion of prestressed concrete box-beams was found to be no more substantial at the beam ends than elsewhere on the beam. Inspection techniques for early identification of distress were identified in the literature review portion of this report.

Field inspection data and literature review indicate that cracking of shear keys are a major cause of deterioration via salt laden water intrusion. In addition, there was evidence of water collecting inside the box-beams. Rust staining around the drain holes and longitudinal cracks along the bottom flange were noted. Longitudinal cracking on the bottom flanges may have occurred due to expansive forces exerted on the beam by corroding tendons or by the freezing of water collected inside the box-beam cavity. Even though Styrofoam is now used to form the box-beam void, moisture can collect between the Styrofoam and concrete on the inside of the bottom flange. Hence, the tendons near the inner cavity may be subject to a more severe exposure than that of the outmost tendon layer. At this stage, it is recommended that the concrete cover of prestressing tendon near the top of the bottom flange be reviewed.

The second project objective was to develop guidelines to assist inspectors in determining when section loss may reduce structural capacity. Any amount of section loss has the potential to reduce structural capacity either immediately or over time. Large spalls with exposed strand lower the structural capacity through the loss of cross-section of the beam. Smaller spalls lessen the concrete cover around the steel reinforcing allowing for the potential of accelerated deterioration of the steel strand or reinforcing steel and future

CENTER FOR STRUCTURAL DURABILITY – Condition Assessment and Methods
of Abatement of Prestressed Concrete Box-Beam Deterioration

151

loss of capacity. Many factors come into play in determining the effect of deterioration on structural capacity; the type, size, and location of distress all play a significant role. For this reason, sample load rating calculations are provided to allow an engineer to determine the effect of distress on a case-by-case basis. The process may be significantly automated through the use of MathCAD or a similar mathematical programming tool.

The next objective was to provide guidelines for the load capacity assessment of bridges with distressed beams based on finite element modeling. Extensive research was conducted in regards to finite element modeling of prestressed concrete beams and deteriorated conditions. The information found in that task was applied to detailed modeling of a single prestressed concrete box-beam. Several forms of distress were simulated and the results were summarized and presented in Chapter 6.

The fourth objective was to identify effective maintenance or repair techniques for deteriorated regions of box-beam bridges considered to be in good or fair condition. Places typically of concern for deterioration on box-beam bridges were identified in the literature review and verified during the field investigations. Effective maintenance and repair techniques were identified in the literature review and in the inspection handbook and repair flowcharts located in Appendix C and E. This objective will be expanded upon during Phase II to include validation of the maintenance and repair techniques.

The final objective of Phase I was to develop recommendations for changes or modifications to the design of side-by-side box-beam bridges based on the results of the analytical modeling. For effective modifications to the design of side-by-side box-beam bridges, the effect of the entire structure must be considered. The finite element model developed for Phase I focused on determining the stress distribution within a single prestressed box-beam. Results of this model showed no significant problems with the existing design; however, several problems found in the field were not addressed by this model. Shear key cracking and differential movement of adjacent beams was observed during the inspections. This distress situation cannot be addressed until a finite element model is developed to represent the entire bridge system; a task planned for Phase II.

Phase I of the box-beam deterioration project provides a solid base for understanding the issues involved in the maintenance of Michigan's side-by-side box-beam bridges. The literature review explains the structural behavior of these bridges and provides a history of box-beam bridge design. Background information on durability and deterioration issues, tools for identifying distress, and the effects of premature deterioration and how to make proper repairs are identified. The Pontis database was used to identify 15 side-by-side box-beam bridges in Michigan to be reviewed during the field inspections. These bridges were inspected and forms of distress identified during the literature review were found and documented. An inspection handbook was created to aid a bridge inspector during a scoping or damage assessment bridge inspection. This handbook provides guidance on what to look for and what impact it may have on the structural integrity of the beam. Flowcharts are included to aid the design engineer in determining proper repair techniques. Additionally, sample load rating calculations are provided to show the engineer how to assess a load rating for a distressed bridge. Lastly, a finite element analysis was conducted for a single box-beam section. The finite element model gave a detailed look at the effects of deterioration on the stresses and strains within a box-beam and provided an advanced method for determining the structural capacity of a single beam.

## 7.2 Recommendations for Future Work

Phase II of this project will expand upon the foundation laid out in Phase I by developing experimental methods of testing the durability and effectiveness of repairs to side-by-side prestressed box-beam bridges. As with most quality research programs, several questions remain and future work is needed. Some tasks for this work are outlined below, many of which are expected to be focused upon during the second phase of this project.

- Applied research of distressed beams should be conducted to provide information for the selection or development of superior materials and repair methods for the forms of distress identified in Phase I.

- The finite element model will be expanded to include the entire bridge system. This will allow for an analysis of the interaction between box-beams placed side-

by-side and the effect that shear key and post-tensioning deterioration has on the load transfer between beams.

- The post-tension losses due to creep and relaxation may have some adverse effects on longitudinal deck cracking along the beam joints. A time delay between post-tension application and deck placement needs further consideration.

- The shear key material in conjunction with post-tensioning is not accomplishing one of the intended functions of sealing the seam between the girders. The shear key materials in conjunction with varying post-tension levels should be investigated further and updated specifications should be considered.

- Unlike reinforced concrete members, prestressed concrete (PC) member strength is provided by the prestressing force. Any loss of prestressing force either by corrosion or by high load hits directly impacts member strength. The state of corrosion of the tendons is concealed except in extreme states when concrete delaminates and spalls on the outside. In the case of tendons near the box-beam cavity, spalling into the interior also cannot be assessed. For accurate assessment of these bridges it is essential to incorporate nondestructive inspection techniques for PC tendon corrosion assessment. Techniques such as resistivity measurements can easily be incorporated.

- Future work is required to better understand the mechanisms that lead to early deterioration of box-beams. Instrumentation and monitoring of several box-beams within a newly constructed bridge would provide information on the stresses and strains that the bridge is subjected to. Locating areas of increased internal stresses could lead to informative design changes to the standard box-beam section. For this study, several types of instrumentation would be located within the concrete and attached to the prestressing strand during fabrication. The instrumentation would be monitored at key periods in the production of the beams, during transport, installation, and for a portion of the service life of the bridge.

- The load rating presented in this report estimated the moment and shear capacity of a distressed section by analyzing the cross-sectional properties and computing capacities based on this information. Future work may indicate that a simplified procedure could be developed for this assessment. This work would likely involve a parametric or Monte Carlo simulation to bound capacity changes to different types of distress. This could then be used to provide a procedure to reduce load ratings based on the type of distress observed within a bridge.

CENTER FOR STRUCTURAL DURABILITY – Condition Assessment and Methods
of Abatement of Prestressed Concrete Box-Beam Deterioration

155

This page intentionally left blank

# References

AASHTO. (2002). *Standard Specifications for Highway Bridges,* 17th Edition, American Association of State Highway and Transportation Officials, 444 North Capitol Street, N.W., Suite 249, Washington, D. C.

AASHTO. (2003). *Interim Revisions to the Manual for Condition Evaluation of Bridges, Second Edition*. American Association of State Highway and Transportation Officials, Washington DC.

AASHTO. (2004). *AASHTO LRFD Bridge Design Specifications*, Third Edition, American Association of State Highway and Transportation Officials, 444 North Capitol Street, N.W., Suite 249, Washington, D. C.

ACI. (1989). "ACI 318-89 – Building Code Requirements for Reinforced Concrete." American Concrete Institute, Farmington Hills, Michigan.

ACI. (1990). "ACI 116R-90 – Cement and Concrete Terminology." American Concrete Institute, Farmington Hills, Michigan.

ACI. (1992). "ACI 201.2R-92 – Guide to Durable Concrete." American Concrete Institute, Farmington Hills, Michigan.

Ahlborn, T. M., Aktan, H. M., Kasper, J. M., Koyuncu, Y., and Rutyna, J. (2002). "Causes & Cures for Prestressed Concrete I-Beam End Deterioration." *Research Report No. RC-1412*, Michigan Department of Transportation, Construction and Technology Division, Lansing, Michigan.

Akbay, Z. (1991). "Actively Regulated Energy Dissipation Devices for Improving Seismic Performance of Buildings." *Ph.D Dissertation*, Wayne State University, Detroit, MI 48202.

Arner, R. C., and Panganiban, R. R. (1986). "Cathodic Deck Protection and Latex Modified Concrete Overlay on Steel I-Beam and on Prestressed Concrete Box-Beam Bridges." *Research Projects No. 83-09A and B,* Pennsylvania Department of Transportation, Harrisburg, Pennsylvania.

Birgul, R. (2001). "Durability Investigation of Concrete Culverts Reinforced with Steel and GFRP by Acoustic Emission." *Ph.D Dissertation*, Wayne State University, Detroit, MI 48202.

Boenig, A., Fúnez, L., Klinger, R. E., and Fowler, T. J. (2000) "Bridges with Premature Concrete Deterioration: Field Observations and Large-Scale Testing." *Research Report 1857-1*, Texas Department of Transportation.

Broomfield, P. P., Davies, K., and Hladky, K. (1999). "Permanent Corrosion Monitoring For New and Existing Reinforced Concrete Structures." *Structural Faults and Repair-99,* 8th International Conference, London, UK, July 13-15.

Brown, D. J. (1993). *Bridges,* Macmillan Publishing Company, N.Y.

Cairns, J., and Millard, S. (1999). "Reinforcement Corrosion and Its Effect on Residual Strength of Concrete Structures." *Structural Faults and Repair-99,* 8th International Conference, London, UK, July 13-15.

Ebeido, T., and Kennedy, J. B. (1996). "Shear and Reaction Distribution in Continuous Skew Composite Bridges." *Journal of Bridge Engineering*, 1(4), 155-165.

El-Remaily, A., Tadros, M. K., Yamane, T., and Krause, G. (1996). "Transverse Design of Adjacent Precast Prestressed Concrete Box-beam Bridges." *PCI Journal*, 41(4), 96-113.

Elzayat, M. H. (1989). "Shear Stress Distribution in RC Structural Walls." *Ph.D Dissertation*, Wayne State University, Detroit, MI 48202.

Emmons, P.H. (1994). *Concrete Repair and Maintenance Illustrated*. R.S. Means Company, Inc. Kingston, Massachusetts.

Enright, M. P., and Frangopol, D. M. (2000). "Survey and Evaluation of Damaged Concrete Bridges." *Journal of Bridge Engineering,* 5(1), 31-38.

FHWA. (1997). "Evaluation of Digital Camera Technology for Bridge Inspection." Federal Highway Administration, *Publication No: FHWA-SA-97-100.*

FHWA. (2002). Hartle, R. A., Ryah, T. W., Mann, J.E., et.al. "Bridge Inspector's Reference Manual." Federal Highway Administration, *Publication No:* FHWA NHI 03-001.

Fereig, S. M. (1994). "Preliminary Design of Precast Prestressed Concrete Box-beam Bridges." *PCI Journal*, 39(3), 82-90.

Galuta, E. M., and Cheung, M. S. (1995). "Combined Boundary Element and Finite Element Analysis of Composite Box-beam Bridges." *Computers & Structures*, 57**,** 427-437.

Ganji, V., Tabrizi, K., and Vittilo, N. (2000). "Project Level Application of Portable Seismic Pavement Analyzer." *Structural Material Technology IV- an NDT Conference, 2000,* S. Allampalli, Ed., Technomic, 205-210.

Gifford, F. W. (1961). "Test on a Prestressed Concrete Hollow-box Bridge Deck." *Magazine of Concrete Research,* Vol. 13, No. 39, pp. 149-156.

Graybeal, B. A., Rolander, D. D., Phares, B. M., Moore, M. E., and Washer, G. A. (2001). "Highway Bridge Inspection : State of the Practice Survey." *Transportation Research Board*, 80th Annual Meeting, Conference Paper, Washington D. C., January 7-11.

Gucunski, N., Vittilo, N., and Maher, A. (2000). "Bridge Deck Delamination using Integrated Seismic Devices." *Structural Material Technology IV_ and NDT Conference, 2000*, S. Alampalli, Ed., Technomic, 329-334.

Hag-Elsafi, O., and Alampalli, S. (2000). "Strengthening Prestressed Concrete Beams Using Bonded FRP Laminates." *Structural Material Technology IV_ and NDT Conference, 2000*, S. Alampalli, Ed., Technomic, 287-292.

Halstead, J. P., O' Conner, J. S., Alampalli, S., and Minser, A. (2000). "Evaluating FRP Wrap with NDT Methods." *Structural Material Technology IV_ and NDT Conference, 2000*, S. Alampalli, Ed., Technomic, 275-280.

Hartle, R. A., Amrhein, W. J., Wilson, K. E., Baughman, D. R., and Tkacs, J. J. (1995). "Bridge Inspector's Training Manual 90." *Report No. FHWA-PD-91-015*, Federal Highway Administration (FHWA), Washington, D. C.

Henderson, M. E., Costley, R. D., and Dion, G. N. (2000). "Acoustic Inspection of Concrete Bridges with the Hollow Deck." *Structural Material Technology IV_ and NDT Conference, 2000*, S. Alampalli, Ed., Technomic, 184-189.

Huckelbridge, A. A. Jr., El-Esnawi, H., and Moses, F. (1995). "Shear key Performance in Multibeam Box-beam Bridges." *Journal of Performance of Constructed Facilities*, 9(4), 271-285.

HyperMesh user's manual – version 6.0. (2003). Altair Engineering, Inc., 1820 E Big Beaver, Troy, Michigan 48083. (http://www.altair.com).

Juntunen, D. (2000). *Cracks and Deterioration of Prestressed Beams (Draft)*. Structural Research Unit, Construction and Technology Division, Michigan Department of Transportation, Lansing, MI 48909.

Kosmatka, S. H., and Panarese, W. C. (2000). *Design and Control of Concrete Mixtures*, EB001, 14th Edition, Portland Cement Association, Skokie, Illinois.

Legat, A., Kahur, V., Bevc, L., and Vehovar, L., (1996). "Some Considerations of Potential Mapping as a Method for the Detection of Corrosion in Reinforced and Prestressed Concrete Structures." *13th International Corrosion Congress Proceedings*, Paper 186, 1-6.

Leonhardt, F. (1964). *Prestressed Concrete Design and Construction*, Second Edition, C. van Amerogen, translator, Wilhelm Ernst & Sohn, Berlin, Munich.

Liu, W., Hunsperger, R., and Kunz, E. (2001). "Nondestructive Corrosion Monitoring of Prestressed HPC Bridge Beams Using Time Domain Reflectometry." *Transportation Research Board*, 80th Annual Meeting, Washington D. C., January 7-11.

Mari, A. R., and Valdès, M. (2000). "Long-Term Behavior of Continuous Precast Concrete Girder Bridge Model." *Journal of Bridge Engineering*, 5(1), 22-30.

MDOT. (1958). *Specifications for Design of Highway Bridges, 1958 Edition,* Michigan State Highway Department.

MDOT. (1999). Pontis Bridge Inspection Manual.  Michigan Department of Transportation, Lansing Maintenance Division, Lansing MI.

MDOT. (2003a).  *Bridge Analysis Guide*, Michigan Department of Transportation, Construction and Technology Support Area, Lansing MI.

MDOT. (2003b).  *Michigan Design Manual, Vol 5: Bridge Design*.  Michigan Department of Transportation, Lansing MI

MDOT. (2003c).  *Standard Specifications for Construction*, Michigan Department of Transportation, Lansing MI.

MDOT. (2003d).  *Michigan Structure Inventory and Appraisal Coding Guide.*, Michigan Department of Transportation, Lansing MI.

MDOT. (2003e).  *Bridge Design Guide*.  Michigan Department of Transportation, Lansing MI.

Memberg, L.S., Klingner, R.E., Fowler, T.J. (2002) "Bridges with Premature Concrete Deterioration: Damage Indices, Strand-Pullout Tests, and Field Observations." *Research Report 1857-4*, Texas Department of Transportation.

Menn, C. (1990).  *Prestressed Concrete Bridges*.  Birkhäuser Verlag AG Basel, Germany.

Miller, R.A., Hlavacs, G.M., and Long, T.W. (1998).  "Testing of Full Scale Prestressed Beams to Evaluate Shear Key Performance." *FHWA report # OH-98/019,* Federal Highway Administration.  FHWA report # OH-98/019

Miller, R., Hlavacs, G. M., Long, T., and Greuel, A. (1999). "Full-Scale Testing of Shear keys for Adjacent Box-beam Bridges." *PCI Journal*, 44(6), 80-90.

Monterio, P. J. M., Frank, M., and Frangos, W. (1998). "Nondestructive Measurement of Corrosion State of Reinforcing Steel in Concrete." *ACI Material*, 95(6), 704-709.

Moore, D. G., Klodt, D.T., and Hensen, R. J. (1970). "Protection of Steel in Prestressed Concrete Bridges." *NCHRP Report No .90*.  National Research Council, Washington D.C.

NACE, National Association of Corrosion Engineers. (1970). "NACE Basic Corrosion Course." *NACE*, Houston, Texas.

Needham, D., and Juntunen, D. A. (1997). "Investigation of Condition of Prestressed Concrete Bridges in Michigan." *Research Report R-1348*, Research Project 85 F-0164, Michigan Department of Transportation, Materials and Technology Division, Lansing, MI 48909.

Nogueira, C. L. (1999). "Bridge Evaluation Using Nondestructive Testing in Bridge Inspections as a Tool for Bridge Management Systems." *Structural Faults and Repair-99*, 8th International Conference, London, UK, July 13-15.

Pascale, G., Bonfiglioli, B., Carli, R., and Arduini, M. (1999). "Bridge RC Beams: Repair and Monitoring." *Structural Faults and Repair-99*, 8th International Conference, London, UK, July 13-15.

PCI. (2003). *Precast Prestressed Bridge Design Manual*. Precast/Prestressed Concrete Institute, 175 W. Jackson Boulevard, Chicago, IL 60604

Roche, J.M., Klingner, R.E. and, Fowler, T.J. (2001). "Bridges with Premature Concrete Deterioration: Fatigue Testing of Full-Scale, Prestressed Concrete Box Girders Failing in Shear." *Research Report 1857-3,* Texas Department of Transportation.

Rolander, D. D., Phares, B. M., Graybeal, B. A., Moore, M. E., Washer, G. A. (2001). "Highway Bridge Inspection: State-of-the-Practice Survey." TRB 2001 80th Annual Meeting CD-ROM, Paper No: 01-2867, Transportation Research Board, 500 Fifth Street, NW, Washington, DC 20001.

Ryall, M.J. (2001). *Bridge Management*, Butterworth-Heinemann, Woburn, MA.

Sennah, K. M., and Kennedy, J. B. (1999). "Load Distribution Factors for Composite Multi-cell Box-beam Bridges." *Journal of Bridge Engineering*, 4(1), 71-78.

Settipani, A. (1987). "Inspection of Reinforced and Prestressed Concrete by means of Gammagraphy." *Bridge Evaluation Repair and Rehabilitation*, E. Absi, and A.S. Nowak, Ed., The University of Michigan, Ann Arbor, Michigan, 498-505.

Shanafelt, G. O., and Horn, W. B. (1980). "Damage Evaluation and Repair of Prestressed Concrete Bridge Members." *NCHRP Report No.226,* Transportation Research Board, Washington D.C.

Shanafelt, G. O., and Horn, W. B. (1985). "Guidelines for Evaluation and Repair of Prestressed Concrete Bridge Members." *NCHRP Report No.280,* Transportation Research Board, Washington D.C.

Teng, T. P. (2000). "Materials and Methods for Corrosion Control of Reinforced and Prestressed Concrete Structures in New Construction." *FHWA-RD-00-081.* Federal Highway Administration.

Timoshenko, S. (1940). *Theory of Plates and Shells*, First edition, McGraw-Hill, New York.

Tinkey, B.V., Fowler, T.J. and, Klingner, R.E. (2000). "Nondestructive Testing of Prestressed Bridge Girders with Distributed Damage.", *Research Report 1857-2,* Texas Department of Transportation.

CENTER FOR STRUCTURAL DURABILITY – Condition Assessment and Methods
of Abatement of Prestressed Concrete Box-Beam Deterioration

161

Titman, D. J. (2001). "Applications of Thermography in NDT of Structures." *Structural Faults and Repair-99*, 8th International Conference, London, UK, July 13-15.

Troitsky, M. S. (1994). *Planning and Design of Bridges,* John Wiley & Sons, Inc. N.Y.

Van Dam, T.J., Sutter, L.L., Smith, K.D., Wade, M.J., and Peterson, K.R., (2002). *Guidelines For Detection, Analysis, and Treatment of Materials-Related Distress in Concrete Pavements – Volume 2: Guidelines Description and Use.* FHWA-RD-01-164. Federal Highway Administration. Turner-Fairbank Highway Research Center, McLean, VA. March. pp. 233.

Vaysburg, A. M., Emmons, P. H., Mailvaganam, N. P., McDonald, J. E., Bissonnette, B. (2004). "Concrete Repair Techonology- A Revised Approach is Needed." *Concrete International*, January 2004

Whiting, D. A., Stejkal, B.G., and Nagi, M. A. (1993). "Conditions of Prestressed Concrete Bridge Components: Technology Review and Field Surveys." *FHWA-RD-93-037*, Federal Highway Administration, Washington, D.C.

Whiting, D. A., Stejkal, B.G., and Nagi, M. A. (1998). "Rehabilitation of Prestressed Concrete Bridge Components by Non Electrical Methods." *FHWA-RD-98-189*, Federal Highway Administration, Washington, D.C.

Xanthakos, P. P. (1996). *Bridge Strengthening and Rehabilitation*, Prentice –Hall PTR, New Jersey.

Yaman, O. (2000). "Numerical Simulation Models for the Verification of NDT Procedures based on Ultrasonic Pulse Propagation in Reinforced Concrete Structure." *Ph.D Dissertation*, Wayne State University, Detroit, MI 48202.

Yamane, T., Tadros, M. K., and Arumugasamy, P. (1994). "Short to Medium Span Pre-cast Prestressed Concrete Bridges in Japan." *PCI Journal*, 39(2), 74-100.

Zhang, J., Monterio, P. M., and Morrison, F.H. (2001). "Non Invasive Surface Measurement of the Corrosion Impedance of Rebar in Concrete Part I." *ACI Material Journal*, 116-126.

Zokaie, T. (2000). "AASHTO-LRFD Live Load Distribution Specifications." *Journal of Bridge Engineering*, 5 (2), 131-138.

# Additional Related Works

AASHTO. (1989). *AASHTO Guide Specifications for Strength Evaluation of Existing Steel and Concrete Bridges*, Second Edition, American Association of State Highway and Transportation Officials, 444 North Capitol Street, N.W., Suite 249, Washington, D. C.

AASHTO. (2003). *Manual for Condition Evaluation and Load and Resistance Factor Rating (LRFR) of Highway Bridges*, American Association of State Highway and Transportation Officials, Washington DC.

ABAQUS/Standard User's Manual - Version 6.3. (2002). Hibbitt, Karlson & Sorensen, Inc., Pawtucket, RI. (http://www.abaqus.com).

Abdullah, M. A., and Abdul-Razzak, A. A. (1990). "Finite Strip Analysis of Prestressed Box-beams." *Computers & Structures*, 36**,** 817-822.

ACI. (1996). "ACI 222R-96 – Corrosion of Metals in Concrete." American Concrete Institute, Farmington Hills, Michigan.

ACI. (1999). "ACI 318-99 – Building Code Requirements for Structural Concrete and Commentary." American Concrete Institute, Farmington Hills, Michigan.

Amer, A., Arockiasamy, M., and Shahawy, M. (1999). "Load Distribution of Existing Solid Slab Bridges Based on Field Tests." *Journal of Bridge Engineering*, 4(3), 189-306.

Bathe, K. (1982). *Finite Element Procedures in Engineering Analysis*. Prentice-Hall, Inc., Englewood Cliffs, New Jersey 07632

Behr, R. A., Cundy, E. J., and Goodspeed, C. H. (1990). "Cost Comparison of Timber, Steel, and Prestressed Concrete Bridges." *Journal of Structural Engineering, ASCE,* 116**,** 3448-3457.

Bennett, R. M., Hufstetler, M. L., and Carver, M. (2002). "50-Year-Old Prestressed Segmental Concrete Bridges." *Journal of Professional Issues in Engineering Education and Practice,* 128**,** 83-87.

Birgul, R., Koyuncu, Y., Ahlborn, T. M., and Aktan, H. M. (2003). "A 40-Year Performance Assessment of Prestressed Concrete (PC) I-Girder Bridges in Michigan." *TRB 2003 Annual Meeting CD-ROM*, Transportation Research Board, 500 Fifth Street, NW, Washington, DC 20001.

Boswell, L. F. (1998). "The Ultimate Load Analysis of Thin-Walled Concrete Box-beam." *Thin-Walled Structures*, 34, 181-198.

Casas, J. R. (2000). "Safety of Prestressed Concrete Bridges to Fatigue: Application to Serviceability Limit State of Decompression." *ACI Structural Journal,* 97**,** 68-74.

Casas, J. R., and Crespo-Minguillon, C. (1998). "Probabilistic Response of Prestressed Concrete Bridges to Fatigue." *Engineering Structures,* 20**,** 940-947.

Chan, T. H. T., and Yung, T. H. (2000). "A Theoretical Study of Force Identification Using Prestressed Concrete Bridges." *Engineering Structures,* 22**,** 1529-1537.

Chan, T. H. T., Law, S. S., & Yung, T.H. (2000). "Moving Force Identification using an Existing Prestressed Concrete Bridge." *Engineering Structures,* 22**,** 1261-1270.

Cheung, Y. K., and Au, F. T. K. (1992). "Finite strip analysis of right box-beam bridges using computed shape functions." *Thin-Walled Structures,* 13**,** 275-298.

Choi, C-K., Kim, K-H., and Hong, H-S. (2002). "Spline Finite Strip Analysis of Prestressed Concrete Box-beam Bridges." *Engineering Structures,* 24**,** 1575-1586.

Choi, S., Park, S., Bolton, R., Stubbs, N., and Sikorsky. (2003). "Periodic Monitoring of Physical Property Changes in a Concrete Box-beam Bridge." *Journal of Sound and Vibration* In Press, Corrected Proof.

Cook, R. D., Malkus, D. S., and Plesha, M. E. (1989). *Concepts and Applications of Finite Element Analysis*, Third Edition, John Wiley & Sons, Inc.

Crespo-Minguillon, C., and Casas, J. R. (1998). "Fatigue Reliability Analysis of Prestressed Concrete Bridges." *Journal of Structural Engineering, ASCE,* 124**,** 1458-1466.

Davis, R. E., Bon, V. D., and Semans, F. M. (1982). "Live Load Distribution in Concrete Box-beam Bridges." *Transportation Research Record 871*, Transportation Research Board, 2101 Constitution Avenue, NW, Washington, DC

Deng, L., Ghosn, M., Znidaric, A., and Casas, J. R. (2001). "Nonlinear Flexural Behavior of Prestressed Concrete Girder Bridges." *Journal of Bridge Engineering*, 6(4), 276-284.

Derobert, X., Aubagnac, C., and Abraham, O. (2002). "Comparison of NDT Techniques on a Post-tensioned Beam Before its Autopsy." *NDT & E International,* 35**,** 541-548.

Dritsos, S. E. (1991). "Distortion of Concrete Box-beams due to Eccentric Transverse Loads*." Journal of Structural Engineering*, 117(1), 29-47.

Dundar, C. (1990). "Concrete Box Sections under Biaxial Bending and Axial Load*." Journal of Structural Engineering*, 116(3), 860-865.

Dunker, K. F., and Rabbat, B. G. (1992). "Performance of Prestressed Concrete Bridges in the United States – The First 40 Years." *PCI Journal*, 37(3), 47-64.

French, C., Mokhtarzadeh, A., Ahlborn, T., and Roberto, L. (1998). "High-Strength Concrete Applications to Prestressed Bridge Girders." *Construction and Building Materials,* 12**,** 105-113.

Fu, G., Alampalli, S., and Pezze, F. P. (1992). " Long-term Serviceability of Isotropically Reinforced Concrete Bridge Deck Slabs." *Transportation Research Record 1371*, Transportation Research Board; Washington D.C.

Grace, N. F. (2000). "Response of Continuous CFRP Prestressed Concrete Bridges under Static and Repeated Loadings." *PCI Journal,* 45(6)**,** 84-102.

Hambly, E. C. (1976). *Bridge Deck Behavior*, Chapman & Hall, London.

Hayashi, S., and Kokusho, S. (1986). "Bond Behavior in the Neighborhood of the Crack." *Finite Element Analysis of Concrete Structures*, Proceedings of the Seminar Sponsored by the Japan Society for the Promotion of Science and the U.S. National Science Foundation, Structural Division, American Society of Civil Engineers, 364-373.

Heldt, L. D. (2001). Corrosion Workshop at Michigan Technological University, July 11.

Hjorth-Hansen, E., Jakobsen, A., and Strommen, E. (1992). "Wind Buffeting of a Rectangular Box-beam Bridge." *Journal of Wind Engineering and Industrial Aerodynamics,* 42**,** 1215-1226.

Jadun, S. (1990). "Michigan Experience with Prestressed Bridges." *MATES*, Michigan Department of Transportation, Materials and Technology Division, Issue No. 49. December 1990.

Jakobsen, J. B., and Hjorth-Hansen, E. (1998). "Aeroelastic Effects on a Rectangular Box-beam Bridge." *Journal of Wind Engineering and Industrial Aerodynamics,* 74(6)**,** 819-827.

Johnston, D. W., and Zia, P. (1975). "Prestressed Box-beams Under Combined Loading." *Journal of the Structural Division*, Proceedings of the American Society of Civil Engineers, 101 (ST7), 1313-1331.

Jones, D.A. (1992). *Principles and Prevention of Corrosion,* McMillan Publishing Company, New York.

Kermani, B., and Waldron, P. (1993). "Analysis of Continuous Box-beam Bridges including the Effects of Distortion." *Computers & Structures*, 47, 427-440.

Kirkpatrick, J., Long, A. E., Stevenson, W. M. C., and Thompson, A. (1985). "Load Tests on Prestressed Concrete Multi-Girder Bridge Decks." *ACI Special Publications*, 88, 23-38.

Krause, H.-J., Wolf, W., Glaas, W., Zimmermann, E., Faley, M. I., Sawade, G., Mattheus, R., Neudert, G., Gampe, U. and, Krieger, J. (2002). " SQID Array for Magnetic Inspection of Prestressed Concrete Bridges." *Physica C: Superconductivity*, 368, 91-95.

Krauss, P.D., and Rogalla, E.A. (1996). "Transverse cracking in newly constructed bridge decks." *NCHRP Report 380*, Transportation Research Board; Washington D.C.

Křístek, V. (1979). *Theory of box-beams*. John Wiley & Sons, Ltd.

Kuhn, P., and Chiarto, P. T., "Shear Lag in Box-beams Methods of Analysis and Experimental Investigations." Report No 739, *National Advisory Committee of Aeronautics.*

Labia, Y., Saiidi, M.S., and Douglas, B. (1997). "Full Scale Testing and Analysis of 20 Year Old Pretensioned Concrete Box-beam Bridge." *ACI Structural Journal,* 94(5), 471-482.

Levintov, B. (1995). "Construction Equipment for Concrete Box-Beam Bridges." *Concrete International*, 17(2), 43-47.

Luo, Q. Z., Wu, Y. M., Tang, J., and Li, Q. S. (2002). "Experimental Studies on Shear Lag of Box-beams." *Engineering Structures,* 24**,** 469-477.

Maes, M. A., Wei, X., and Dilger, W. H. (2001). "Fatigue Reliability of Deteriorating Prestressed Concrete Bridges due to Stress Corrosion Cracking." *Canadian Journal of Civil Engineering,* 28**,** 673-683.

Megson, T. H. G. (1995). "Finite Element Modeling of Box-beam Diaphragms at Supports." *Thin-Walled Structures*, 22, 25-37.

Mehlhorn, G., and Keuser, M. (1986). "Isoperimetric Contact Elements for Analysis of Reinforced Concrete Structures." *Finite Element Analysis of Concrete Structures*, Proceedings of the Seminar Sponsored by the Japan Society for the Promotion of Science and the U.S. national Science Foundation, Structural Division, American Society of Civil Engineers, 329-347.

Michalopoulos, A., Stavroulakis, G. E., Zacharenakis, E. C., and Panagiotopoulos, P. D. (1997). "A Prestressed Tendon Based Passive Control System for Bridges." *Computers & Structures,* 63**,** 1165-1175.

Mikkola, M. J., and Paavola, J. (1980). "Finite Element Analysis of Box-beams." *Journal of the Structural Division*, Proceedings of the American Society of Civil Engineers, 106(ST6), 1343-1357.

Miller, R., and Parekh, K. (1994). "Destructive Testing of Deteriorated Prestressed Box Bridge Beam." *Transportation Research Record 1460*, Transportation Research Board, 2101 Constitution Avenue, NW, Washington, DC.

Mishra, P. K., Das, S., and Dey, S. S. (1992). "Discrete Energy Method for the Analysis of Right Box-beam Bridges." *Computers & Structures,* 43**,** 223-235.

Mo, Y.L., Jeng, C-H., and Chang, Y.S. (2000) "Torsional Behavior of Prestressed Concrete Box-beam Bridges with Corrugated Steel Webs." ACI Structural Journal, 97(6), 849-859.

Moon, J., and Burns, N. H. (1997). "Flexural Behavior of Member with Unbonded Tendons I: Theory." *Journal of Structural Engineering*, 123(8), 1087-1094.

Moon, J., and Burns, N. H. (1997). "Flexural Behavior of Member with Unbonded Tendons II: Applications." *Journal of Structural Engineering*, 123(8), 1095-1101.

Morita, S., and Fujii, S. (1986). "Bond-Slip Models in Finite Element Analysis." *Finite Element Analysis of Concrete Structures*, Proceedings of the Seminar Sponsored by the Japan Society for the Promotion of Science and the U.S. national Science Foundation, Structural Division, American Society of Civil Engineers, 348-363.

Nielsen, R. J., and Schmeckpeper, E. R. (2002). "Single-Span Prestressed Girder Bridge: LRFD Design and Comparison." *Journal of Bridge Engineering*, 7(1), 22-30.

Niwa, J., Chou, L., Shima, H., and Oakmura, H. (1986). "Nonlinear Spring Element for Strain -Slip Relationship of a Deformed Bar." *Finite Element Analysis of Concrete Structures*, Proceedings of the Seminar Sponsored by the Japan Society for the Promotion of Science and the U.S. National Science Foundation, Structural Division, American Society of Civil Engineers, 374-383.

Nowak, A. S., and Grouni, H. N. (1986). "Serviceability Criteria in Prestressed Concrete Bridges." *Journal of the American Concrete Institute,* 83**,** 43-49.

Oh, B. H. (2000). "Sensitivity Analysis of Time Dependent Behavior in PSC Box-beam Bridges." *Journal of Structural Engineering*, 126(2), 171-179.

Oh, B. H., and Chae, S.T. (2001). "Structural Behavior of Tendon Coupling Joints in Prestressed Concrete Bridge Girders." *ACI Structural Journal,* 98**,** 87-95.

Oh, B. H., and In, H. Y. (2001). "Realistic Long-Term Prediction of Prestress Forces in PSC Box-beam Bridges." *Journal of Structural Engineering*, 127(9), 1109-1116.

Park, R., and Paulay, T. (1975). *Reinforced Concrete Structures*. John Wiley & Sons, Inc.

Perenchio, W. F., Fraczek, J., and Preiffer, D.W. (1989). "Corrosion Protection of Prestressing Systems in Concrete Bridges." *NCHRP Report No. 313,* National Research Council, Washington D.C.

Picard, A., and Massicotte, B. (1999). "Serviceability Design of Prestressed Concrete Bridges." *Journal of Bridge Engineering*, 4(1), 48-55.

Rabbat, B. G., Dunker, K. F., and Dick, J. S. (1992). "Cost Comparison of Timber, Steel, and Prestressed Concrete Bridges." *Journal of Structural Engineering, ASCE,* 118**,** 1151-1153.

Rao, C., and Frantz, G. C. (1996). "Fatigue Tests of 27-Year-Old Prestressed Concrete Bridge Box-beams." *PCI Journal*, 41(5), 74-83.

Rengaswamy, N. S., and Rajagopalan, K. S. (1997). "Corrosion of High Strength Steel in Prestressed Concrete:1-Electrochemical Studies." *Indian Concrete Journal*, 51(10), October, 301-304.

Sampaio, A. Z. (2003). "Geometric Modeling of Box-beam Deck for Integrated Bridge Graphical System." *Automation in Construction,* 12**,** 55-66.

Sandor, B. I. (1972). *Fundamentals of Cyclic Stress and Strain*, The University of Wisconsin Press, Box 1379, Madison, Wisconsin 53701.

Sennah, K. M., and Kennedy, J. B. (2001). "State-of-the-Art in Design of Curved Box-beam Bridges." *Journal of Bridge Engineering*, 6(3), 159-167.

Sennah, K. M., and Kennedy, J. B. (2002). "Literature Review in Analysis of Box-beam Bridges." *Journal of Bridge Engineering*, 7(2), 134-143.

Shiu, K. N. (1984). "Seasonal and Diurnal Behavior of Concrete Box-beam Bridges." *Transportation Research Record 982*, Transportation Research Board, 2101 Constitution Avenue, NW, Washington, DC

Shiu, K. N., and Tabatabai, H. (1994). "Measured Thermal Response of Concrete Box-Beam Bridge." *Transportation Research Record 1460*, Transportation Research Board, 2101 Constitution Avenue, NW, Washington, DC.

Sloan, T. D., and Thompson, A. (1991). "Development of an Automatic Data Collection System for a Major Box-beam Bridge." *Computers & Structures*, 41, 1411-1416.

Srinivasan, S., Saravanan, K., Kapali, V., Nayak, N. U., Bapu, R. H. S., Kalyanasundaram, R. M., Madhavamayandi, A., Iyer, Y. M., Rengaswamy, N. S. (1996). "Radiographic Examination of Prestressed Concrete Box-Beam Bridges." *Materials Performance*, 35, 61-65.

Stanton, J. F. and Mattock, A. H. (1986). "Load Distribution and Connection Design for Precast Stemmed Multibeam Bridge Superstructures." *NCHRP Report No.287*, Transportation Research Board, Washington D.C.

Strommen, E., Hjorth-Hansen, E., and Kaspersen, J. H. (2001). "Dynamic Loading Effects of a Rectangular Box-beam Bridge." *Journal of Wind Engineering and Industrial Aerodynamics,* 89**,** 1607-1618.

Taysi, N., and Ozakca, M. (2002). "Free Vibration Analysis and Shape Optimization of Box-beam Bridges in Straight and Curved Plan Form." *Engineering Structures,* 24**,** 625-637.

Thorkildsen, E., and Holombo, J. (1995). "Innovative Prestressed Concrete Bridges Mark Caltrans Centennial." *PCI Journal,* 40**,** 34-38.

Tilly, G. P. (1987). "Performance and Serviceability of Concrete Bridges." *Bridge Evaluation Repair and Rehabilitation*, E. Absi, and A.S. Nowak, Ed., The University of Michigan, Ann Arbor, Michigan, 119-134.

Upadyay, A., and Kalyanaraman, V. (2003). "Simplified Analysis of FRP Box-beams." *Composite Structures,* 59**,** 217-225.

Van De Lindt, J. W., Fu, G., Zhou, Y., and Pablo, R. M. (2002). "Structural Reliability of Bridges Designed using HS25 in the State of Michigan." *TRB 2003 Annual Meeting CD-ROM*, Transportation Research Board, 500 Fifth Street, NW, Washington, DC 20001.

Virlogeux, M. (2000). "New Trends in Prestressed Concrete Bridges." *Fifth International Bridge Engineering ConferenceProceedings,* Volumes 1, 238-272.

Wang, T. L., Shahawy, M., and Huang, D. Z. (1992). "Impact in Highway Prestressed Concrete Bridges." *Computers & Structures,* 44**,** 525-534.

Weyers, R. E., Prowell, B. D., Sprinkel, M. M., and Vorster, M. (1993). "Concrete Bridge Protection, Repair, and Rehabilitation Relative to Reinforcement Corrosion: A Methods Application Manual," *SHRP-S-360*, National Research Council, Washington DC.

Yang, L. F., Leung, A. Y. T., and Li, Q. S. (2001). "The Stochastic Finite Segment in the Analysis of the Shear lag Effect on Box-beams." *Engineering Structures*, 23, 1464-1468.